INSTITUTO SUPERIOR DE ENGENHARIA DE LISBOA

ÁREA DEPARTAMENTAL DE ENGENHARIA ELECTRÓNICA E TELECOMUNICAÇÕES E COMPUTADORES

RECONFIGURABLE ANTENNA FOR MOBILE DEVICES

Ricardo Miguel Romão Gonçalves

(Licenciado em Engenharia Electrónica e Telecomunicações e Computadores)

Dissertação de Mestrado entregue como requisito para a obtenção do grau de Mestre em Engenharia Electrónica e Telecomunicações pelo Instituto Superior de Engenharia de Lisboa

Júri da prova:

Presidente:	Prof. Doutor Mário Véstias
Vogal - Orientador:	Prof. Doutor Pedro Pinho
Vogal - Arguente:	Prof. Doutor Nuno B. Carvalho

Setembro 2012

Orientação

Prof. Doutor Pedro Renato Tavares Pinho

Área **D**epartamental de **E**ngenharia **E**lectrónica e **T**elecomunicações e **C**omputadores

Instituto Superior de Engenharia de Lisboa

Instituto Politécnico de Lisboa

Júri da Prova

Arguente

Prof. Doutor Nuno Borges Carvalho

Instituto de Telecomunicações

Departamento de **E**ngenharia **E**lectrónica **T**elecomunicações e **I**nformática

Universidade de Aveiro

Coordenador do Curso

Prof. Doutor Mário Pereira Véstias

Área **D**epartamental de **E**ngenharia **E**lectrónica e **T**elecomunicações e **C**omputadores

Instituto Superior de Engenharia de Lisboa

Instituto Politécnico de Lisboa

Orientador

Prof. Doutor Pedro Renato Tavares Pinho

Área **D**epartamental de **E**ngenharia **E**lectrónica e **T**elecomunicações e **C**omputadores

Instituto Superior de Engenharia de Lisboa

Instituto Politécnico de Lisboa

"A man needs to travel. By his account, not through stories, pictures, books or television. Needs to travel by himself, with his eyes and feet, to understand what is yours. For a day plant his own trees and give them value. Meet the cold to enjoy the warmth - and the opposite. Feel the distance and homelessness to be well under his own roof. A man needs to travel to places he doesn't know, to break the arrogance that makes him see the world like he imagines and not simply as it is or can be; which makes him a professor and doctor of what he didn't see, when he should be a student, and simply go see"

Amyr Klink

"Education is an admirable thing, but it is well to remember from time to time that nothing that is worth knowing can be taught."

Oscar Wilde

Abstract

The work reported in this dissertation is focused in the printed antenna research. Basic concepts of printed antennas are presented, along with a few examples that were developed. The main focus however, is around miniaturization and reconfigurability of antennas.

Antenna miniaturization is a long time research subject, however, new techniques and solutions are presented everyday. In this thesis, a recent technique based on the introduction of chip inductors in the resonating element of a printed antenna is used in order to miniaturize a monopole with a resonating frequency at 2.5 GHz.

Another issue approached in this work is antenna reconfigurability. Some common techniques used in antenna reconfiguration are presented and debated. A solution with PIN diodes is used to study this capability. The concepts and characteristics of this type of components are presented and an example of a reconfigurable printed monopole for dual-band operation is designed and fabricated.

At last, miniaturization with chip inductor and reconfigurability through PIN diodes are used together to create a very small antenna for dual-band operation. The simulated and measured results are discussed and upon these, some possible optimizations are proposed.

Keywords: Miniaturization, reconfigurability, chip inductors, PIN diodes

Resumo

O trabalho descrito nesta dissertação de mestrado foca-se em geral na investigação de antenas impressas. São apresentados conceitos básicos, em conjunto com alguns exemplos desenvolvidos. No entanto, o principal foco prende-se com técnicas de miniaturização e reconfigurabilidade de antenas.

A miniaturização de antenas é um tema de investigação de longa data, no entanto, novas técnicas e soluções são apresentadas regularmente. Nesta tese, é aplicada uma técnica recente, baseada na introdução de indutores encapsulados no elemento ressonante de uma antena, que permite miniaturizar um monopolo impresso com uma frequência de ressonância de 2.5 GHz.

Outro assunto abordado neste trabalho é a reconfigurabilidade de antenas. Algumas das técnicas mais comuns na investigação actual são apresentadas e debatidas. Uma solução com recurso a díodos PIN é usada para estudar esta capacidade. Os conceitos e características deste tipo de componentes são apresentadas sendo feito o desenho e fabrico de um possível monopolo impresso reconfigurável para operação em dupla banda.

Por fim, são combinadas as técnicas de miniaturização com inductor encapsulado e reconfigurabilidade através de díodos PIN, por forma a projectar uma antena reconfigurável muito pequena, para operação em duas bandas distintas. Os resultados são discutidos e com base nestes, algumas possíveis optimizações são propostas.

Palavras-chave: Miniaturização, reconfigurabilidade, indutores encapsulados, díodos PIN

Acknowledgements

Agradecimentos

Em primeiro lugar e acima de todos, quero deixar um especial agradecimento aos meus pais. Agradecer por todo o apoio e dedicação que me deram, são eles os pilares da minha existência, nos quais eu me suporto em todos os momentos de maior dificuldade. E estes nunca vacilaram. Sem eles, nada disto seria possível. Tal como eles, quero também agradecer aos meus tios e aos meus padrinhos, que me ajudaram em todo o meu percurso académico, pelo apoio e por sempre acreditarem que era capaz de aqui chegar.

Não posso deixar de agradecer a todos os meus amigos, que conheci ao longo destes anos, que me proporcionaram os melhores momentos da minha vida. Com todas as aventuras e desventuras, todos os momentos de farra e acima de tudo boa disposição. Pela partilha de conhecimentos e companheirismo.

Quero também agradecer ao Intituto de Telecomunicações de Aveiro, por ter disponibilizado material e equipamentos para a fabricação e teste dos protótipos, bem como ter auxiliado nas medições das antenas desenvolvidas neste trabalho.

Por fim, não podia deixar de agradecer ao meu orientador, o professor Pedro Pinho, que me acompanha desde o final da minha Licenciatura, pela disponibilidade, pela boa disposição, e por sempre acreditar em mim e continuar a incentivar-me a chegar mais longe. E essencialmente aos professores que me ensinaram ao longo da vida e estimularam o gosto pelo conhecimento e a aprendizagem contínua.

Contents

List of Figures

List of Tables

Acronyms

DVB	**D**igital **V**ideo **B**roadcast
ESA	**E**lectrically **S**mall **A**ntenna
GPS	**G**lobal **P**ositioning **S**ystem
GPRS	**G**lobal **P**acket **R**adio **S**ervice
GSM	**G**lobal **S**ystem for **M**obile Communication
IC	**I**ntegrated **C**ircuit
LTE	**L**ong **T**erm **E**volution
MEMS	**M**icro **E**lectro **M**echanical **S**witches
MIMO	**M**ultiple **I**nput **M**ultiple **O**utput
NFC	**N**ear **F**ield **C**ommunications
PIN	**P**-**I**ntrinsic-**N**
RF	**R**adio **F**requency
RFID	**R**adio **F**requency **ID**entification
SDR	**S**oftware **D**efined **R**adio
SPST	**S**ingle **P**ole **S**ingle **T**hrow
UMTS	**U**niversal **M**obile **T**elecommunication **S**ystem
WLAN	**W**ireless **L**ocal **A**rea **N**etwork
WiMAX	**W**ireless **I**nteroperability for **M**icrowave **A**ccess

Chapter 1

Introduction

1.1 Motivation

In the last few decades the Telecoms business market has seen a great economic growth due to the incredible technological development that it has been subject. It is responsible for new tendencies and vices, has influenced new habits and expanded the capability but also the necessity for connectivity between people, companies and the Internet.

In a world that gets more digital each day, the access to information has become imperative. The importance of being connected has grown exponentially and there's more and more the need for automation and control of the environment. The Internet of Things [1] takes shape and requires a large develop and implementation of infrastructures, capable of supporting the growing streams of data that crosses the new generation networks. These new requirements for bandwidth arise from the increasing number of devices and sensors that monitor and act on the world.

Besides the technological challenges, an environmental friendly mindset has been noticed given the expansion of electronic devices. In that sense the research for lighter, smaller, with lower power consumption and preferably self-sufficient, this is, able to reuse energy, electronic components and devices, has been of great importance. Development is being held, based on alternative materials, less damaging to the surrounding environment, and with sophisticated integration and miniaturization techniques.

The range of wireless communication technologies that have emerged in the last two decades is immense. And nowadays the tendency is to study new methods of integration and interoperability between devices. Figure 1.1 shows a generic smartphone, a very common wireless communication device nowadays, and lists some of the different radio frequency systems it has to aggregate in itself.

FIGURE 1.1: Generic mobile device

The electronics for wireless devices are being designed in the perspective of shrinking and group multiple functions in one single IC (Integrated Circuit), also the software and firmware on the processing units are being developed to be faster and less energy consuming. But besides streamlining the electronics and processing techniques, one can do improvements in the radio interface, namely in the antennas.

There is already different solutions to address the interoperability capacity of the antennas. From multi-band antennas to wideband and ultra-wideband antennas, a lot of approaches have been presented in the past years. However, this type of antennas have some disadvantages. Multi-band antennas are not versatile, they're dificult to design and not always present a good performance for all the bands, besides, most of them ain't very small, which can arouse size concerns. Ultra wideband antennas can cover very large frequency bandwidths with semingly performance, however this performance isn't good for any particular band, which leads to low to moderate gains and they're also quite large.

Another way to achieve versatility is with the application of reconfigurable antennas; these allow reducing the number of antennas present in a given device, ensuring the

interoperability between systems. But this can also be integrated in more complex systems such as MIMO (Multiple-Input Multiple-Output) and/or cognitive radio systems, also known as SDR (Software Defined Radio).

Reconfigurability allows an antenna to adapt in real time different parameters like the resonant frequency, the polarization or even the radiation pattern to some extent. These are extremely useful features for mobile devices when considering the expansion of the different communication systems in the near future. As seen in Figure 1.1, an illustration of a generic mobile terminal and the wireless communication interfaces currently required.

Given the versatility and advantages these antennas can provide for new wireless devices, these have been subject of much attention in the investigation field in the past few years and there are already many different solutions presented to acquire different reconfigurability to different systems.

Reconfigurability can be achieved with resource to electronic components such as varactors, RF (Radio Frequency) switches or PIN (P-Intrinsic-N) diodes, which allow modifying the current flow on the structures and so changing the resonating frequency. Another recent approach is with the use of MEMS (Micro Electro Mechanic Switches). This solution is rather complex, and difficult to model and especially very difficult to execute, because these kind of structures are, still nowadays, somewhat difficult to build.

Another important factor to take in account in antenna engineering these days, especially when designing antennas for mobile devices, is their sizes. Antenna miniaturization is a long time subject of study in antenna engineering, however, there are always new developments and updates of the literature in this aspect. Much due to the constant demand for ever-smaller structures, which allow the construction of ever more compact equipment, without compromising too much the gain and radiation pattern of the same.

1.2 Objectives

The purpose of the work being developed based on this MSc dissertation is to design a printed antenna for mobile communication devices, which should be reconfigurable in frequency and have the smallest form factor possible. It should work properly in the

most common communication frequency bands used these days, such as GSM (Global System for Mobile Communication), UMTS (Universal Mobile Telecommunication System), WLAN (Wireless Local Area Networks) and LTE (Long Term Evolution).

During the course of development it's required to study a few methods to miniaturize the antenna and obtain reconfigurability, and to choose the best ones to accomplish the requirements of possible applications for the antenna while being able to build a prototype.

1.3 Document Organization

This dissertation is organized as follows. As seen, in the first chapter, an introduction and framework for the work developed is presented. Along with some examples of related work, and that was studied in order to step forward in the development of this thesis.

The second chapter shows the basic concepts of antennas, particularly, printed monopoles. Some examples of printed monopoles are explored, and their basic characteristics are presented and discussed.

The third chapter introduces the miniaturization techniques. The state of the art on this matter is presented, followed by two miniaturized printed monopoles that were developed to study some of the existing techniques.

In the fourth chapter reconfigurable antennas are presented. Some possible techniques for antenna reconfigurability are presented, followed by an ideal and a real implementation of a reconfigurable printed monopole for UMTS, WLAN and LTE.

In the fifth chapter the techniques explored in the previous chapters are combined, to create very small reocnfigurable printed monopoles. A first solution is an inverted L-monopole, and a second solution, even smaller, is a C-monopole.

The sixth and last chapter presents the conclusions and proposes some future work possibilities based on the work developed so far.

1.4 Author Contributions

[1] - Ricardo Gonçalves, Pedro Pinho, Nuno B. Carvalho. Compact Frequency Reconfigurable Printed Monopole, *Submitted to International Journal of Antennas and Propagation.*

[2] - Ricardo Gonçalves, Pedro Pinho. Antena Impressa Reconfigurável de Pequena Dimensão para Dispositivos Móveis, *Submitted to 6° Congresso do Comité Português da URSI*

Chapter 2

Printed antennas

2.1 Introduction

An antenna is an essential device in every existing radio frequency system. It is responsible for converting the electrical current in electromagnetic waves and vice-versa, responsible for interfacing the electrical system and a non-guided propagation environment, usually the air.

Printed antennas have been the subject of much research and development through the last thirty years, since they became popular in the late 70s. However, the origins of this kind of antenna back to the year of 1953, when G.A. Deschamps proposed the first microstrip antenna [2].

Printed antennas are widely used in microwave systems nowadays, especially in devices with physical dimension constraints, since these have a few advantages that make them very good candidates for applications that require low profile and lightweight antennas and a surface adaptable structure. They're also easy to fabricate, through common electronic printed circuit board methods, and easy to install, which means low production costs. Moreover, they are very versatile in terms of resonance frequency, radiation pattern, and adjustment of input impedance.

The main disadvantages of these types of antennas are: low operation power, narrow bandwidths, low efficiency and gain, and low polarization purity. Although there are

several techniques to improve these characteristics, that should be used to enhance the most of the antenna features regarding the requirements for a given application.

2.2 Basic concepts

Figure 2.1 shows an example of a printed antenna. This consists essentially of a very thin conductive material, usually copper, deposited over a dielectric material, at a distance h of the ground plane, which is a large deployment of the same conductive material.

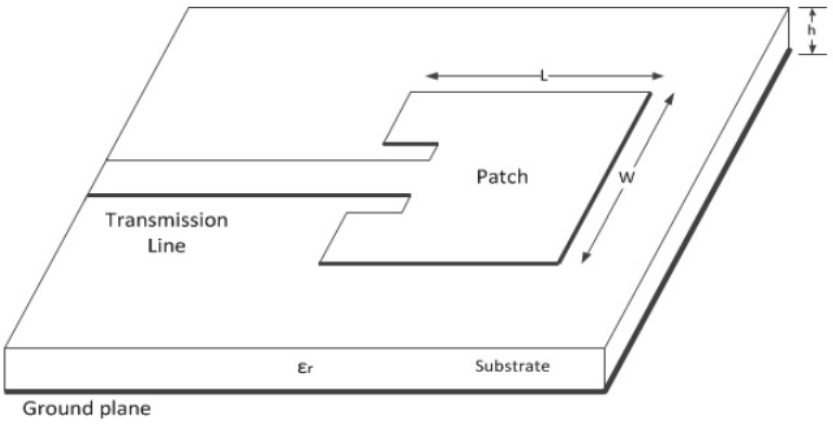

FIGURE 2.1: Patch antenna example

The electrical and mechanical characteristics of the dielectric surface, commonly known as the substrate, have a great influence in the antenna behavior and radiation characteristics. The thickness of the dielectric (h) influences the propagation of surface waves, resulting in a higher bandwidth antenna for thicker substrates at the expense of lower efficiencies. The relative permittivity of the material also influences the radiation. Lower values of dielectric constant allow more space and leakage waves, which is rather preferable for radiation concerns, whereas highest values of permittivity generate more guided waves, which are better suited for printed transmission lines.

There are lots of different geometries to create a printed antenna, in Figure 2.2 is shown some examples that are usually found.

To feed these antennas four different methods can be considered. Its possible to feed with a printed transmission line, as in Figure 2.1, through a coax cable, proximity-coupled feed or aperture-coupled feed. It is not a main issue of this thesis to discuss the feeding methods, in that sense, more information about feeding techniques for printed

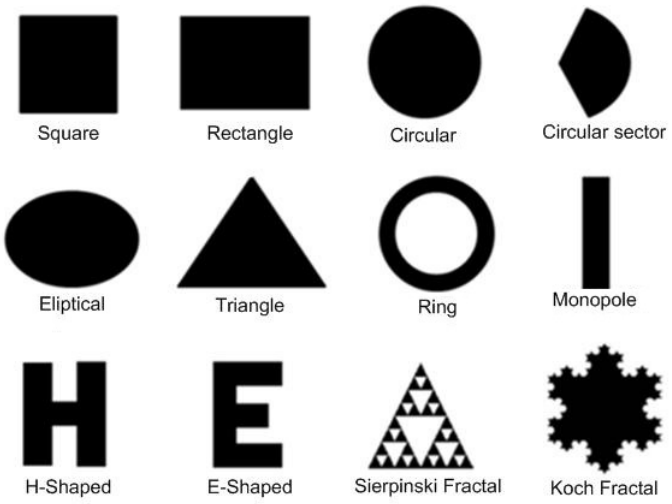

FIGURE 2.2: Patch antenna types [3]

antennas can be found at [4]. However more information regarding printed transmission lines, which were mainly used in these studies, can be found further in this document in appendix A.

2.3 Monopoles

A monopole is a type of antenna that has a lot of practical applications. This is essentially built of one single conducting arm of length L upon a conducting plane. To understand the monopole, first we should review the basic concepts of the dipoles, especially the $L = \lambda/2$ dipoles.

According to [4], the radiated power can be calculated with the expression (2.1) which can be obtained from the power density of the antenna.

$$P_{rad} = \eta \frac{|I_0|^2}{8\pi} \{C + \ln 2\pi - C_i(2\pi)\} \tag{2.1}$$

Where I_0 is the source current, C is a constant of value $C = 0.5772, \eta$ is the efficiency, and $C_i(x)$ can be obtained from expression (2.2).

$$C_i(x) = \int_{\infty}^{x} \frac{\cos y}{y} dy \tag{2.2}$$

The radiation intensity can be written as in expression (2.3), which leads to a maximum directivity of the half-wavelength dipole, as seen in (2.4).

$$U = \eta \frac{|I_0|^2}{8\pi^2} \sin^3 \theta \tag{2.3}$$

$$D_0 = 4\pi \frac{U_{max}}{P_{rad}} = 4\pi \frac{U|_{\theta=\frac{\pi}{2}}}{P_{rad}} = 1.643 \tag{2.4}$$

The typical input impedance of a half-wavelength dipole is around $Z_{in} = 73 + j42.5$, thus to eliminate the complex part of the impedance (the reactance), the dipole is shortened, so the first resonance is obtained with a dipole of length $L = 0.47\lambda$ to $L = 0.48\lambda$. This leads the input impedance to take the value of the radiation resistance, which according to [4] can be obtained from expression (2.5).

$$R_r = \frac{2P_{rad}}{|I_0|^2} = \frac{\eta}{4\pi}\{C + \ln 2\pi - C_i(2\pi) = 73\Omega \tag{2.5}$$

Based on the image theory, which is rather complex and is not the purpose of this document to describe it (further details can be obtained at [4]), a monopole structure with half the length of the dipole, will have twice the value of maximum directivity and half the value of the input impedance.

$$Z_{in(monopole)} = \frac{1}{2} Z_{in(dipole)} = 36.5 + j21.25\Omega \tag{2.6}$$

When considering the design of a dipole or monopole, usually, the input impedance is given and so the first step is to determine the length of the element. It's shown in [5] that one can determine the length easily following a few steps as shown in (2.7) and (2.8). First let G be defined as

$$\begin{aligned} G_{dipole} &= \frac{kL}{2} \\ G_{monopole} &= kL \end{aligned} \tag{2.7}$$

Where k is the angular wavenumber ($k = \omega\sqrt{\mu\varepsilon} = \frac{2\pi}{\lambda}$). So the input resistance of the dipole can be computed as

$$\begin{cases} R_{in} = 20G^2, & 0 < L < \lambda/4 \\ R_{in} = 24.7G^{2.5}, & \lambda/4 < L < \lambda/2 \\ R_{in} = 11.14G^{4.17}, & \lambda/2 < L < 0.6366\lambda \end{cases} \tag{2.8}$$

Whilst the input impedance for the monopole is, of course, half of this values.

As an example, to calculate a rough measure for the length of a monopole with characteristic impedance of 50 Ω, a resonating frequency of 1 GHz and considering the air as the environment, the monopole will be slightly longer than $\lambda/4$, according to (2.9) and (2.10).

$$G_{monopole} = \sqrt[2.5]{\frac{R_{in}}{12.35}} = 1.75 \tag{2.9}$$

$$G_{monopole} = kL \Leftrightarrow L = \frac{G_{monopole}}{\frac{2\pi}{\lambda}} = 0.278\lambda \tag{2.10}$$

Having studied the printed antennas and the common monopoles, it's shown in the following sections a few approaches to printed monopole antennas that were simulated and evaluated. It is presented a few descriptions of each, with the view to select the best candidate to the final prototype of the reconfigurable antenna.

2.3.1 Printed simple monopole

In order to get acquainted with the software tools for this project, a first attempt was made to design a simple printed monopole, that could work in the WLAN lower band. In order to do so, an appropriate substrate must be selected. In this case, the choice was based on the material availability, so that prototypes could be produced without much more expense.

The selected substrate was Arlon CuClad 217 [6], with dieletric (ϵ_r) of 2.17, tangent loss (δ) of 0.0009 and 0.787 mm height. Which is not the best option of all, since the dielectric and height are quite low. An higher dielectric constant and thicker substrate would allow for smaller and slimmer feeding lines, but would also result in higher return losses, and so would be harder to size.

For simulation purposes, the selected conductor was an infinitely thin copper padding with a conductivity of 5.8×10^7 S/m.

The simple monopole is an arm, of approximately a quarter of wavelength, of conductive material deposited upon a dielectric material, as it is shown in Figure 2.3.

For this example, the width of monopole is the same as the feeding transmission line. The transmission line is a quarter wavelength transformer, designed to adapt the input

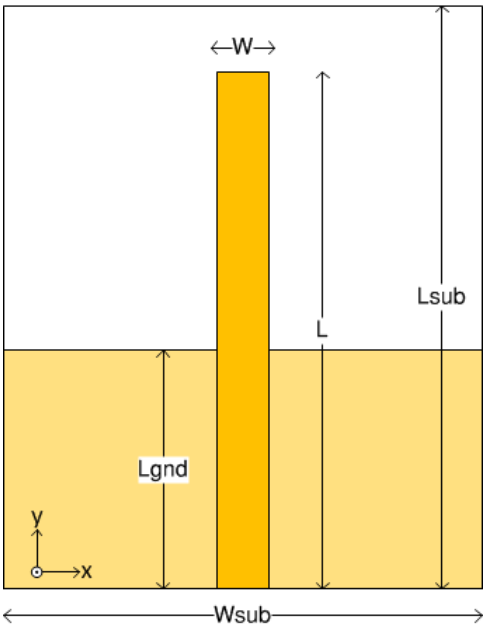

FIGURE 2.3: Simple monopole model.

impedance of the monopole to 50 Ω. More information about printed transmission line can be found in appendix A and in [7]. The dimensions considered to this design are present in Table 2.1.

TABLE 2.1: Printed line monopole dimensions.

Parameter	**Value [mm]**
L0	37.475
W0	3.35
Lgnd	13.775
Lsub	45.00
Wsub	33.5

The impedance response of the antenna, can be analysed in order to verify the diferent resonant frequencies of a given antenna. An antenna resonate at every frequency where the resistance achieves a relative maximum value and the reactance has a sudden slope. The impedance response for this monopole can be seen in Figure 2.4. From the graphic analysis, the resonating frequency is achieved at around 2.49 GHz.

In order to evaluate the bandwidth of the antenna, the return loss at the entrance of the system can be observed. The return loss is the relation between the power that is injected in the antenna and the power reflected by it. The feeding system is usually designed to 50 Ω impedance, if the antenna is perfectly matched to this impedance value, then the power injected is all radiated and none is reflected, which means no return loss.

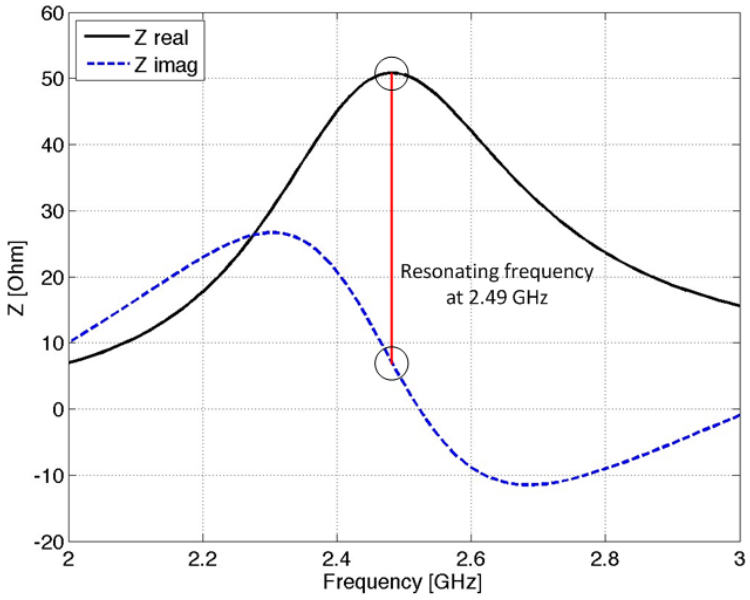

FIGURE 2.4: Impedance of the printed simple monopole.

However, an antenna can only be approximately matched to this impedance, at one frequency.

From the impedance graphic in Figure 2.4 one can see that very close to the resonating frequency, there's a point at 2.52 GHz where the resistance (impedance's real part) is very close to 50 Ω while the reactance (impedance's imaginary) is practically 0. At this point is where the return loss (S_{11} parameter) will be lowest. The bandwidth of the antenna can be extracted from this parameter as the set of frequencies that satisfies the condition $S_{11} < -10$ dB.

For this example, the simulated return loss, which is also the S11 parameter, can be observed in Figure 2.5.

The bandwidth is around 2.35 to 2.75 GHz, this is a 16% bandwidth, which is fairly good. Also, the purpose of covering the WLAN and LTE 2.6 bands was fulfilled.

The radiation pattern of this printed monopole has an omnidirectional characteristic. The simulated radiation pattern is presented in Figure 2.6. It presents a radiation efficiency of 93%, however, the small area of the antenna, and the proximity of the ground plane to the radiator, results in a small gain of 1.5 dBi[1].

[1]The radiation patterns are in linear scale

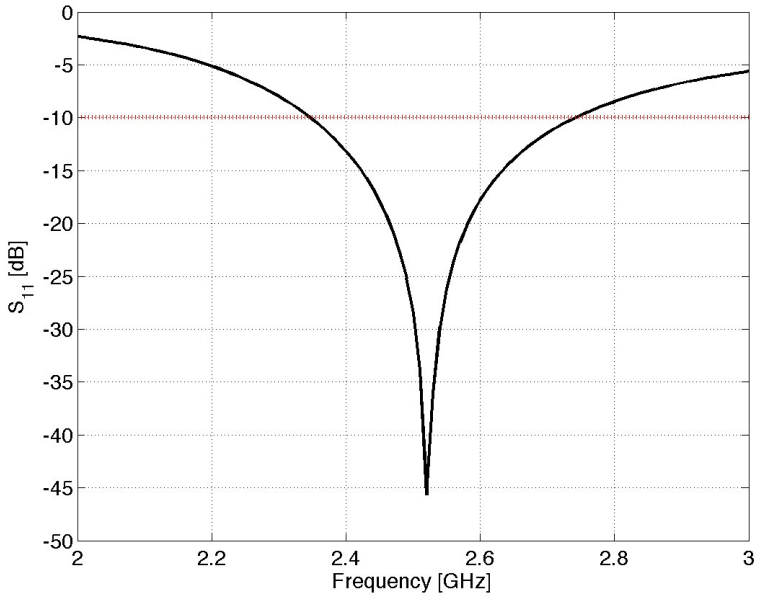

FIGURE 2.5: Return loss of the printed simple monopole.

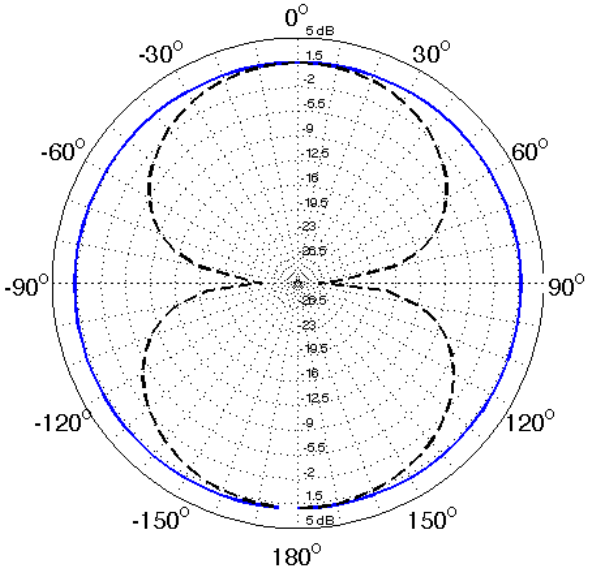

FIGURE 2.6: Radiation pattern of the simple monopole on YZ plane (dashed) and XZ plane (solid).

2.3.2 Printed L-monopole

The L-monopole is a common printed monopole antenna. Compared to the simple monopole, this one occupies a smaller area due to the curved arm. This model is presented here because it will serve as a base of comparison to another antenna presented further on this dissertation.

The design is presented in Figure 2.7 and the corresponding dimensions are found in Table 2.2. The area of this antenna is $14.0 \times 17.0\text{mm}^2$ while the total area of the antenna plus the feeding line and support structure is $30.0 \times 40.0\text{mm}^2$.

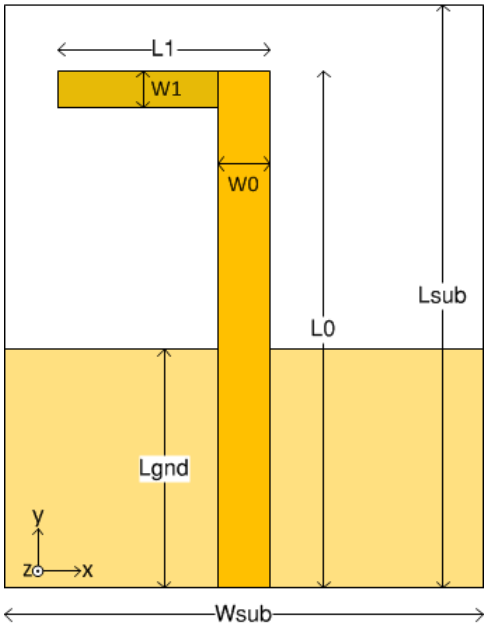

FIGURE 2.7: L monopole model.

TABLE 2.2: Printed L monopole dimensions.

Parameter	Value [mm]
L0	38.0
L1	14.0
W0	3.00
W1	2.00
Lgnd	21.0
Lsub	40.0
Wsub	30.0

This monopole was designed to work at the same frequency as the previous example. That can be proved by looking at the return loss response present in Figure 2.8.

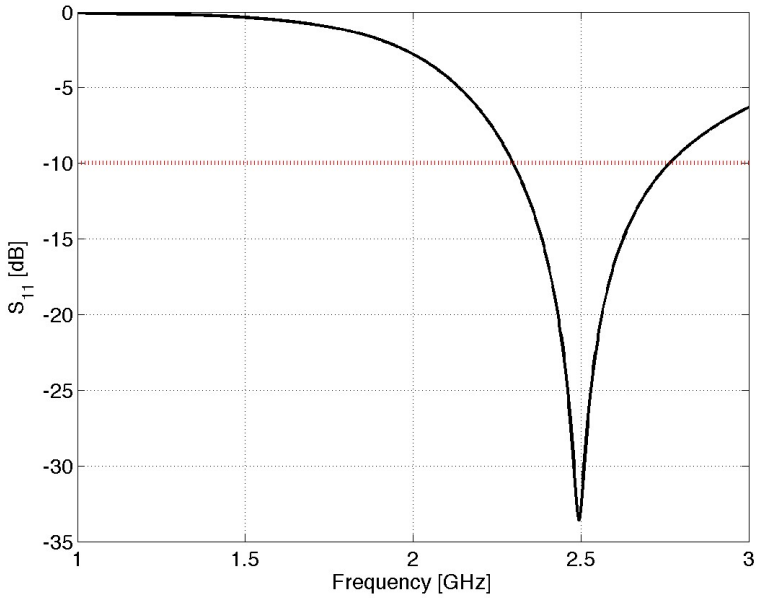

FIGURE 2.8: Return loss of the printed L monopole.

From the return loss plot one can extract the -10 dB bandwidth, which is closely 450 MHz, this means a 18% bandwidth. Which is slightly higher than the example shown in the previous section. The monopole arm bending, creates an increased impedance that can help explain this result. Watching the surface current distribution in Figure 2.9 one can see an accumulation of current in the corner, which is a result of the increased impedance.

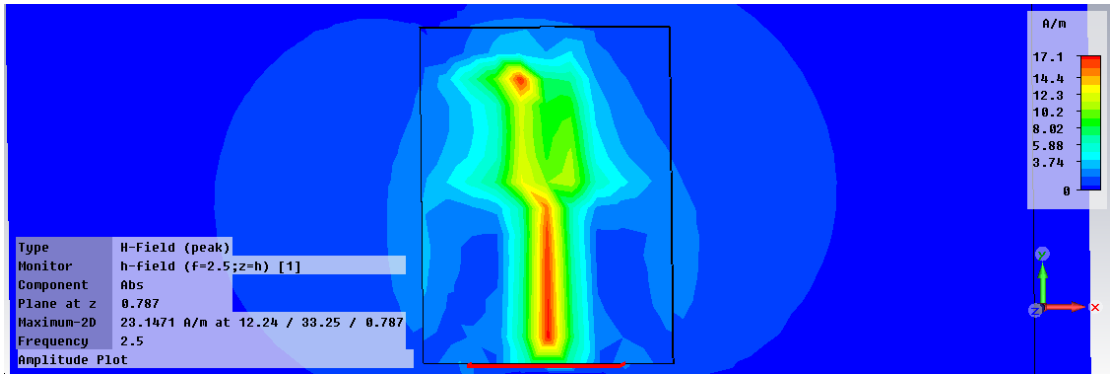

FIGURE 2.9: Surface current of the printed L monopole at 2.5 GHz.

The bended arm of the monopole has a very small effect on the radiation pattern and this presents an omnidirectional caractheristic like the previous example, as can be seen in Figure 2.10. However, the gain obtained by simulation for this monopole is higher than the simple monopole, in this case is 2.50 dBi, to a 99% radiation efficiency.

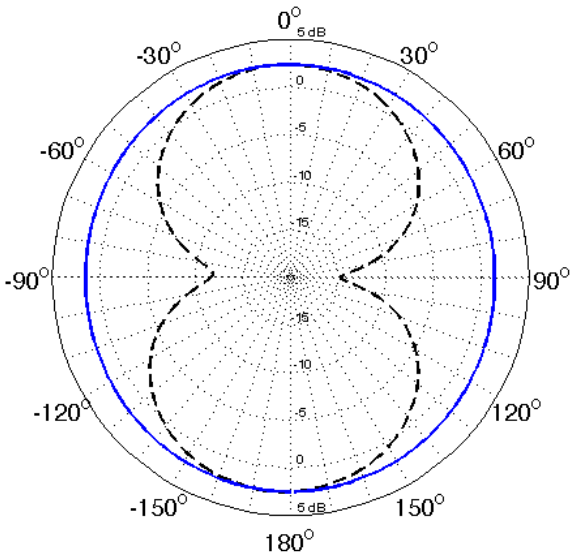

FIGURE 2.10: Radiation pattern of the L monopole on YZ plane (dashed) and XZ plane (solid).

2.3.3 Printed C-monopole

The C-Monopole is another common printed monopole antenna, that when compared to the previous example, has the advantage of having an even smaller form factor, although the electrical area of the antenna remaining the same. Two different C-monopoles of different lengths were designed for comparison, a shorter version and a longer version. The C-monopole is presented in Figure 2.11. Its dimensions can be found on Table 2.3.

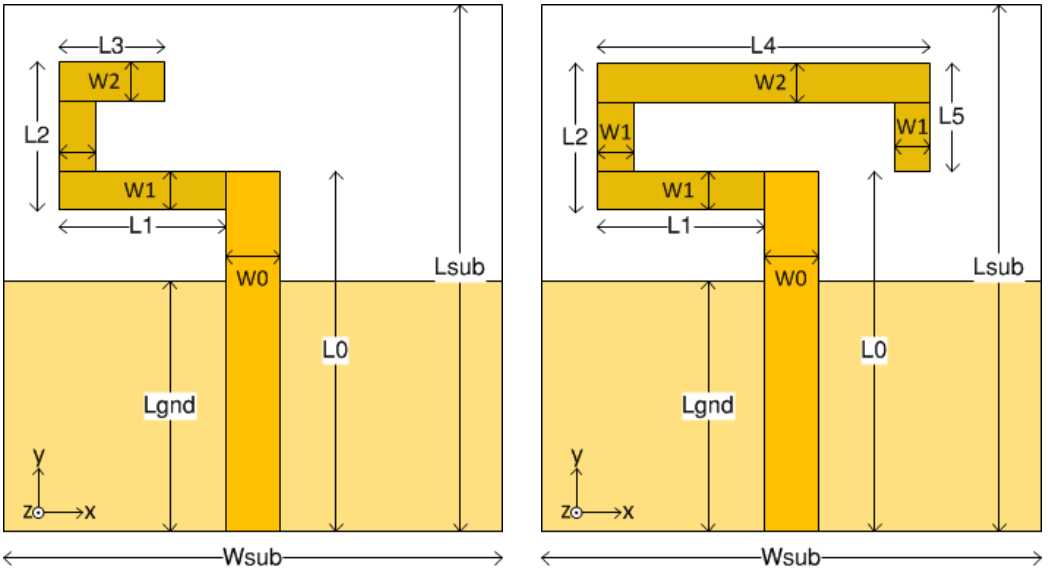

(a) (b)

FIGURE 2.11: C monopole models (a) short version, (b) long version.

TABLE 2.3: Printed C monopoles dimensions.

Parameter	**Value [mm]**
L0	24
L1	3.35
L2	6.0
L3	4.0
L4	13.6
L5	5.0
W0	3.35
W1	1.5
W2	2.0
Lgnd	21
Lsub	30
Wsub	20

Through the impedance response analysis, it is clear, that the resonating frequency is higher than the previous examples, and it is not intend to work with any common wireless technology, but it is particularly interesting in order to compare a few results, further on this document.

As the resonating frequency is not the same, the dimensions cannot be compared directly, but if we assume that the monopole has to have the same length, then the meanderline will result in a smaller overall volume of the antenna.

For the reasons already mentioned, the longer monopole will present a lower resonating frequency, and *vice-versa*, as can be seen in Figures 2.12 and 2.13, it is presented the impedance response for the longer and shorter version of the C-monopole respectively.

From the impedance response simulated for both monopoles, it is clear, that the longer version has resonating frequencies at 3.1 GHz and 5 GHz and the shorter version has a resonating frequency around 4.5 GHz and another one at 6.8 GHz.

The return loss of the given antenna is closely related to the impedance variation of the antenna, and the value is lower where the impedance is closest to a resistance of 50 Ω, and a reactance of 0 Ω. Which results, in the return loss, for both monopoles, present in Figure 2.14.

From the graphic present in Figure 2.14, it can be concluded that the longer monopole has a bandwidth of approximately between 3 to 3.4 GHz, as the shorter monopole has a bandwidth between 6.3 to 7 GHz. So far, the absolute bandwidth is very similar to the simple line monopole example, nevertheless mean lower ratios.

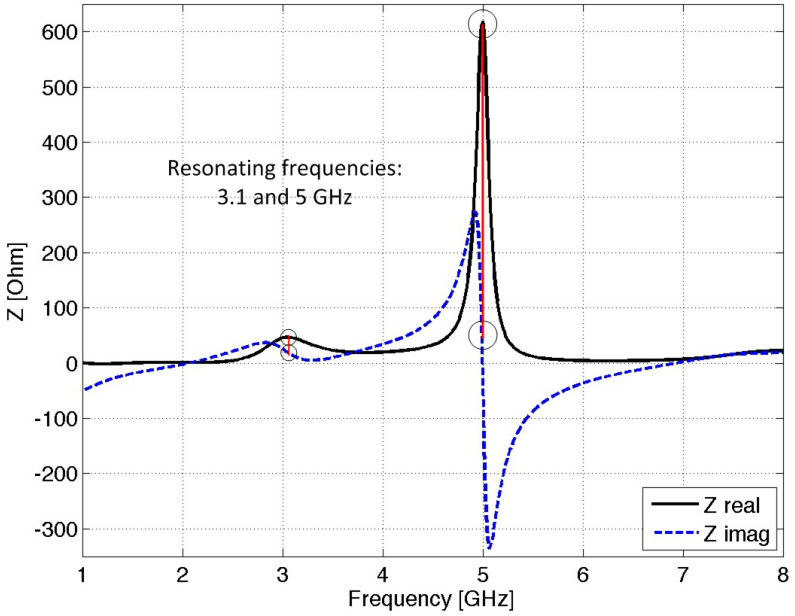

FIGURE 2.12: Impedance response of the longer C monopole.

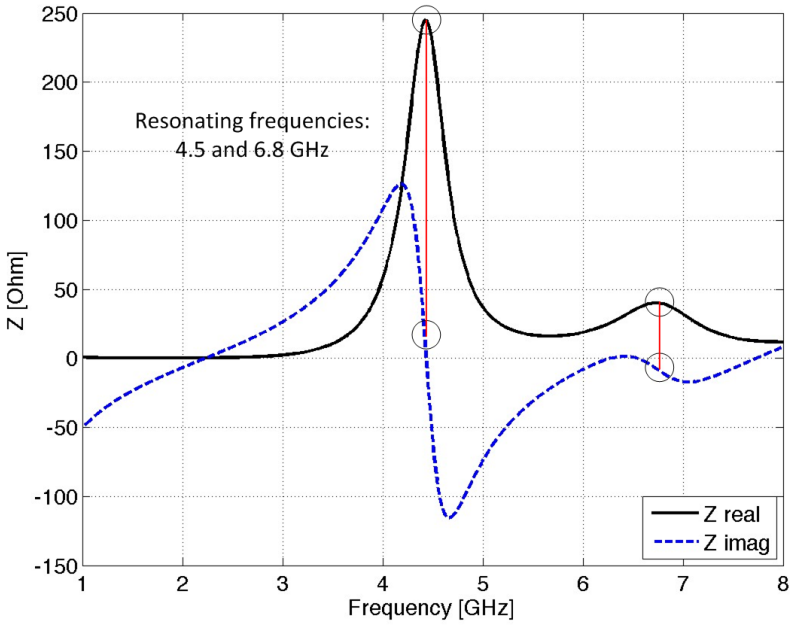

FIGURE 2.13: Impedance response of the shorter C monopole.

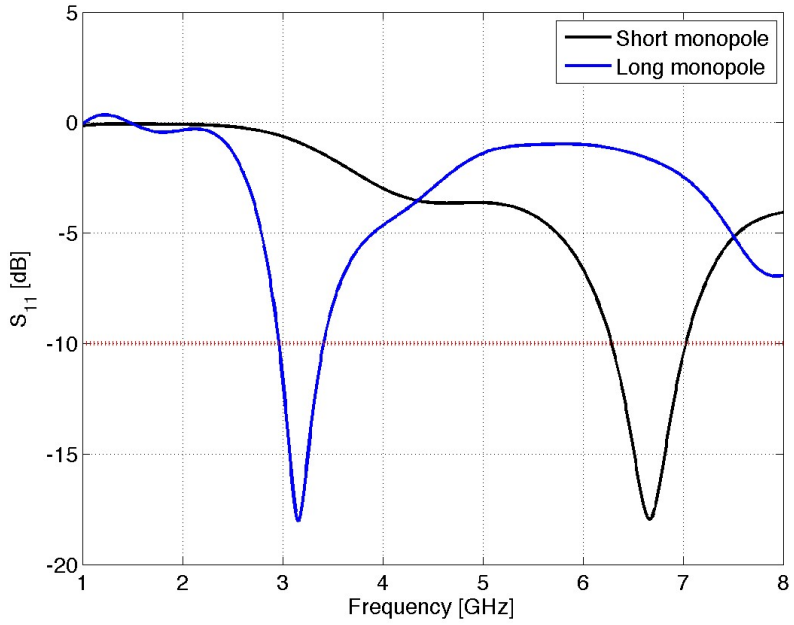

FIGURE 2.14: Return loss for both C-monopole examples.

The biggest issue about this monopole regards the radiation pattern. Which no longer presents a seemingly perfect 'donnut' shape, but instead, has an increased directivity through certain angles, as can be observed in Figure 2.15. This behaviour can occur due to different reasons, one of them being the size and proximitty of the ground plane to the radiator element, and also, because of the meanderline type structure.

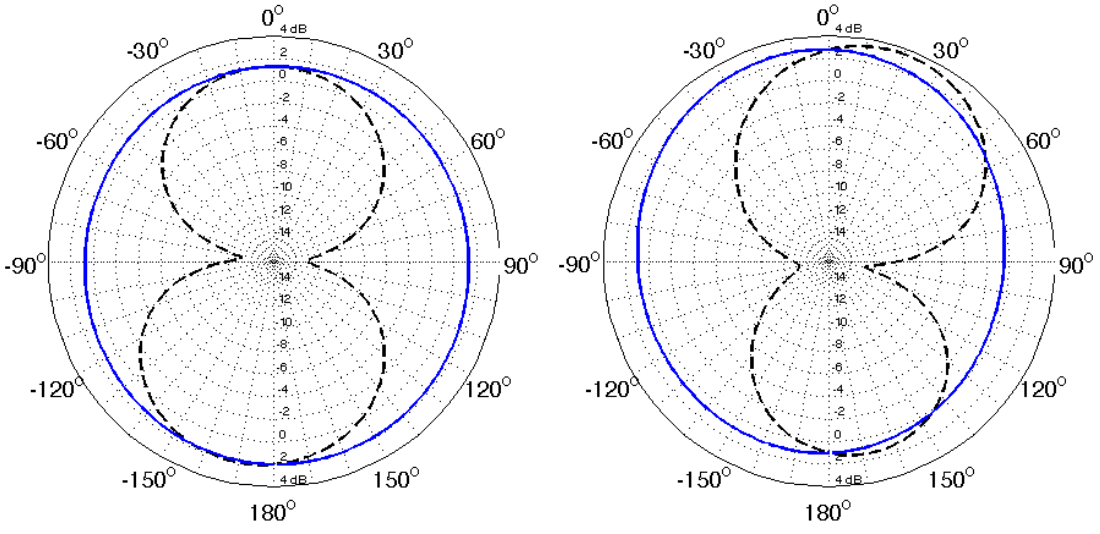

(a) (b)

FIGURE 2.15: Radiation pattern for both C monopoles on YZ plane (dashed) and XZ plane (solid) (a) longer version, (b) shorter version.

Chapter 3

Miniaturization

3.1 Introduction

Antenna miniaturization is a well documented research subject and which is regularly complemented with new techniques and new approaches to certain techniques, a few examples can be found at [8, 9]. This research is motivated by today's needs for more multifunctional systems that further drive the requirements for small mobile terminals, like cellphones, tablets, laptops, short and long-range communication devices, RFID (Radio Frequency Identification), GPS (Global Positioning System), etc.. These applications and the continuous growth of wireless devices will continue to support the search for smaller and compact antennas, that can present the same or even better performance.

In this chapter we intend to present some recent techniques applied in the field of antenna miniturization and in further sections, to explore it's applicability to printed monopoles for WLAN operation.

There are a lot of examples of techniques used for antenna miniaturization of different kinds of antennas for different kinds of applications that can be found in [10]. Also in printed antennas, an approach is presented in [11–13] in which pins are used to *chunt* patch antennas in a certain point, which results in a decrease in the resonating frequency of the first mode of operation. In [14, 15], metamaterials are used, in one approach an SRR (Split Ring Resonator) is used between the radiating element and the ground plane of a printed circular patch, on the second article a magneto-dielectric material is used as

substrate. Other examples are presented in [16–18], where fractal geometries are used, to reduce the size of printed antennas.

A recent approach was presented in [19, 20], where a chip inductor is used in order to reduce the resonating frequency of a printed monopoles, without changing the size and radiation characteristics and with minor losses to the radiating efficiency and gain. This is an interesting approach, since its quite simple to fabricate, and it's not very expensive. However, the use of the chip inductor reduces the overall bandwidth of the antenna.

3.2 Definition of small antennas

Wheeler [21] proposed the ESA (Electrically Small Antenna) definition has an antenna whose maximum dimension is smaller than $\lambda/2\pi$, known as the radianlength. Another equivalent and more commonly used definition for ESAs, is presented in [8], is an antenna that satisfies the condition

$$ka < 0.5 \tag{3.1}$$

where k is the wavenumber $(2\pi/\lambda)$, and a is the radius of the minimum size sphere that encloses the antenna (see Figure 3.1). That enclosure sphere can be refered as *Chu Sphere*.

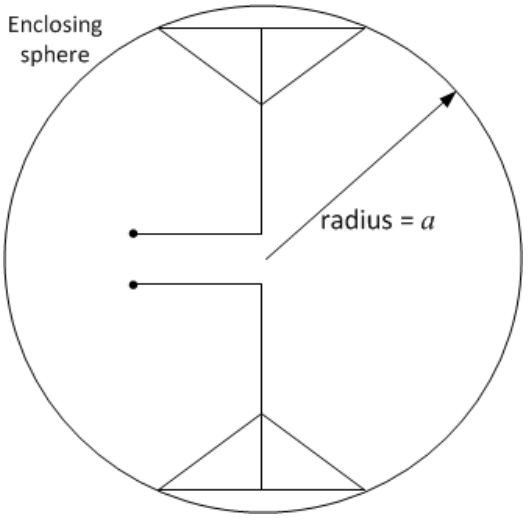

FIGURE 3.1: *Chu Sphere* of radius a.

The limitations of the small antennas were also studied by Wheeler [21], and the efficiency and bandwidth of an antenna are related to its radiation power factor. Wheeler

stated that an antenna within the size limit refered earlier can be made to behave as a lumped capacitor or inductor, and its radiation power factor, p_e or p_m can be represented as

$$p_e = \frac{G_e}{wC} \tag{3.2}$$

if it behaves as a capacitor, or

$$p_m = \frac{R_m}{wL} \tag{3.3}$$

if it behaves as an inductor. In (3.2) and (3.3), G_e is the radiation conductance in parallel with the antenna, R_m is the radiation resistance in series with the antenna, w is the radian frequency, C is antenna's capacitance and L is the antenna's inductance.

Limitations of small antenna were further investigated, stating that the limits of quality factor (Q) of an antenna are shown to be inversely proportional to the size of the antenna. In [22] the relation between the bandwidth and Q factor of an antenna is presented as

$$B = \frac{1}{Q} \tag{3.4}$$

This equation is relatively accurate for $Q \gg 1$. When $Q < 2$ the result ain't so precise, however the relationship is maintained.

The Q factor of a given antenna, according to [23], can be determined by equation 3.5.

$$Q(w_0) = \frac{2\sqrt{\beta}}{FBW_v(w_0)} \tag{3.5}$$

where

$$FBW_v = \frac{w_+ - w_-}{w_0} \tag{3.6}$$

$$\sqrt{\beta} = \frac{s-1}{2\sqrt{s}} \tag{3.7}$$

In which s is the maximum VSWR criterion, w_+, w_- and w_0 are the higher and lower frequency bounds and the antenna central frequency respectively. From the same source, it is presented an approximation to calculate the quality factor lower bound as

$$Q_{lb} = \left[\frac{1}{(ka)^3} + \frac{1}{ka}\right]\eta_r \tag{3.8}$$

From the previous equations it is clear that the smaller the antenna is, the higher the quality factor gets. Which means that the smaller the antenna is, the narrower the bandwidth it will have. And, although the quality factor can be reduced, by introducing losses to the antenna, the radiation efficiency will suffer from that. This leads to a clear trade-off between the antenna miniaturization and its radiation performance. This expressions are used further in order to prove the effectiveness of the proposed miniaturization methods.

The following sections are dedicated to the study of miniturization techniques for printed monopoles. The application of a shorting pin to miniaturize a simple monopole and the application of a chip inductor to miniaturize a C-monopole. Both models are compared to the monopoles presented in the previous chapter.

3.3 Shorting pin miniaturization

There are a few examples for antenna miniaturization, that are achieved by pinning a microstrip antenna to ground in a certain spot. By grounding the microstrip antenna, the current flowing through the patch on that point is changed, and so is the global impedance response. This gives the ilusion that the patch is bigger around that section which leads to a decrease in the resonating frequency.

In this section, this technique was used to try to miniaturize a printed monopole antenna. However the results were not very satisfactory, as it will be clear further on. The proposed design in presented in Figure 3.2, the dimensions are presented in Table 3.1. The design is a simple line monopole, placed on top of the substrate, with the ground plane on the bottom. The pin, is a filled copper wire, of 0.6mm diameter, on the edge of the monopole arm, that connects to the ground plane on the bottom side by a slim chunt connection,as shown in Figure 3.2.

TABLE 3.1: Miniaturized monopole with shorting pin dimensions

Parameter	**Value [mm]**
L0	18.5
W0	1.5
Lgnd	10.0
Lsub	19.5
Wsub	9.0

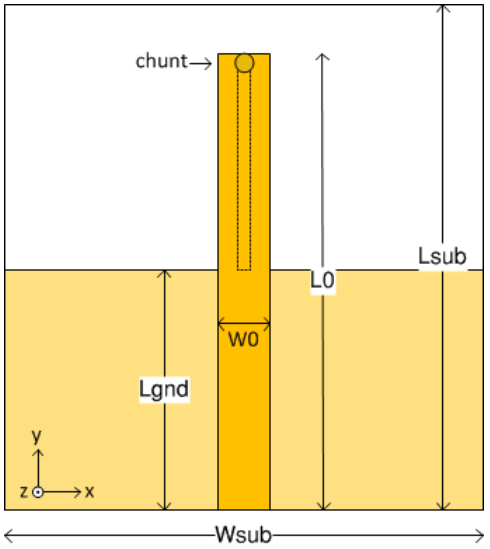

FIGURE 3.2: Miniaturized monopole with shorting pin.

The application of this shorting pin technique effectively reduce the size of the antenna. Since this monopole is shorter than the monopole presented in the previous chapter and still resonates at around 2.5 GHz. That is clear by the impedance response presented in Figure 3.3.

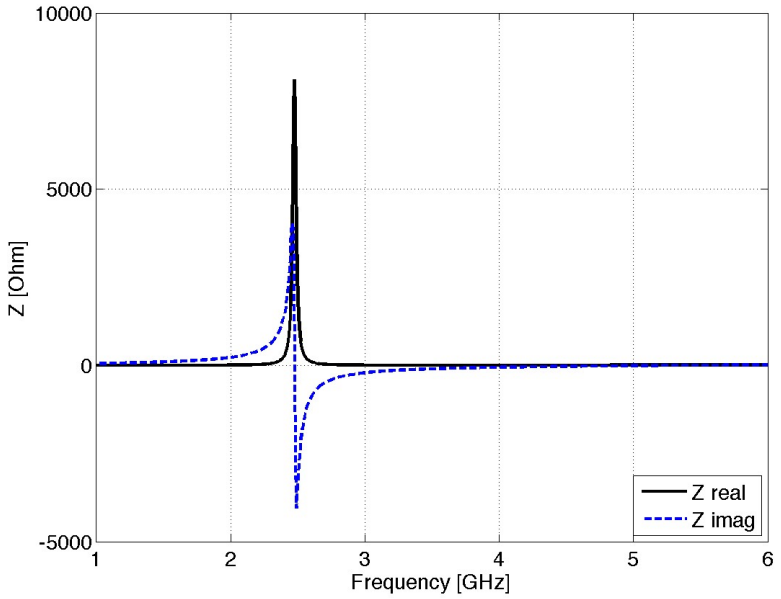

FIGURE 3.3: Impedance for shorting pin miniaturized monopole.

However, the impedance match is very bad. The resistance is extremely high, and it is nearly impossible to match this antenna to 50 Ω, whatever the method chosen. It is than irrelevant to check the return loss in this case, since the impedance match is not very

good, the return loss will of course show high values, rendering this antenna unusable for this application. Even if with some more elaborate matching circuit, it would be possible to match the entrance impedance to 50 Ω, the low gains, shown in Figure 3.4, dictate the unsuccess of this technique when applied to printed monopoles.

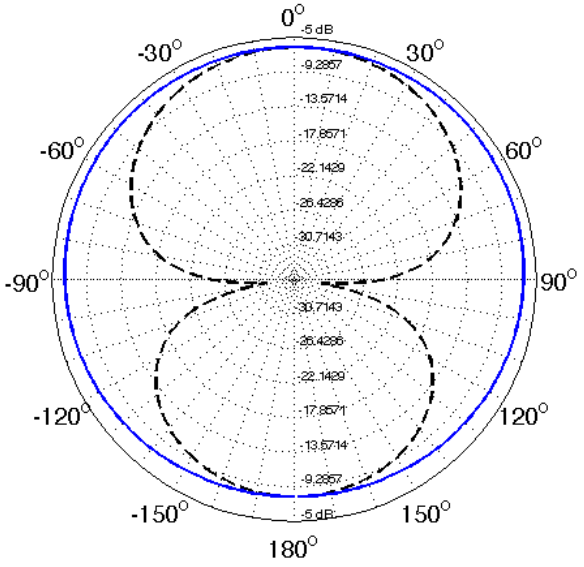

FIGURE 3.4: Radiation pattern for shorting pin miniaturized monopole on YZ plane (dashed) and XZ plane (solid).

3.4 Chip inductor miniaturization

As shown in the introduction of this chapter, one recent approach to antenna miniturization was achieved by introducing a chip inductor in the antenna. As the previous technique, this is a very interesting solution due to its simplicity and low cost. In this section, it is pretended to further investigate this technique, by applying the same concept to a printed monopole. The results are then compared to the simple structures presented in the previous chapter, and this knowledge is further used for other applications.

3.4.1 Simulation model

The chosen inductor for this application was the 0402HP series from Coilcraft© [24]. According to the datasheet, the lumped-element frequency dependent behavior, can be emulated by the following circuit in Figure 3.5.

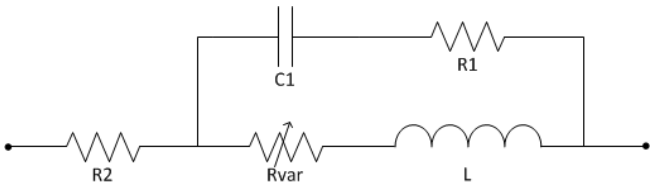

FIGURE 3.5: Lumped-element equivalent circuit of the chip inductor.

It is a series and parallel of resistances, capacitors and inductors. According to the datasheet, the variable resistance R_{VAR} has a relationship with frequency as follows

$$R_{VAR} = k \times \sqrt{f} \tag{3.9}$$

where k is a constant, and f is the frequency in Hertz. The values for the diferent elements of the equivalent circuit and also for k are given by the manufacturer and are present in the datasheet. It is important to have present that this equivalent circuit and its values are only valid from 1 MHz to an upper frequency that depends on the component value.

By resolving the above ciruit, the total impedance is given by

$$Z = R_2 + \frac{(R_1 - j/\omega C_1)(R_{VAR} + j\omega L)}{(R_1 + R_{VAR}) + j(\omega L - 1/\omega C_1)} \tag{3.10}$$

Although possible, this circuit can be quite difficult to introduce in the EM (Electro Magnetic) simulation software. To ease the antenna simulation process, the previous circuit can be simplified to the one presented in Figure 3.6.

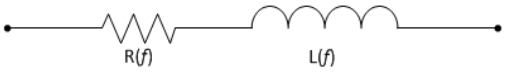

FIGURE 3.6: Lumped-element simplified circuit of the chip inductor.

This can be introduced in the EM software simulation as a lumped element, or a RLC boundary. The resistance and inductance of this equivalent circuit are frequency variable, due to the R_{VAR} of the original circuit. Resolving the impedance of both circuits,

the values of $R(f)$ and $L(f)$ can be defined as

$$R(f) = \frac{E \times A + D \times B}{A^2 + B^2} + R_2 \tag{3.11}$$

$$L(f) = \frac{D \times A - B \times (R_1 R_{VAR} + L/C_1)}{\omega \times (A^2 + B^2)} \tag{3.12}$$

where

$$\begin{aligned} A &= R_1 + R_{var} \\ B &= \omega \times L + \frac{1}{\omega} \times C_1 \\ D &= \omega \times L \times R_1 - \frac{R_{var}}{\omega} \times C_1 \\ E &= R_1 \times R_{var} \\ \omega &= 2\pi \times f \\ R_{VAR} &= k \times \sqrt{f} \end{aligned} \tag{3.13}$$

Being this values frequency dependent, the variation in the operating frequency will change the parasitic values of this component. The values of the equivalent circuit components are presented in the datasheet, but they depend on the inductors series number, a table with the values for the 0402HP series can be found on Appendix B. Still, given that this values are all positive and similar, the response of the resistance and inductance with frequency will be somewhat the same for all of them. The $R(f)$ and $L(f)$ variation with frequency is shown in Figures 3.7.

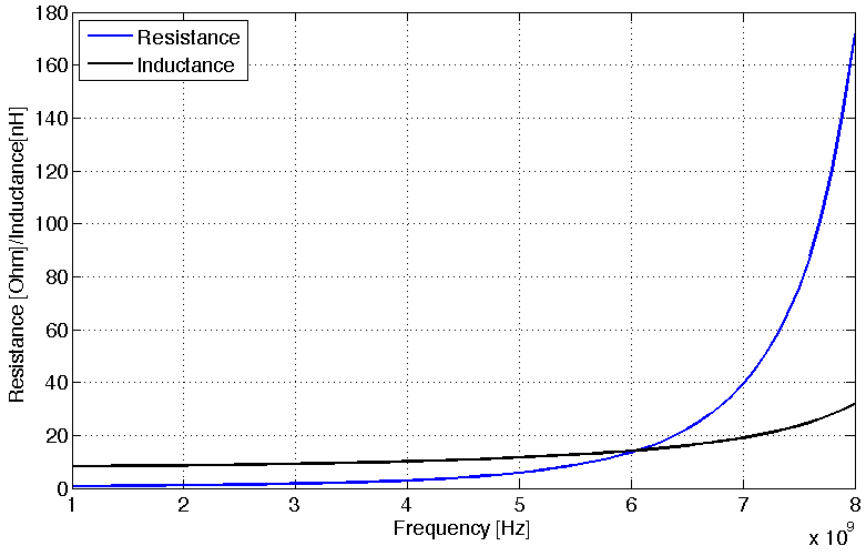

FIGURE 3.7: Variation of the chip inductor's resistance and inductance with frequency.

From the variation of the inductor parameters with frequency it is easy to see that the resistance for frequencies above 3 GHz increases significantly. While for the lowest frequencies, it's value is rather small, above 3 GHz it's value increases in such a way that can render unusable the application of this particular chip inductor on the antenna. Lower inductor values, will have less variation.

The variation of the inductance is also considerable, being the inductance very similar to the resistance variation. The resonating frequency of the antenna is largelly defined by the inductor, which means that these large variations on the inductor values can be a large source of error between simulated models and prototypes.

3.4.2 Antenna design

The proposed antenna is a C-monopole like the one in the previous chapter, with the chip inductor introduced in the middle of the left arm of the structure, as shown in Figure 3.8.

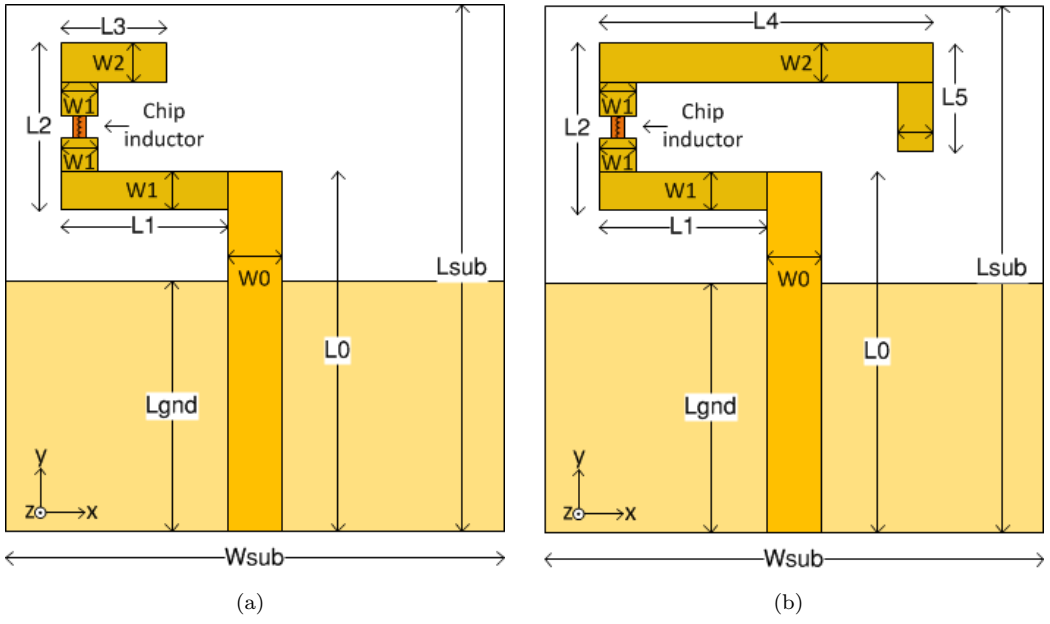

FIGURE 3.8: Miniaturized monopole with chip inductor (a) short version, (b) long version.

The dimensions of this antenna are exactly the same as the previous chapter model, with a narrower feeding line, to account for decrease in the resistance. The width of the feeding line for the miniaturized monopole was reduced to 2.8 mm. The chip inductor

used for this simulation was the 0402HP-20N, which according to the expressions in the previous section, can be emulated by a resistance of 5 Ω and a inductance of 24 nH.

The impedance response simulated for this antenna is shown in Figure 3.9. The resonating frequency in this case is around 1.85 GHz, which means a reduction of 2.6 GHz, or 59% of the resonating frequency, compared to the monopole without the chip inductor in the previous chapter.

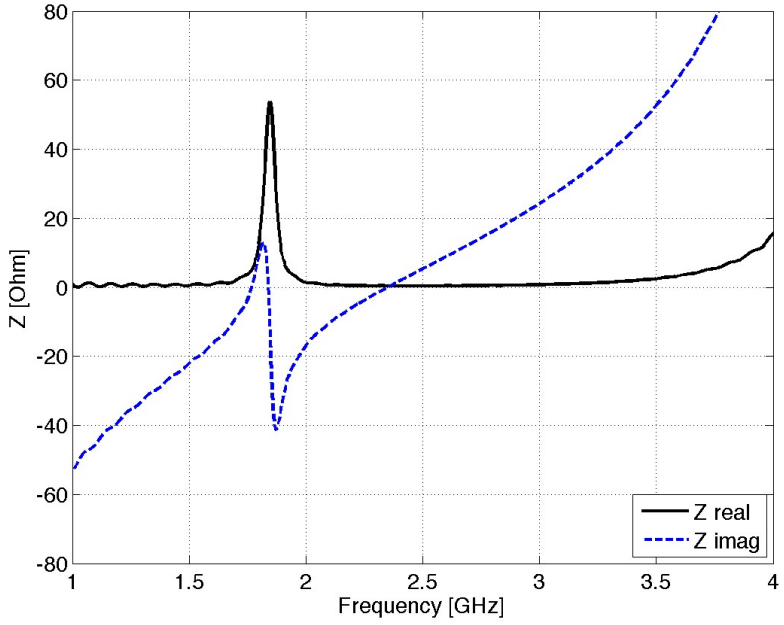

FIGURE 3.9: Impedance for the miniaturized short monopole.

From the impedance response, which has a much more abrupt response than the simple model, it's clear that the bandwidth is now narrower. The return loss present in Figure 3.10 can clarify that the obtained bandwidth is around 40 MHz, this is a bandwidht of 2.2%, a big reduction when compared to the simple monopole.

The resonating frequency of the antenna is mostly determined by the chip inductor itself. Otherwise, the longer monopole would allow for a similar reduction in frequency, as the example shown in section 3.4.2, but that is not the case. Although the stretching of the monopole allows for a lower resonating frequency, the scale is not the same. That can be observed in the impedance response of the longer monopole, present in Figure 3.11.

In this case, the resonating frequency occurs at 1.35 GHz, which means 500 MHz less than the shorter version. Whilst the monopole presented in the previous chapter had

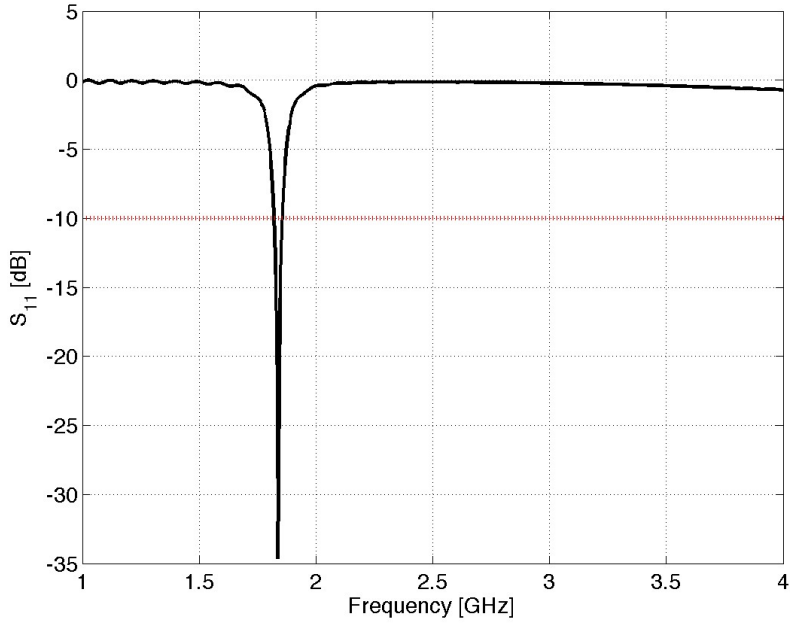

FIGURE 3.10: Return loss for the miniaturized short monopole.

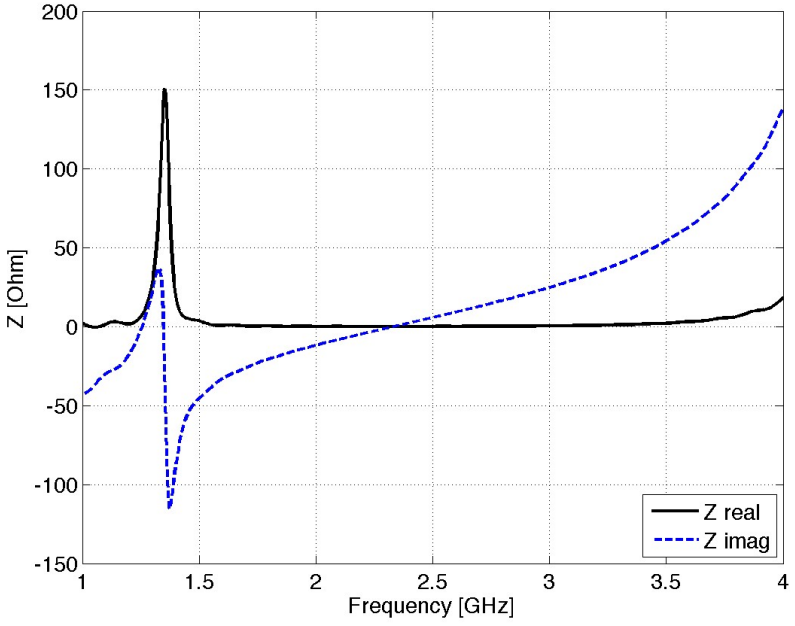

FIGURE 3.11: Impedance for the miniaturized long monopole.

a difference of 1.4 GHz between versions. Moreover, the impedance response is also severely influenced by the introduction of the chip inductor. While the monopole in section 2.3.3 had a similar impedance response for the shorter and the longer version, although slightly different, in this case, when comparing both impedance responses from Figures 3.9 and 3.11, it's clear that the impedance is increased significantly in the longer version.

These facts mean that the size/frequency reduction depends on different factors, and it's not a constant value dependant solomnly on the inductor.

The value of the inductor change the resistance and reactance response, as is shown in Figure 3.12. This effect also affects the bandwidth, the higher the inductor value, the tighter the impedance response is, which means narrower bandwidths. Which means that it can play a big role in the tunning of the monopole.

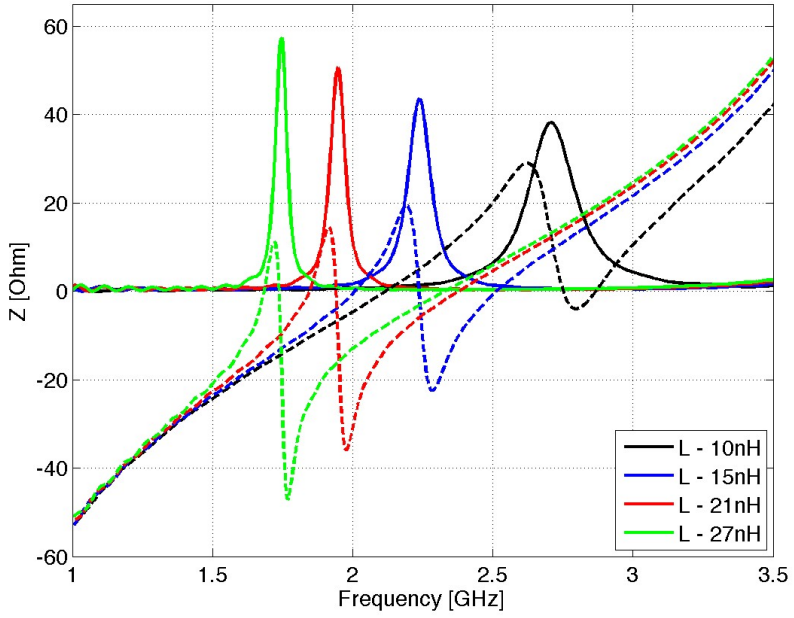

FIGURE 3.12: Simulated impedance of chip inductance sweep for the miniaturized monopole.

Like the inductor value, the position also changes the impedance response and hence the frequency. The inductor was dislocated along the left arm of the monopole, as indicated in Figure 3.13 by x milimeters.

The resulting impedance response of the position sweep are shown in Figure 3.14. The frequency shift can be explained by the difference in the antenna length, between the

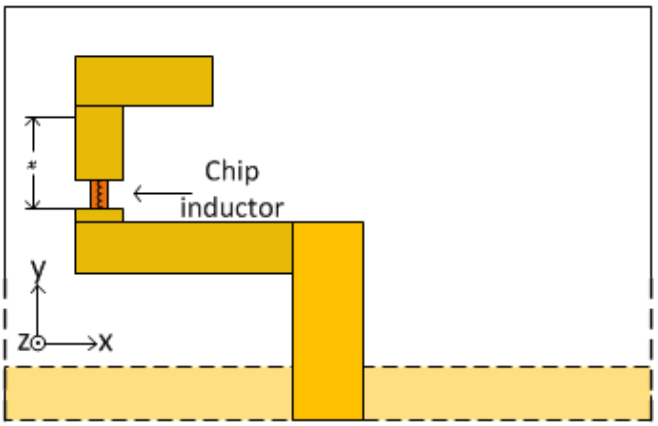

FIGURE 3.13: Chip inductor sweep ilustration.

entrance and the inductor position. However, there's also the changes in the resistance and reactance, the impedance absolut value decreases as x increases, and at some point the best impedance match can be found.

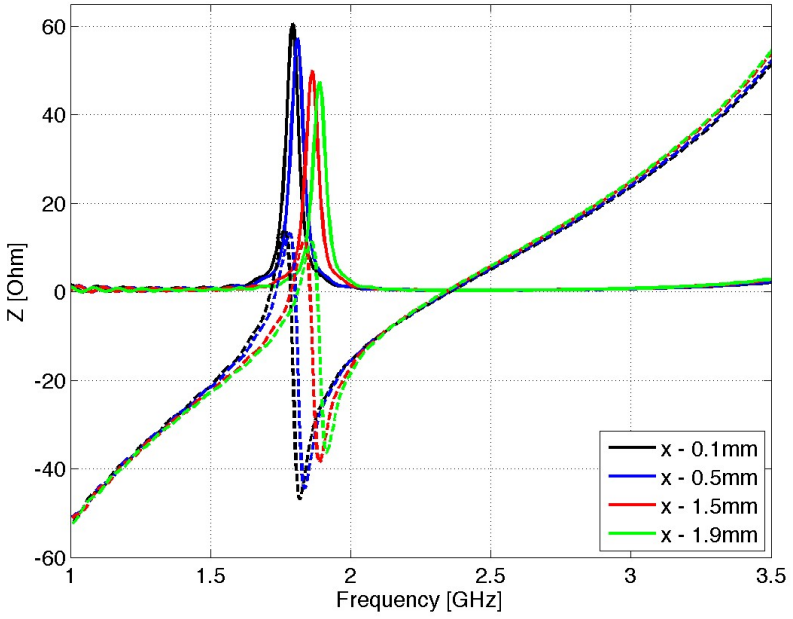

FIGURE 3.14: Simulated impedance of chip inductor's position sweep for the miniaturized monopole.

Another way to understant the influence of the chip inductor on the antenna resonance and overall performance is to watch the surface current for both monopoles. In Figure 3.15 the surface current for both C-monopoles is presented, and one can see that it is more intense near the chip inductor, when compared to the rest of the monopole sections. Which, once again, leads to the conclusion that the chip inductor is the main responsible for the resonant frequency of the antenna.

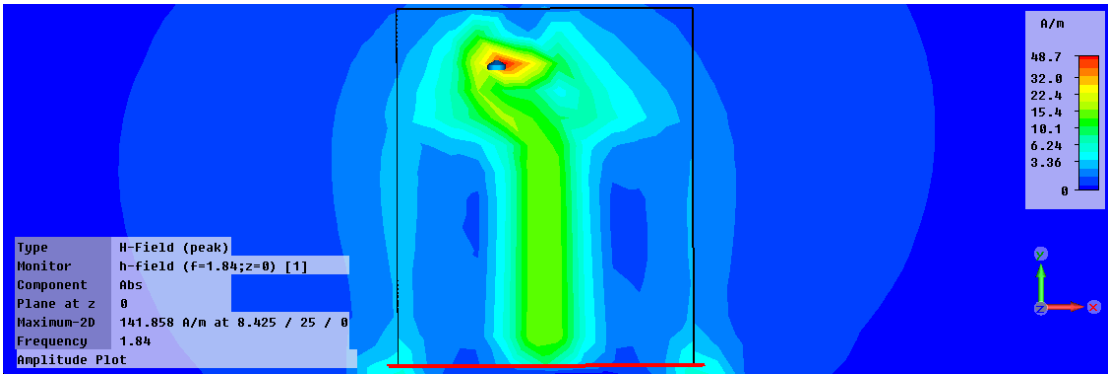

(a)

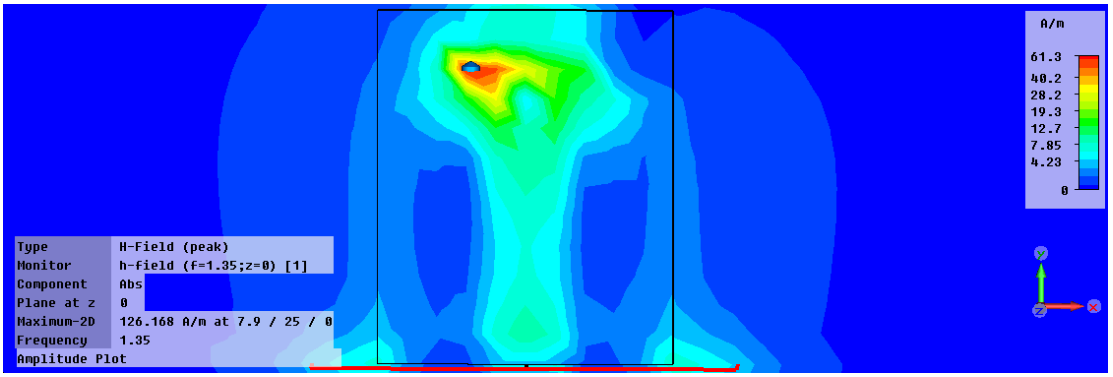

(b)

FIGURE 3.15: Simulated surface current for the miniaturized monopole (a) short version, (b) long version.

Albeit the bandwidth, the radiation efficiency also suffers a considerable loss, to 33% for the shorter version and 22% for the longer version, which are very low. However, the radiation pattern is barely the same, and a gain of 2.26 dBi and 2.15 dBi respectivelly, are just slightly lower that the simple monopole from section , as seen in Figure 3.16.

It was known, according to the literature, that the radiation characteristics would not be much affected, and it is proved by the small loss in the gain and equivalent radiation pattern. However, the large reduction in radiation efficiency goes against the information stated on the articles seen before. Losses associated with impedance match wouldn't have this effect, since the matching is rather good for the short version, in that, sense it's hard to explain or predict this behavior. This can be an effect of this particular geometry, but that's a long shot explanation.

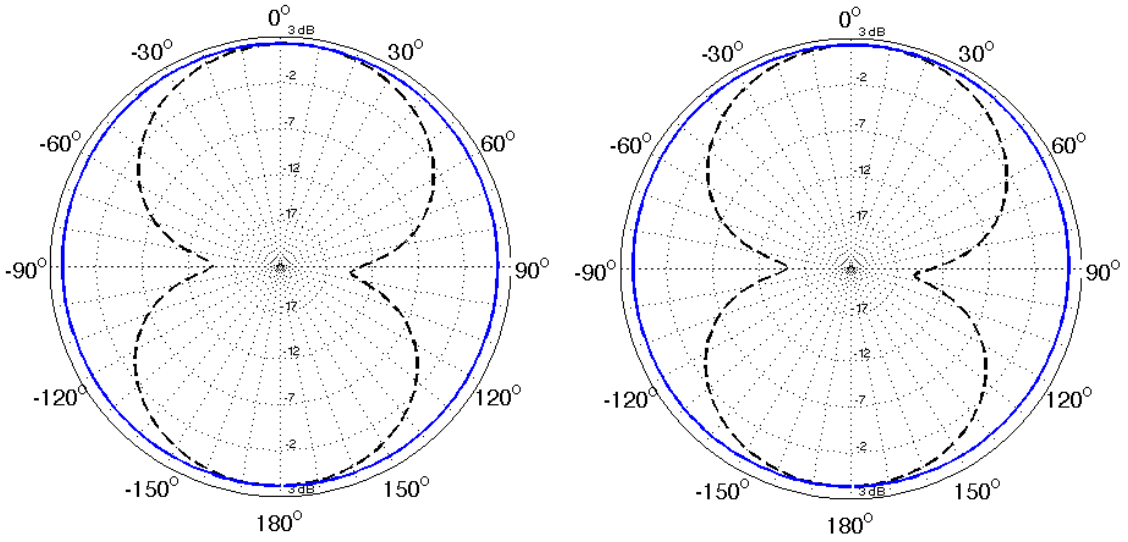

(a) (b)

FIGURE 3.16: Simulated radiation pattern for chip inductor miniaturized monopole on YZ plane (dashed) and XZ plane (solid) (a) shorter, (b) longer.

Following the expressions presented in section 3.2 the quality factor of the antennas was calculated for both monopoles. The *ka* relation was also determined in order to prove that these monopoles can be characterized as small antennas. The results are present in Table 3.2.

TABLE 3.2: Calculated Q factor for the C-monopoles.

Parameter	**Shorter**	**Longer**
Frequency (GHz)	1.85	1.35
a (mm)	6.1	8.6
k	38.75	28.3
ka	0.236	0.243
Radiation Efficiency (%)	33	22
Q_{lb}	26.5	16.2
Bandwidth (%)	2.0	3.1
Q	36	23

Chapter 4

Reconfigurability

4.1 Introduction

There are many different kinds of antennas that have been developed along the years. Each has his own benefits and disadvantages that make them better suited for certain kinds of applications. When considering a certain application, the antenna to choose must be carefully thought, because the characteristics of the antenna are fixed. Creating reconfigurable antennas, so that their behavior can adapt to the system requirements and transmission conditions, brings more versatility and enhances functionality of wireless equipment.

Reconfigurable antennas can possibly reduce the number of needed antennas in wireless equipment, which is a very important feature for mobile terminals such as smartphones, laptops and tablets nowadays, but they can also be used for more complex tasks, such as being able to increase the throughput, reduce errors and noise, and increase security. [8]

In this work, more attention is given towards reconfigurable printed antennas. However there's lots of work around other kinds of antennas, such as aperture, traveling wave, slot and others that can be found in several publications and books [8, 25, 26].

4.2 Reconfigurability in antennas

Reconfigurability is the ability for an antenna to change its operation characteristics, either by electrical, mechanical, electromechanical or other ways. This means that the simple signal phase shift of array elements to achieve the beam redirection is not considered reconfigurability, because the antenna operation remains the same.

So a reconfigurable antenna must be able to change, independently, one or more of the following parameters: resonant frequency, bandwidth, radiation pattern and polarization.

There are several techniques that have been studied in order to achieve reconfigurability in antennas. In [27] one approach is presented, in this solution a group of printed antennas, with different resonant frequencies, are displaced upon a circular section that can be rotated by the means of a stepper motor. This solution is a simple approach, however, can become expensive and is big and heavy, due to the usage of a motor. Besides, the different antennas are printed very close to each other, which lead to coupling effects between them. Another possibility is to use MEMS, which is a good solution and have been subject to several studies and attempts, as seen in [28], in which a frequency reconfigurable PIFA antenna for tri-band operation is presented, in this case, MEMS are used to connect and disconnet certain elements of ground plane, changing its operating mode. In [29–31] other examples on creating frequency reconfigurable antennas are presented. Another good reference on this subject can be found at [32], in which a compilation of some applications using MEMS are presented, in this case, mechanical and capacitive MEMS are used to create frequency or polarization reconfigurability and also to create phased arrays. Although MEMS can be a good solution, regarding it's adaptability and good behavioral response, this are hard to model and can be quite dificult to fabricate and hence become expensive.

There's also the active AMC (Artificial Magnetic Conductor) solution, as presented in [33], this is an interesting solution, but still hard to model, and it has a certain volume, which is not indicated for applications with space constraints.

Among others, there is also the possibility to use PIN diodes. These can be used, so as the MEMS, to connect or disconnect certain elements of a given antenna, and thus change its shape. Many solutions are presented in the literature, as in [34] where PIN

diodes are used in between slots cutted on the antenna, ir order to null some of them, and this way grant a frequency change of the antenna. In [35] a MIMO antenna for dual-band operation is presented. This is achieved with PIN diodes, that can actively change the shape of the elements of the antenna, transforming C-monopoles on inverted F-monopoles and thus change the resonating frequency.

Frequency reconfigurability is well documented and some good examples can be found at [36–40]. But, besides the frequency reconfigurability, polarization and radiation pattern reconfigurability may also be achieved using PIN diodes. Two versatile solutions are presented in [41, 42], in which reconfigurable antennas using PIN diodes, capable of changing its radiation pattern and its frequency, are presented. In what concerns polarization reconfigurability, in [43–45] two approaches for obtaining polarization diversity with PIN diodes are presented. A radiation pattern reconfigurable antenna can also be found in [46].

There are many different PIN diodes that are easily found on market, with different characteristics and in many different package configurations, besides, they're usually non-expensive. In that sense, PIN diodes are a very versatile component, that allows very adaptable solutions. This kind of antennas are also quite easy to fabricate.

4.3 PIN diodes

In order to use PIN diodes in antennas their electrical characteristics must be addressed first. This components have very specific operating characteristics, that make them widelly used in RF systems. Although they're also used as keys in low frequency and digital electronics and have also been used in optics as photodetectors.

A PIN diode is a silicon semiconductor consisting of a layer of intrinsic (high resistivity) material of finite area and thickness which is contained between highly doped P and N type material, as shown in Figure 4.1.

The characteristic of this type of components that make them so viable for so many applications, its his response to the bias current. A PIN diode acts like a current controled resistor, the more current that it is injected through the I region, the lower the resistance at RF frequencies. Because of this particular behavior the PIN diode can

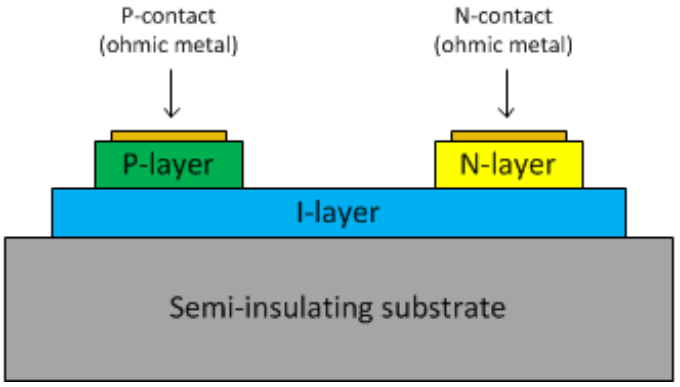

FIGURE 4.1: Example of PIN diode stacking.

be applied in different ways for RF circuits and applications. When the forward bias control current of the PIN diode is varied continuously, it can be used for attenuating, leveling, and amplitude modulating an RF signal. When the control current is switched on and off, or in discrete steps, the device can be used for switching, pulse modulating, and phase shifting an RF signal [47].

4.3.1 Simulation model

According to [47], when the diode is forward biased, holes and electrons are injected into the I-region. This charge does not recombine instantaneously, but has a finite lifetime (τ) in the I-region. This results in a quantity of stored charges Q which reduces the resistance (R_S) of the I-region, and thus the diode behaves like a current controled resistance. If the PIN diode is reverse biased, there is no stored charge in the I-region and the device behaves like a capacitance (C_T) shunted by a parallel resistance (R_P).

The schematic of the component and the equivalent circuits, for the diode 'ON' and 'OFF' state, are presented in Figures 4.2 and 4.3 respectively.

The equivalent circuit for the forward biased PIN diode, Figure 4.2 (b), consists of a series combination of the series resistance (R_s) and a small inductance (L_s). R_s is a function of the forward bias current (I_f) and this function, although with sligth differences between manufacturers, is essentially as the one presented in Figure 4.4. L_s depends on the geometrical properties of the package such as metal pin length and diameter. L_s is a small parasitic element with little to no effect for frequencies below 1 GHz. Which means, that at RF frequencies or microwave frequencies, this small parasitic value, can, and probably will, affect the circuit or antenna behavior.

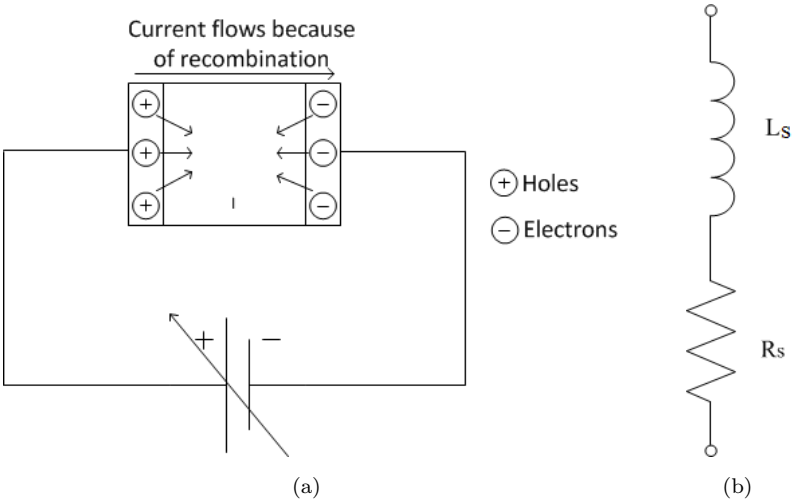

FIGURE 4.2: Forward bias model: (a) Carriers flux, (b) Equivalent circuit.

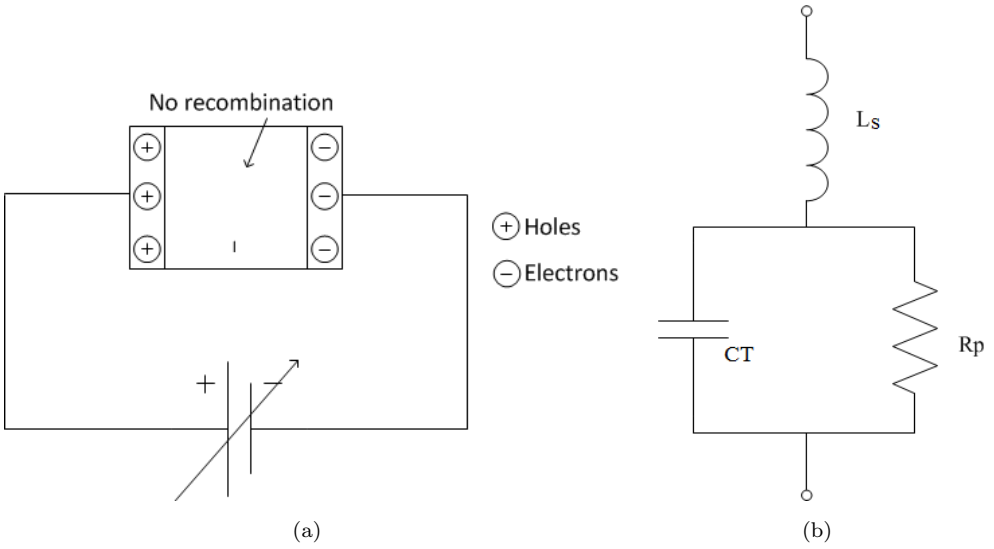

FIGURE 4.3: Reversed bias model: (a) Carriers flux, (b) Equivalent circuit.

This response is useful, for instance, in low distortion attenuators and amplitude modulator applications. The R_s vs I_f relationship is described as

$$R_s = \frac{W^2}{(\mu_n + \mu_p).I_f.\tau} \quad [\Omega] \tag{4.1}$$

where W is the width of the intrinsic region, μ_n and μ_p are the electron and holes mobility, I_f is the forward bias current and τ is the carrier lifetime.

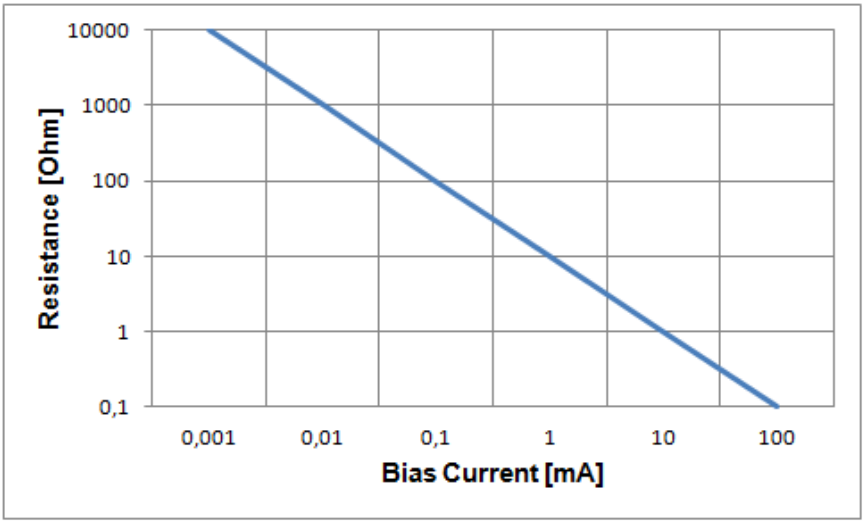

FIGURE 4.4: Example of PIN diode RF resistance response.

The reversed bias equivalent circuit consists of the diode capacitance (C_T), a shunt loss element (R_p) and again the parasitic inductance (L_s). C_T can be expressed as

$$C_T = \frac{\epsilon A}{W} \tag{4.2}$$

where ϵ is the dielectric of the silicon, A is the junction area and W is the intrinsic zone width. This expression is valid for frequencies above the dielectric relaxation frequency of the I-region, i.e.

$$f > \frac{1}{2\pi\rho\epsilon} \tag{4.3}$$

where ρ is the silicon resistivity.

C_T decreases from 0 V to the "punch-through" voltage from where it remains constant to the increase in the reverse bias voltage (V_r). This is different from the common PN-junction diode, where the capacitance vs voltage behavior continuosly varies out to the breakdown voltage (VBr). This makes the PIN diode easier to impedance match, because of its flat C_T vs V_r characteristic. R_p is minimum at 0 V and increases to a fixed value as V_r increases.

The upper cutoff frequency for the PIN diode can be defined as the frequency at which L_s resonates with the average value of C_T. The lower cutoff frequency is defined by the

carrier lifetime (τ) as shown in 4.4 according to [48].

$$f_c = \frac{1}{2\pi\tau} \tag{4.4}$$

For frequencies lower than f_c and DC, the PIN diode behaves like a PN junction diode, this is, the incident RF signal will be rectified and distorted. Just below and just above f_c frequencies, it behaves like a linear resistance, but the equivalent circuit, although similar to those shown before, can reflect a stronhly inductive or strongly capacitive characteristic depending on the device design. Operation at this frequency ranges with moderate bias levels will result in large amounts of distortion. At frequencies much higher than f_c ($f > 10.f_c$) the diode behaves as a pure linear resistance, which can be controled by a DC current [47–49].

4.4 Reconfigurable printed monopole

In order to further investigate the printed reconfigurable antennas. A first approach was made by designing a printed monopole, which could work in two different frequency bands, namely between 2.4-2.7 GHz and 1.9 - 2.2 GHz, so that this could be used for UMTS, WLAN and LTE applications. For this first attempt, it was considered an ideal connector between the antenna elements, instead of any real component such as MEMS or PIN diodes.

4.4.1 Ideal model

The proposed monopole is presented in Figure 4.5, and the corresponding dimensions are in Table 4.1. As the previous models, this was build in an Arlon CuClad 217 [6] substrate.

From the design analysis, the proposed antenna is a square monopole, with a meanderline in order to reduce the substrate size needed and the second element is another square. This geometry was chosen and adapted, in order to allow the highest bandwidth possible, for a modestly small antenna. The monopole size is $18.3 \times 26.0\text{mm}^2$, whilst the total size of the structure is $40.0 \times 50.0\text{mm}^2$.

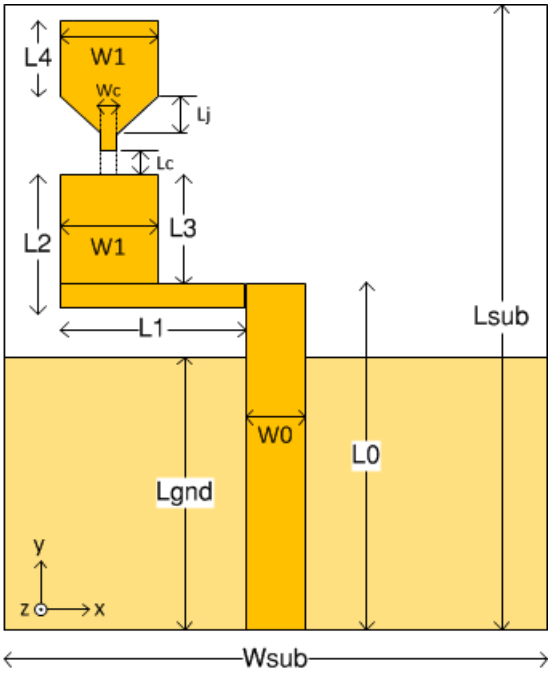

FIGURE 4.5: Ideal reconfigurable monopole.

TABLE 4.1: Printed ideal reconfigurable monopole dimensions.

Parameter	**Value [mm]**
L0	28.0
L1	15.0
L2	11.2
L3	7.7
L4	5.5
Lc	1.6
Lj	3.3
W0	3.1
W1	8.5
Wc	1.5
Lgnd	21
Lsub	50
Wsub	40

One of the challenges of this kind of design is the impedance match of the antenna. Since there is two different operating frequency bands, the width of the feeding line must be optimized in order to achieve a fairly good performance for both operating bands. Therefore, after balancing this issue, which led to the line width presented in the previous table, the simulated return loss obtained for this antenna can be viewed in Figure 4.6 and it is clear that the impedance matching is fair enough for both operating bands.

A better impedance matching is very dificult to perform, given the differences in the

obtained impedances for both modes. In Figure 4.7, the impedance response for both modes can be observed.

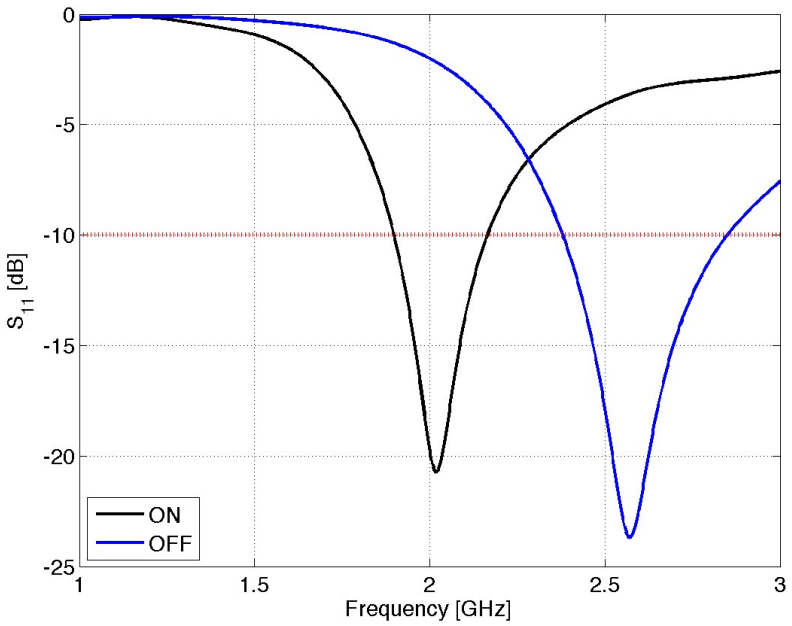

FIGURE 4.6: Simulated return loss for 'ON' state (black) and 'OFF' state (blue).

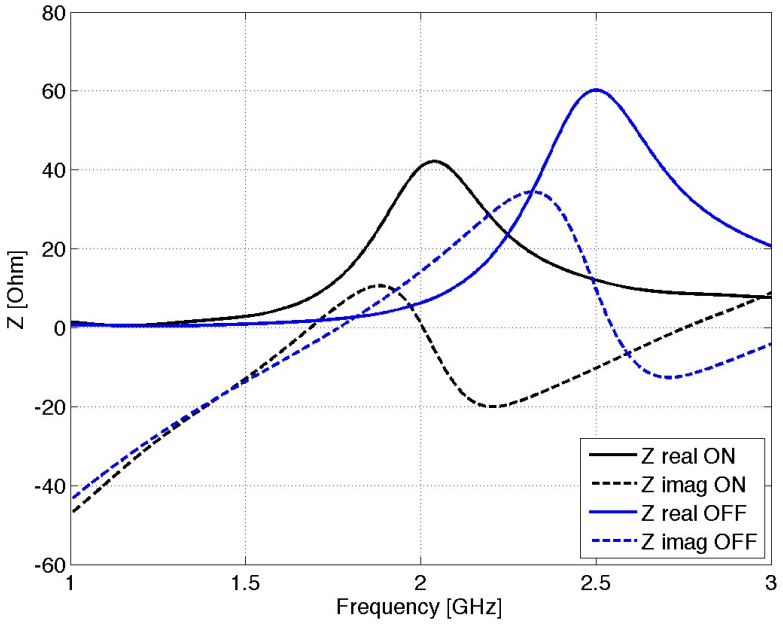

FIGURE 4.7: Simulated impedance for 'ON' state (black) and 'OFF' state (blue).

In the 'OFF' state, the real part of the impedance is around 60 Ω, while in the 'ON' state the real part is around 40 Ω, the imaginary part, this is the reactance, follows the

same course. Given the impedance matching method used, only the real part can be manipulated, but to achieve 50 Ω for both modes is impossible, since that would imply increasing the resistance in one mode and decreasing another.

Even so, simulation results are very good for the proposed design, and from the return loss it is clear that UMTS, WLAN and LTE operating frequency bands were achieved. This monopole was then prototyped, in order to compare results. The prototype is presented in Figure 4.8.

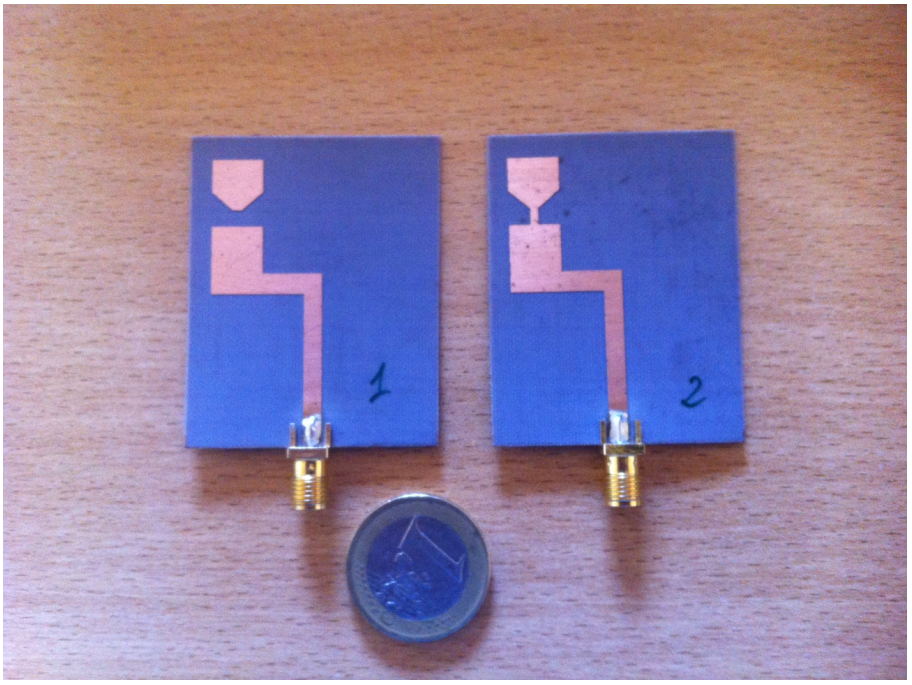

FIGURE 4.8: Prototype of ideal reconfigurable monopole.

The comparison between the simulated and measured return loss, for both states, can be observed in Figures 4.9 and 4.10.

The prototype shows some deviations regarding the operation frequencies, which might be due to the fabrication proccess. Still, the prototyped monopole shows a fairly good agreement with the simulated results. It has a bandwidth from 2-2.4 GHz when in 'ON' state, which means it is capable of working in the UMTS band, although only in the downlink band. Also, it has a bandwidth from 2.5-2.8 GHz, which means it is capable of supporting LTE service.

In Figure 4.11 the surface current for both modes of operation is presented. The difference in the current distribution is clear.

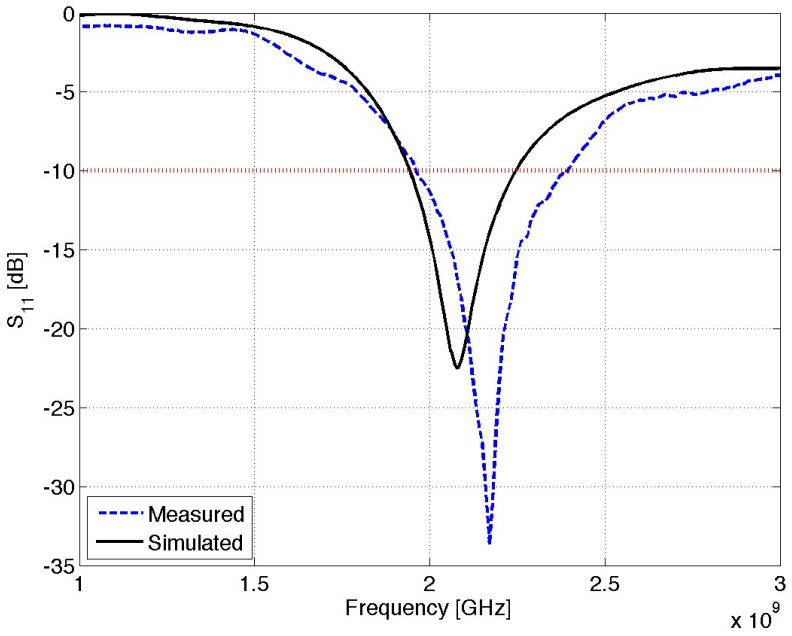

FIGURE 4.9: Return loss for 'on' state; Simulated (solid) and Measured (dashed).

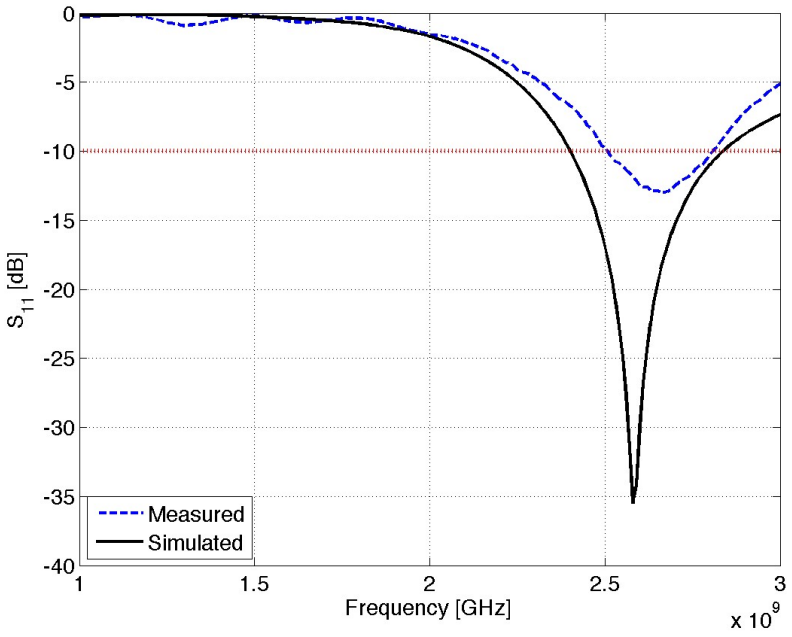

FIGURE 4.10: Return loss for 'off' state; Simulated (solid) and Measured (dashed).

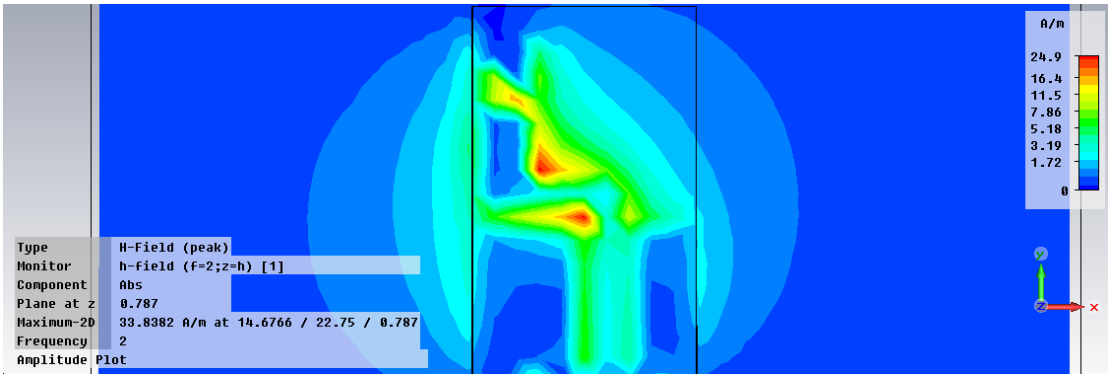

(a)

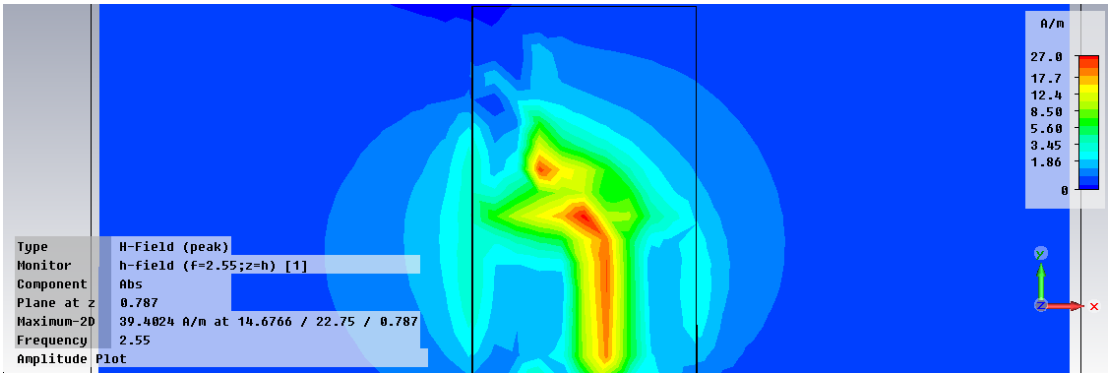

(b)

FIGURE 4.11: Simulated surface current for the reconfigurable ideal monopole (a) 'ON' state, (b) 'OFF' state.

When the parasitic antenna element is connected ('ON' state) the current flow reaches the connector between the base monopole and the parasitic element, which indicates that current flows through this section of the antenna. Whilst when the parasitic element is disconnected ('OFF' state), the current is more intense in the base monopole and barely no current reaches the parasitic element. There is therefore, low coupling effect.

In what concerns the radiation characteristics, the results for both operating frequencies of the ideal model are presented in Figure 4.12. It is essentially an omnidirectional pattern, as expected since this is a monopole antenna.

The gains are also quite good, with a maximum gain of 2.63 dBi for the lowest frequency and 2.38 dBi for the higher frequency of operation. Although not very high, they can be considered quite good given the fact that this is a quite small printed monopole in a low height substrate. These gains are also associated with a simulation result of 100%[1] radiation efficiency, which preconizes a very good radiation efficiency for a real

[1]Simulation results for the radiation efficiency always have an error margin

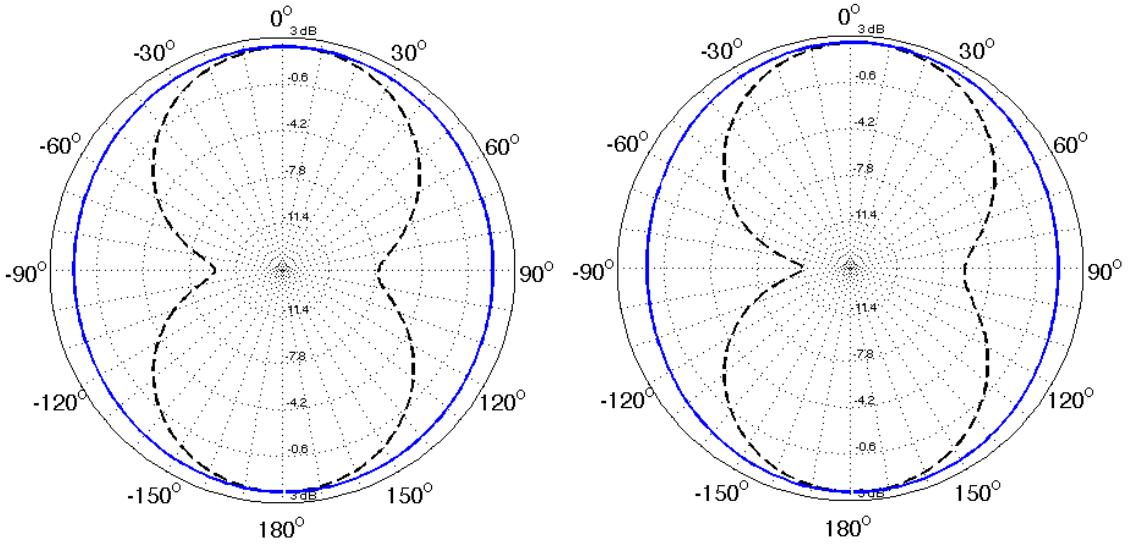

(a) (b)

FIGURE 4.12: Radiation pattern for the ideal reconfigurable monopole on YZ plane (dashed) and XZ plane (solid) at (a) 2.0 GHz, (b) 2.5 GHz.

prototype.

Overall the results are quite good. Albeit some optimizations could be made, in order to fabricate a new monopole that could show better agreement and, of course, could support the proposed services. However, this was an ideal model, a first approach in order to understand the concept of reconfigurability, and the effects of the parasitic element in the antenna. In that sense, on a seccond approach, a model of the PIN diode was introduced, instead of the line connection, and so, no further changes were performed upon this model.

4.4.2 Real model

The proposed antenna design is essentially the same as the previous example from Figure 4.5, but instead of the line connection, a PIN diode was used in its place. With the anode connected to the monopole, and the cathode connected to the parasite element.

The PIN diodes considered to develop the reconfigurable antennas where the HSMP-3860 from Avago Technologies© [50] and the BAP64-03 from NXP© [51]. Although the parasitic value of the PIN diodes can introduce certain changes in the results, those are not so significative, as will be shown further, which makes it little relevant the choice of

some diodes in detriment of others. So these choices was made based on cost, availability and the quality of the information presented in the datasheets.

A lumped element like the equivalent circuits of the PIN diodes, as described in the previous section, was used in the simulations to emulate the PIN diode. According to the datasheet of the BAT64-03 PIN diodes, the corresponding values of the equivalent circuit are 2 Ω if $I_f > 10$ mA, 10 kΩ if $I_f < 0.001$ mA, 0.48 pF and 1.68 nH, for R_s, R_p, C_T and L_s respectivelly. For the HSMP-3860 PIN diode, the corresponding values of the equivalent circuit are around 3 Ω if $I_f > 10$ mA, 10 kΩ if $I_f < 0.001$ mA and 0.2 pF, for R_s, R_p and C_T respectivelly. The L_s value is not mentioned, but it is always present, as it is a small value, a value of 1.68 nH (equal to the other manufacturer) was assumed in the simulations.

The impedance response suffered some changes, which was expected. In consequence, the impedance match is no longer accurate, and thus, the return loss for the antenna gets a lot worst. The difference between the ideal model and the real model can be seen in Figure 4.13.

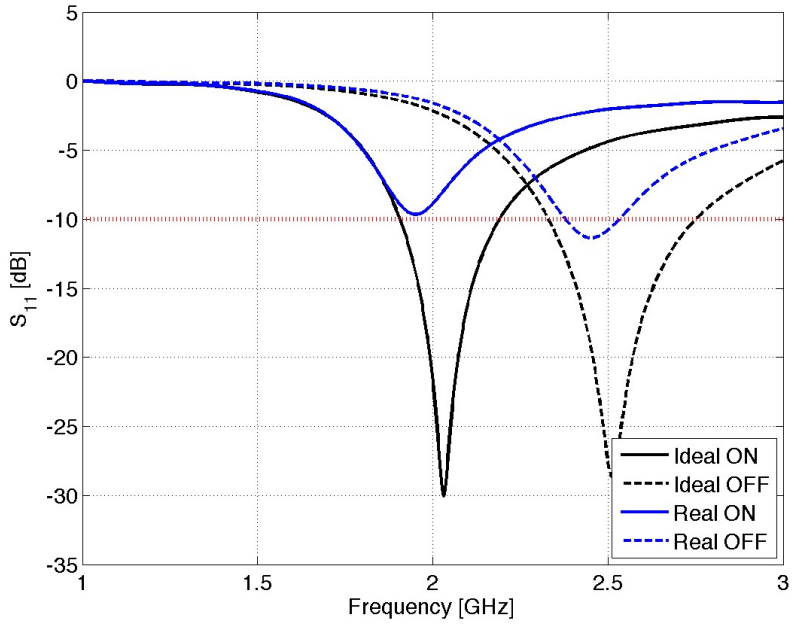

FIGURE 4.13: Return loss comparison for ideal (black curves) and real (blue curves) models for 'ON state' (solid) and 'OFF state' (dashed).

Although there is a slight reduction in the resonating frequencies, the operation remains essentially the same. The change in the resonating frequency was somewhat expected,

given the parasitic inductance of the PIN diode. As seen in the previous chapter, where an inductor was used to effectivelly reduce the resonating frequency of the antenna.

The increase in the return loss is a direct consequence of the lowering of the entrance resistance of the antenna due to the introduction of the PIN diode. The reactance also changes, but the most contributing factor is the real part of the impedance. A comparison between the impedance of the ideal and the real model can be seen in Figures 4.14 and 4.15.

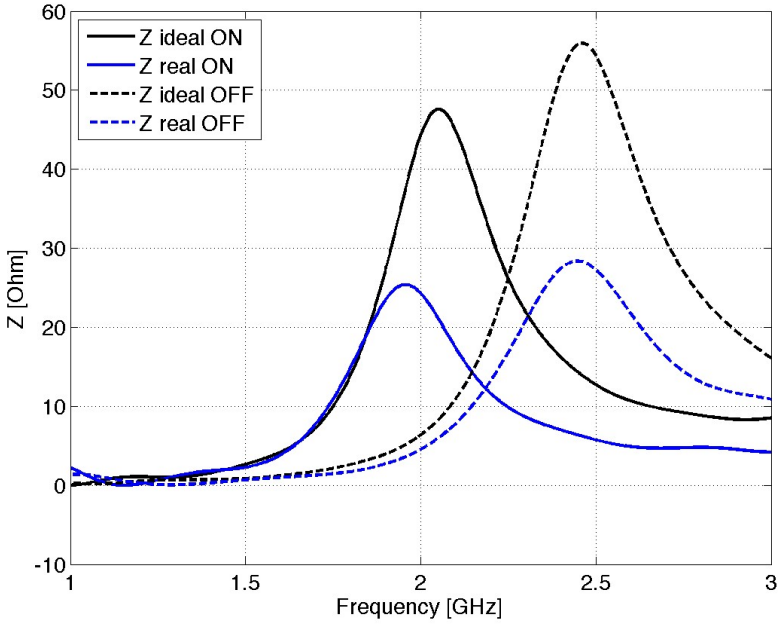

FIGURE 4.14: Resistance comparison for ideal (black curves) and real (blue curves) models for 'ON state' (solid) and 'OFF state' (dashed).

It is clear then, that the introduction of the PIN diode has a considerable effect on the impedance response of the antenna. Fortunately the major effect is felt in the resistance. Not only that, one can see a smoother reactance response curve, which means, that the bandwidth can be sligthly improved.

As the impedance matching of this monopole is done merely with a $\lambda/4$ microstrip transmission line, the resistance can be easily increased, by narrowing the line width. Again, the impedance matching can not be optimized directly, as two different frequencies are being considered. However, after a few runs a good balance can be achieved.

The resulting return loss for the antenna after the impedance rematching, can be observed in Figure 4.16.

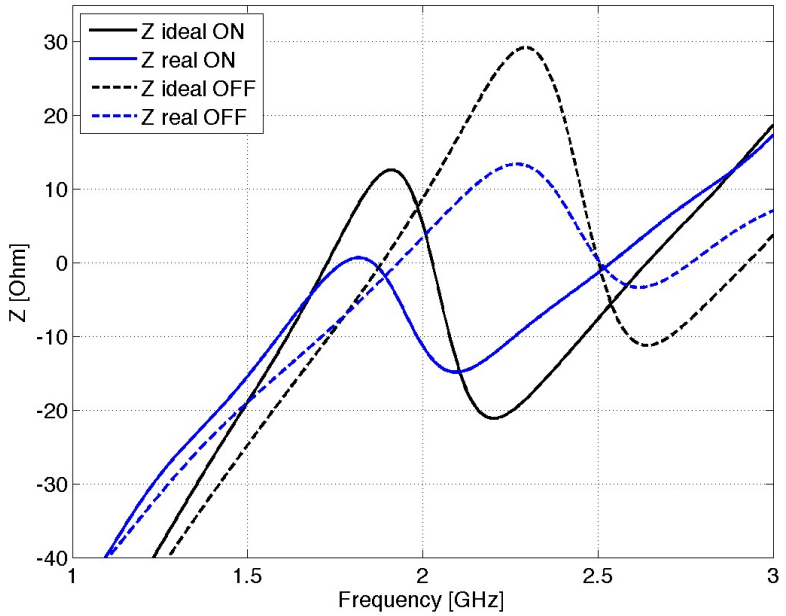

FIGURE 4.15: Reactance comparison for ideal (black curves) and real (blue curves) models for 'ON state' (solid) and 'OFF state' (dashed).

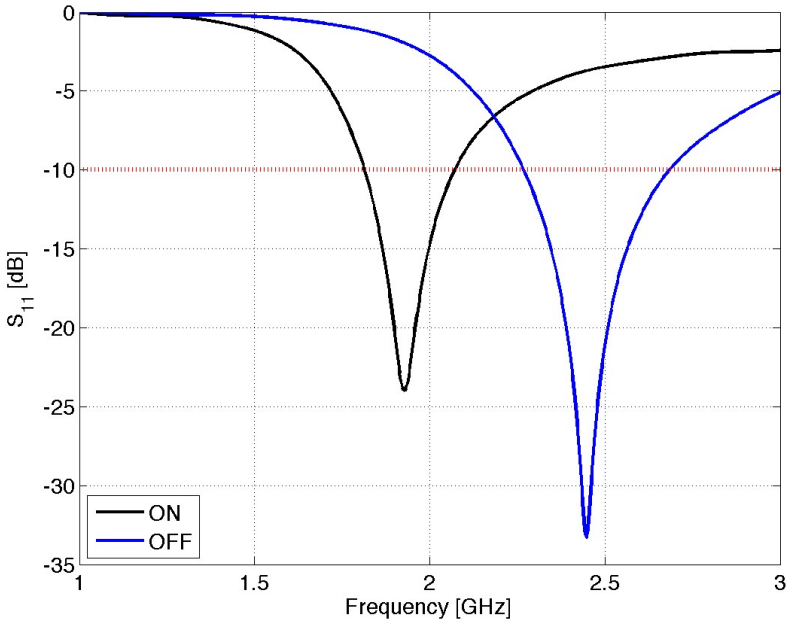

FIGURE 4.16: Return loss for real model for 'ON state' (black) and 'OFF state' (blue).

Besides adjusting the feeding line width, it was also considered a small adjustment to the monopole dimensions, in order to compensate for the small decrease in frequency. The optimized antenna dimensions are present in Table 4.2. Which resulted in the return loss presented in Figure 4.17.

TABLE 4.2: Printed real reconfigurable monopole dimensions

Parameter	Value [mm]
L0	28.0
L1	15.0
L2	10.6
L3	7.1
L4	4.2
Lc	1.6
Lj	2.5
W0	1.62
W1	8.5
Wc	1.5
Lgnd	21
Lsub	50
Wsub	40

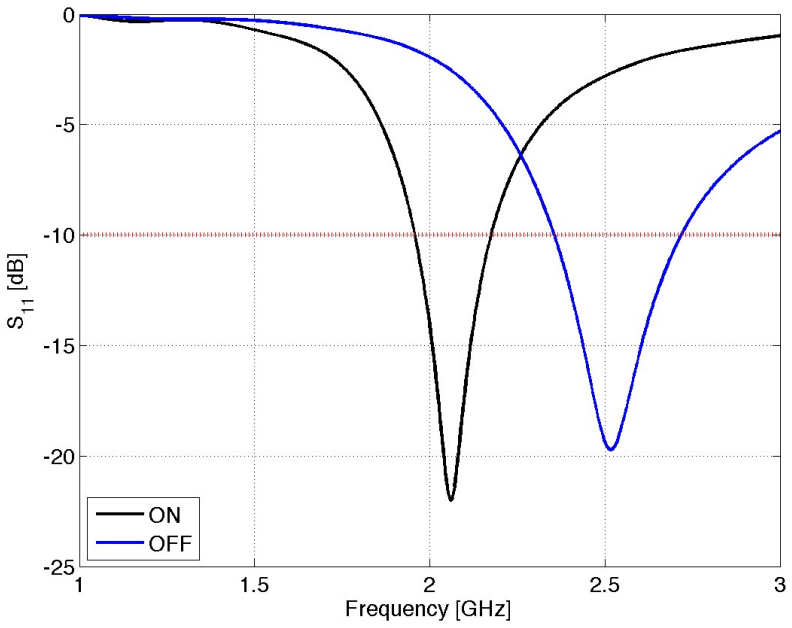

FIGURE 4.17: Return loss of optimized model for 'ON state' (black) and 'OFF state' (blue).

After the final adjustments one can see from the obtained return loss, that the bandwidths for all the applications are garanteed. Also, due to the impedance response being more smooth with the introduction of the PIN diode, there was a better matching which

resulted in a slight improvement in the return losses for both states. The antenna dimension was also slightly reduced by the use of the PIN diode, because of the parasitic inductance associated to it. Resulting in an antenna of $16.6 \times 23.3\text{mm}^2$, less 1.5 mm in width and 3 mm in length.

As mentioned before, the PIN diode has some influence over the resonatinhg frequency of the antenna. Watching the surfce current of the antenna gives another insight over this issue. Figure 4.18 shows the surface current of the antenna for both diode states.

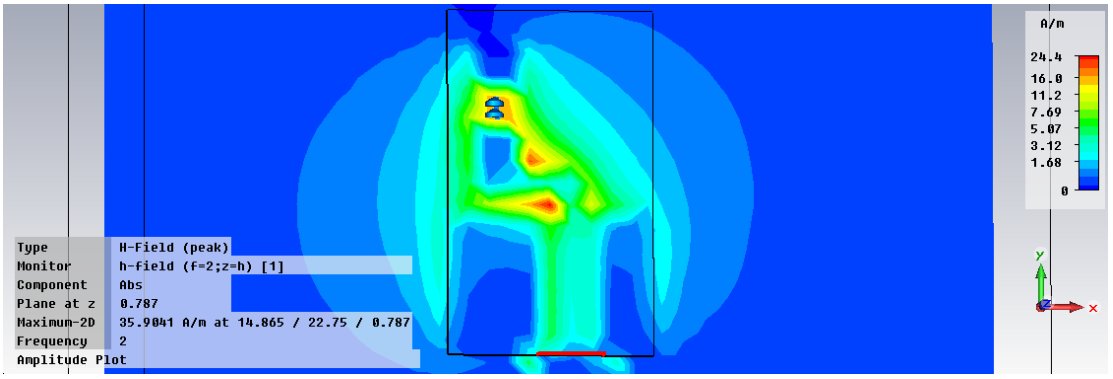

(a)

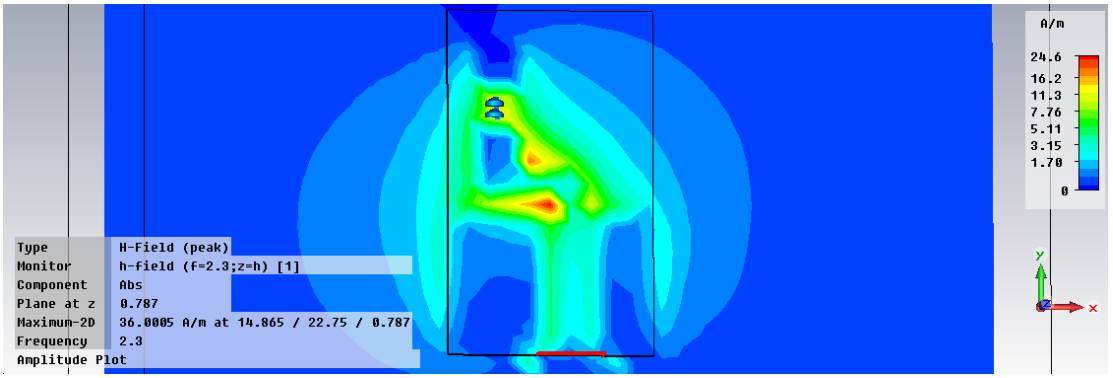

(b)

FIGURE 4.18: Simulated surface current for the reconfigurable real monopole (a) 'ON' state, (b) 'OFF' state.

The current flow concentrates near the PIN diode whichever the state of this component, contrary to the ideal model, in which the current flow was different between states. Still, an higher current flow near the parasitic element of the antenna when the diode is in forward bias can be discerned.

The radiation characteristics are essentialy the same as the ideal model. There was no change in the pattern due to the introduction of the PIN diode, as can be comproved by the simulated radiation pattern present in Figure 4.19. However, the gains were very

slightly reduced to 2.45 dBi at 2.5 GHz and 2.2 dBi at 2.0 GHz. The power dissipation of the PIN diode might be responsible for this small loss in the gain of the antenna, but it's hard to tell to what extent. That led to a small reduction (although not very relevant) in the radiation efficency, to 98.8% at 2.0 GHz and 97.5% at 2.5 GHz.

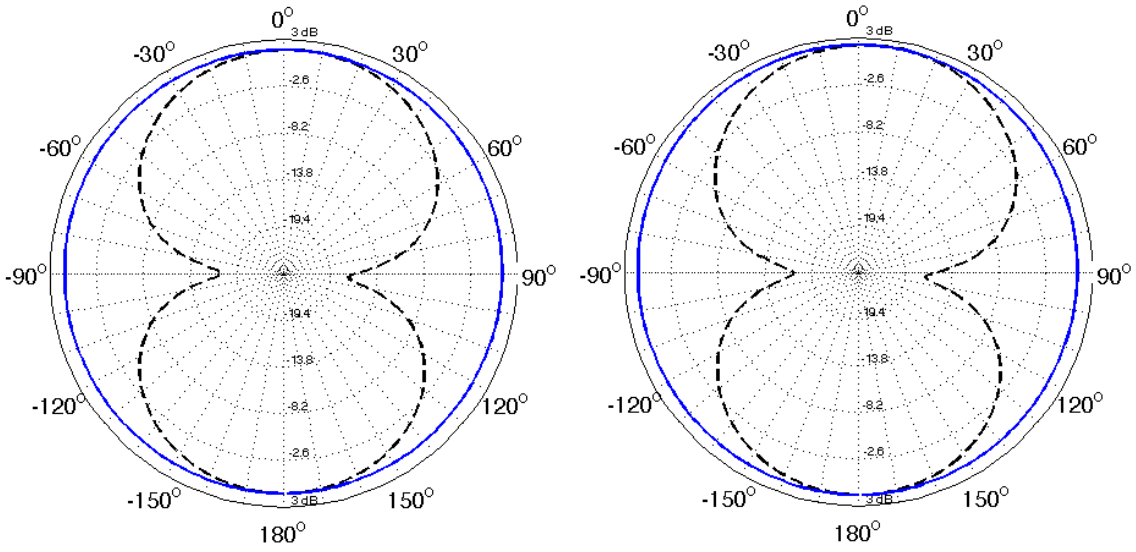

FIGURE 4.19: Radiation pattern for the real reconfigurable monopole on YZ plane (dashed) and XZ plane (solid) at (a) 2.0 GHz, (b) 2.5 GHz.

4.4.3 Lumped element effects

The PIN diode has a few parasitic elements such as the inductance and a capacitance, that affect the impedance response and ence the characteristics of the antenna. This values, although presented in most of the datasheets of these components, may not always be very accurate. Not only that, but most of the times, it's value is dependent on other parameters.

For the chosen PIN diodes for this project, the capacitance is dependent on the frequency and on the reverse bias voltage. The inductance is not even present in the datasheet for the HSMP-3860 PIN diode, and being this value dependent on the structure of the diode itself, it can present some deviations to the given information. The series resistance of the diode is also dependent on the bias current, and although easy to control, can be hard to garantee an exact value for it, which means that one must account for a range of values.

In this section some attention was given towards those factors and a small analysis to the effects of their variations was performed.

The series resistance of the diode is controled by the bias current. Supposing that the activation source of the PIN diode would be a microcontroler, having a strict control of the current is very hard and besides there's the purpose of keeping this antenna simple and inexpensive. In that sense, it's hard to garantee an exact bias current and therefore an exact equivalent series resistance of the PIN diode.

In order to understand if the deviations that can occur, due to the series resistance variation, a sweep to the PIN diode series resistance was performed for both modes of operation. The impedance response of the antenna for those variations can be seen in Figures 4.20 and 4.21.

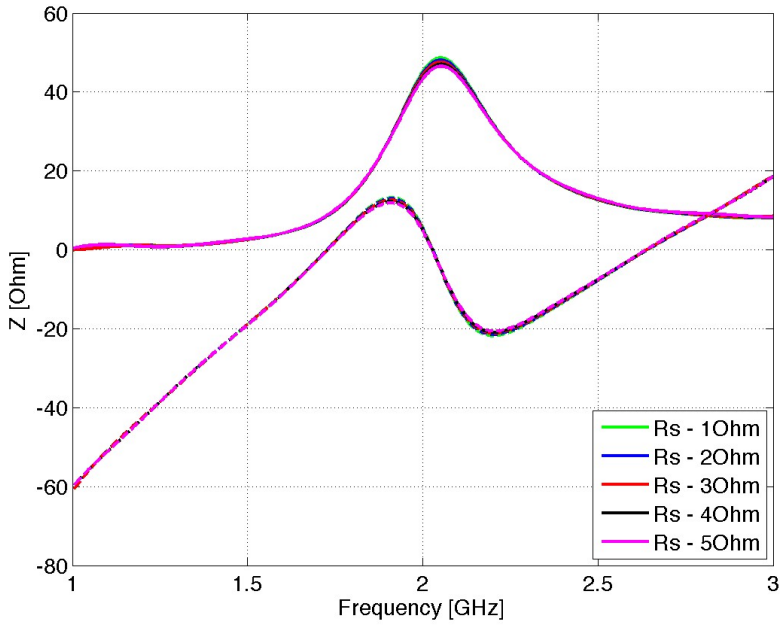

FIGURE 4.20: Impedance for the PIN diode's equivalent series resistance value sweep of the reconfigurable monopole in 'ON' state.

From the graphics in Figures 4.20 and 4.21 it is clear that the series resistance doesn't play a relevant change in the impedance response of the antenna, neither in 'ON' nor 'OFF' state. There is no shifts in resonant frequency, and the impedance absolut values changes only slightly to the variation of R_s. This means that the poor control of the bias current will not produce any considerable changes to the antenna operation. However,

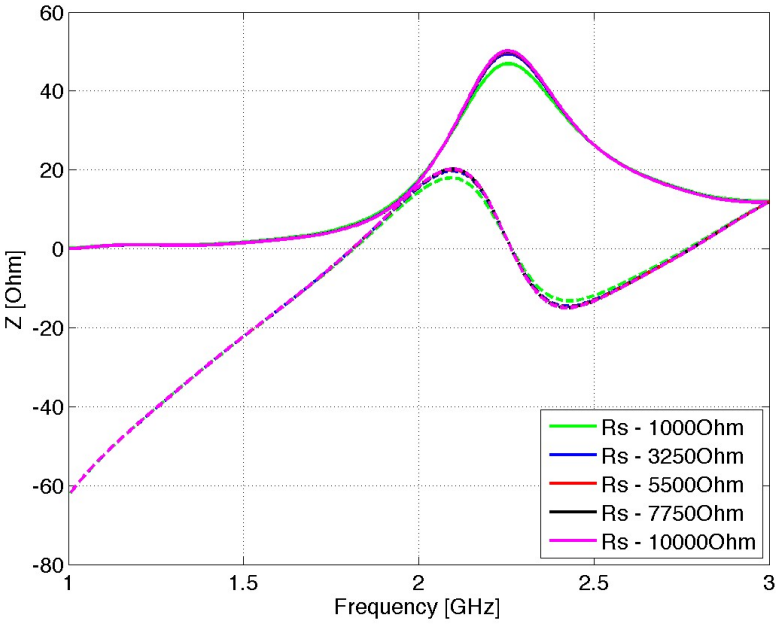

FIGURE 4.21: Impedance for the PIN diode's equivalent series resistance value sweep of the reconfigurable monopole in 'OFF' state.

the 'OFF' state must be taken into careful account, since the variation from 1 kΩ to 10 kΩ mean an increase in the impedance of roughly 5 Ω.

The parasitic capacitance of the PIN diode, has a very small variation with frequency, but it exists. Besides, the values indicated by the datasheet are merely indicative, which means there's no certainty that those values are 100% accurate. In that sense, a sweep to this parasitic value was performed in order to understand its influence in the antenna impedance response. The results are presented in Figure 4.22.

The variation of the parasitic capacitance value has a considerable effect on the antenna operation. From Figure 4.22, one can see that the higher the capacitance is, the lower the resulting resonant frequency. Not only that, the impedance absolut value also changes and all this, for a very small sweep in values. This means that a practical implementation of the antenna may show a different resonant frequency than the simulated, due to a small variation in this factor.

The last of the parasitic values of the diode is the series inductance. This is a result of the package geometrie of the diode, which means that it's value may not be very accurate, some manufacturers don't even mention it in the datasheets. Besides, the soldering of the PIN diode to the antenna, might even change it.

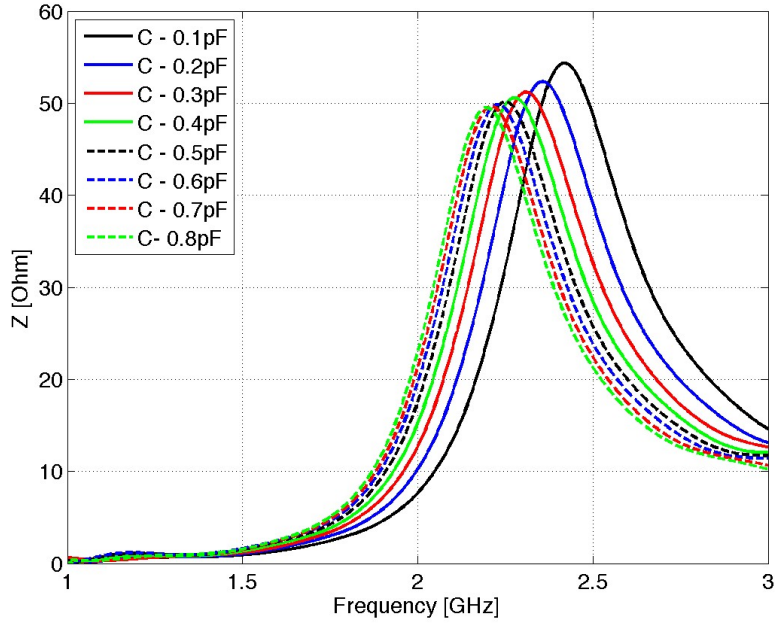

(a)

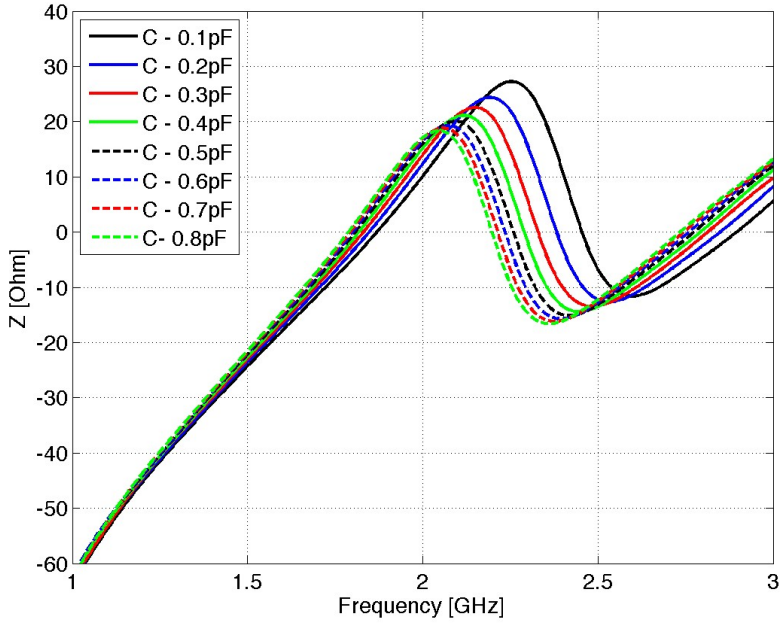

(b)

FIGURE 4.22: Impedance for the PIN diode's parasitic capacitance value sweep of the reconfigurable monopole (a) resistance, (b) reactance.

In the previous chapter, an inductor was used to reduce the resonant frequency of a printed antenna, this means that the parasitic impedance of the PIN diode will also have an effect in the resonant frequency. Figures 4.23 and 4.24, show the impedance response to the parasitic inductance sweep value.

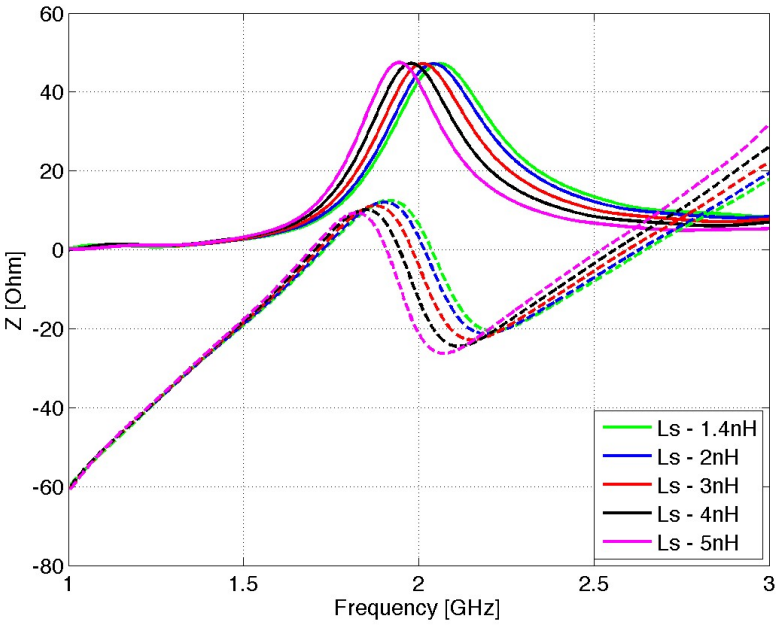

FIGURE 4.23: Impedance for the PIN diode parasitic inductance value sweep of the reconfigurable monopole in 'ON' state.

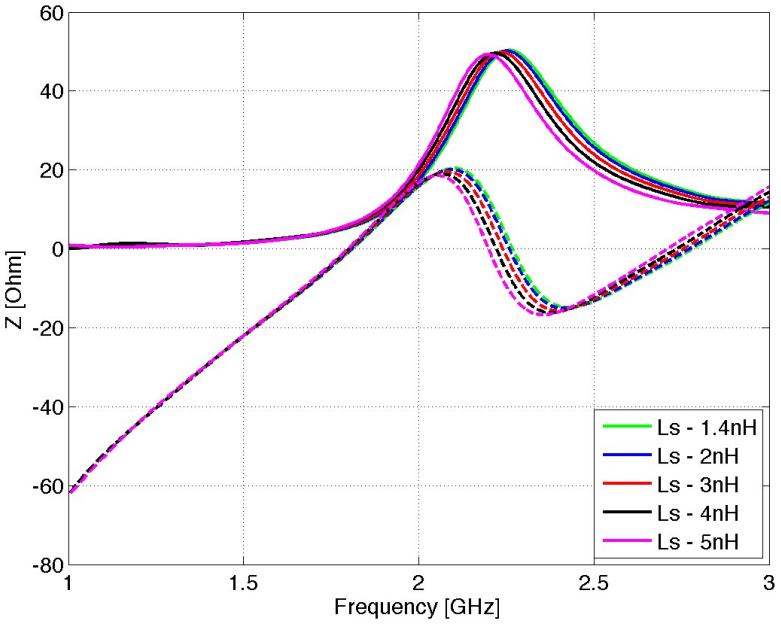

FIGURE 4.24: Impedance for the PIN diode parasitic inductance value sweep of the reconfigurable monopole in 'OFF' state.

The inductance plays a major role for the resonant frequency definition when in 'ON' state. This is due to the fact that in the 'ON' state, the equivalent capacitance of the PIN diode is null. However it also influences the resonant frequency in 'OFF' state. Just as the results obtained in the previous chapter about miniaturization, the higher the inductance, the lower the resonant frequency of the antenna.

4.4.4 C-monopole

The C-monopole has already been introduced in this dissertation in the previous chapters. First a simple version and then a miniturized version of it. In this chapter, an approach to make this monopole reconfigurable is investigated.

The antenna design is presented in Figure 4.25 and the corresponding dimentions are presented in Table 4.3.

This version of the C-monopole is bigger than the C-monopole presented in the previous chapters. This was designed to resonate at WLAN and UMTS bands. The purpose of making this design bigger, is to be able to further compare the size reduction, resulting from the introduction of the chip inductor.

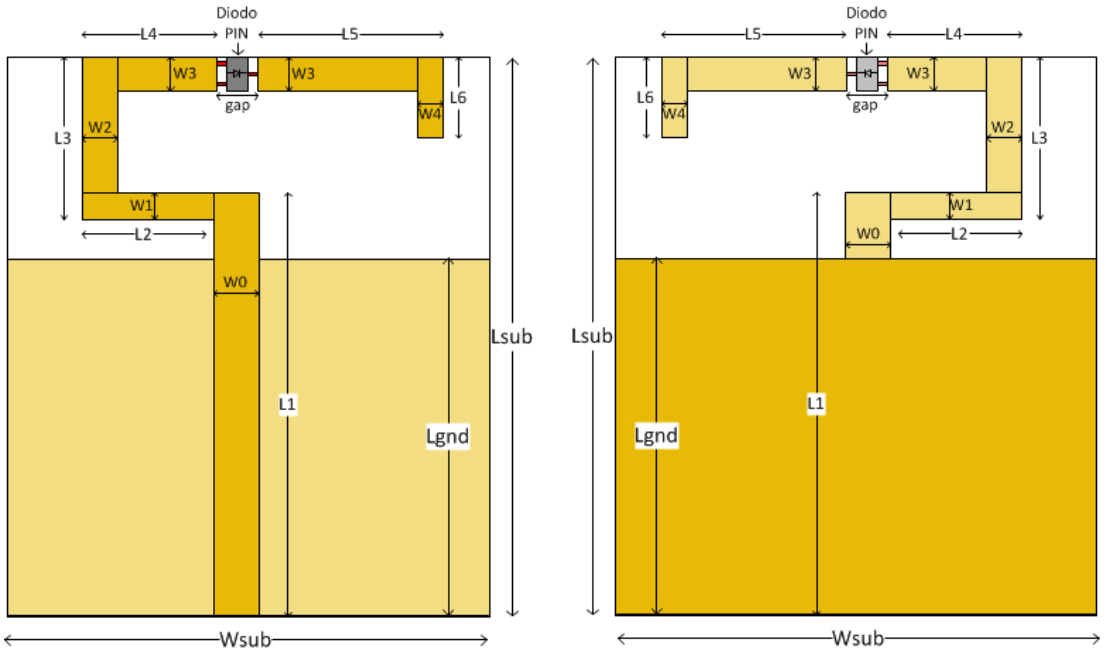

FIGURE 4.25: Reconfigurable C-monopole model (a) front view, (b) back view.

TABLE 4.3: Reconfigurable C-monopole dimensions.

Parameter	Value [mm]
L1	29.5
L2	6.20
L3	10.0
L4	4.00
L5	10.1
L6	5.00
Lgnd	21.0
Lsub	38.0
Wsub	25.0
W0	2.60
W1	1.50
W2	1.50
W3	2.00
W4	1.50
gap	2.00

The resulting resonating frequencies for this antenna, according to the simulated impedance on Figure 4.26, are 2.05 GHz and 2.5 GHz, for 'ON' and 'OFF' modes respectively. Once again, the impedance differences make the impedance matching quite challenging.

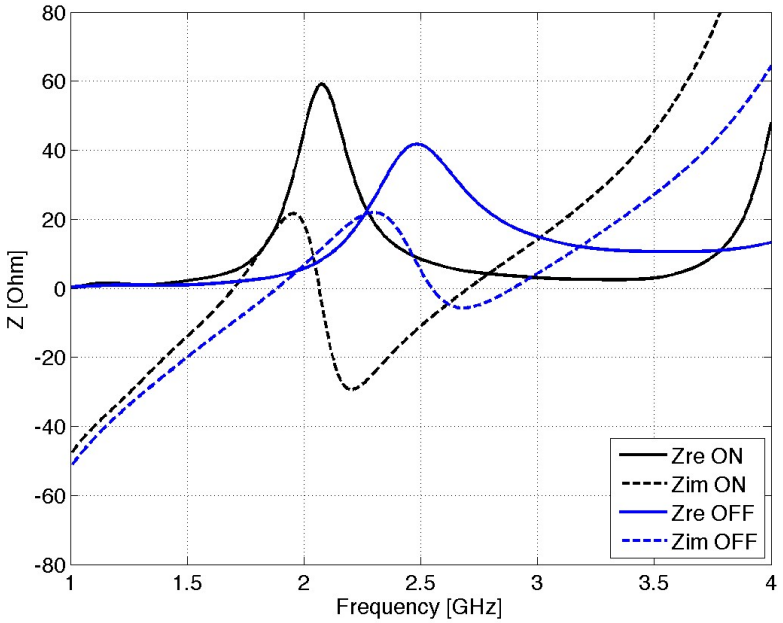

FIGURE 4.26: Impedance for the reconfigurable C-monopole in 'ON state' (black) and 'OFF state' (blue).

The resulting return loss for this antenna is presented in Figure 4.27. It is clear, that this antenna has a smaller bandwidth than the previous example, although it can still

support UMTS, WLAN and LTE. The bandwidth reduction, when compared to the reconfigurable monopole in the previous section, is a consequence of the size reduction of the antenna.

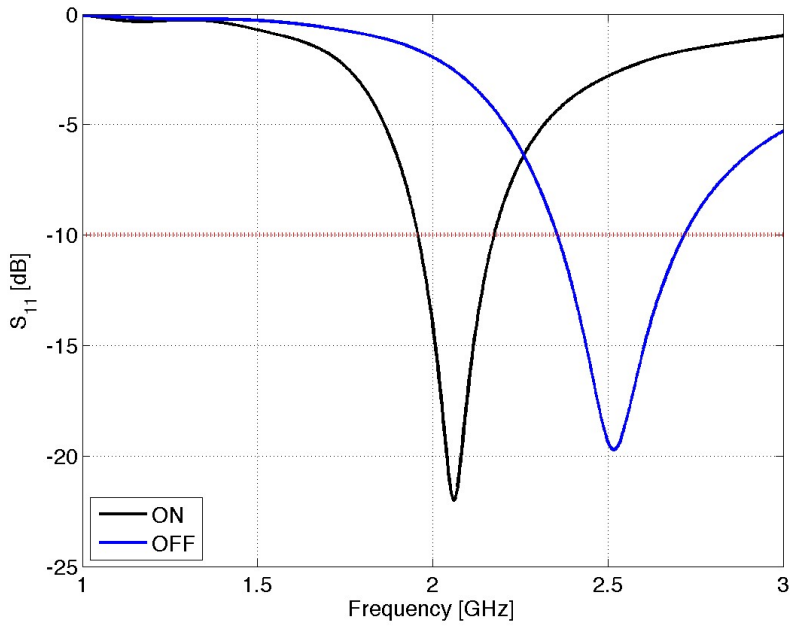

FIGURE 4.27: Return loss for reconfigurable C-monopole in 'ON state' (black) and 'OFF state' (blue).

The resulting radiation pattern from this antenna, is not much different from the previous examples, as shown in Figure 4.28 it is still omnidirectional.

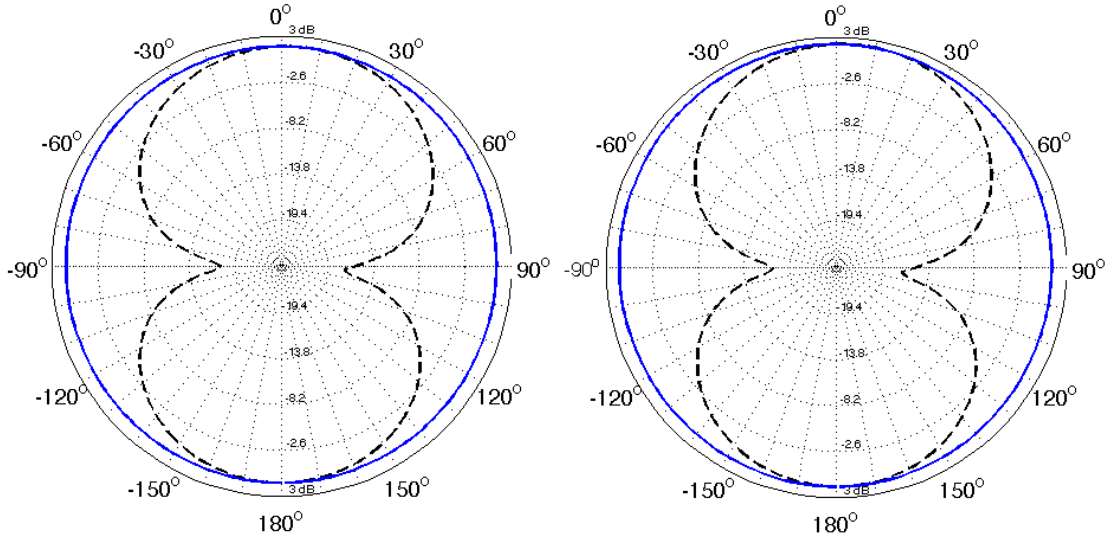

(a) (b)

FIGURE 4.28: Radiation pattern for the reconfigurable C-monopole on YZ plane (dashed) and XZ plane (solid) at (a) 2.0 GHz, (b) 2.5 GHz.

However, the gains and efficiencies are lower than the example in section 4.4.2. The gain is reduced to 2.21 dBi in 'OFF' state and 1.71 dBi in 'ON' state, which led to an efficiency of 93% and 87% in 'OFF' and 'ON' state respectively. This losses were expected, once again, given the smaller size of the antenna.

Chapter 5

Miniaturized reconfigurable antennas

5.1 Introduction

In Chapter 3, miniaturization techniques were presented, and special attention was given to the miniaturization of a printed monopole with a chip inductor, also in Chapter 4, reconfigurability techniques were presented, and a possible implementation of a reconfigurable monopole with PIN diodes was presented.

As shown in the previous chapter, there is a good range of sources for the study of miniaturization and reconfigurability, by many means and techniques. In some of the reconfigurable antenna's articles exposed in the previous chapter, a certain concern to design small antennas is noted, however, the search for the miniaturization of this kind of antennas was never researched.

The search for a very small reconfigurable antenna is presented in this chapter. Two possible implementations for a very small reconfigurable printed monopole, for dual band operation to support UMTS and WLAN, are presented and discussed. The first approach is a printed inverted L-monopole and the second approach, in order to further reduce the antenna size, is a printed C-monopole.

As seen in the previous chapters, chip inductors and PIN diodes, both influence the impedance response of the antenna and produce some other constraints in bandwidth

and gain. In this chapter the effects on the combination of both elements, for the purpose of antenna design, is studied.

5.2 Very small reconfigurable printed antennas

As stated in the introduction, the first approach on this study was a L-monopole, that was miniaturized and able to work in two different frequency bands through reconfigurability. The results obtained with this design are compared to the results obtained in Chapter 2, in which a normal inverted L-monopole was presented and Chapter 3, in which the miniaturization techniques were discussed.

The second approach was a C-monopole, with the same working bands, that allowed to further reduction the size of the antenna. The results obtained with this design are also compared to the studied conducted in previous chapters.

5.2.1 L-monopole

The printed L-monopole is a simple and common printed antenna and that has already been shown in this dissertation on Chapter 2. The advantages of this design are the reduction in the size of the antenna structure, by bending the monopole arm, without changing the characteristics of the antenna neither the radiation performance.

In the previous chapters miniaturization and reconfigurability techniques applied to printed monopoles were studied. The advantages and disadvantages of each were discussed and the problems arousing from these were presented.

The proposed reconfigurable miniaturized L-monopole is presented on Figure 5.1, and the corresponding dimensions can be found on Table 5.1.

For this implementation the chosen PIN diode was the HSMP-3860 which has lower series resistance ($R_s = 3.8\ \Omega$) with lower forward bias current $I_f = 1$ mA, and lower capacitance ($C_T = 0.2$ pF). In the previous chapter, the effect of this parameters on the impedance response of the antenna were observed. For the proposed reconfigurable monopole it was seen that this values almost had no influence on the antenna response.

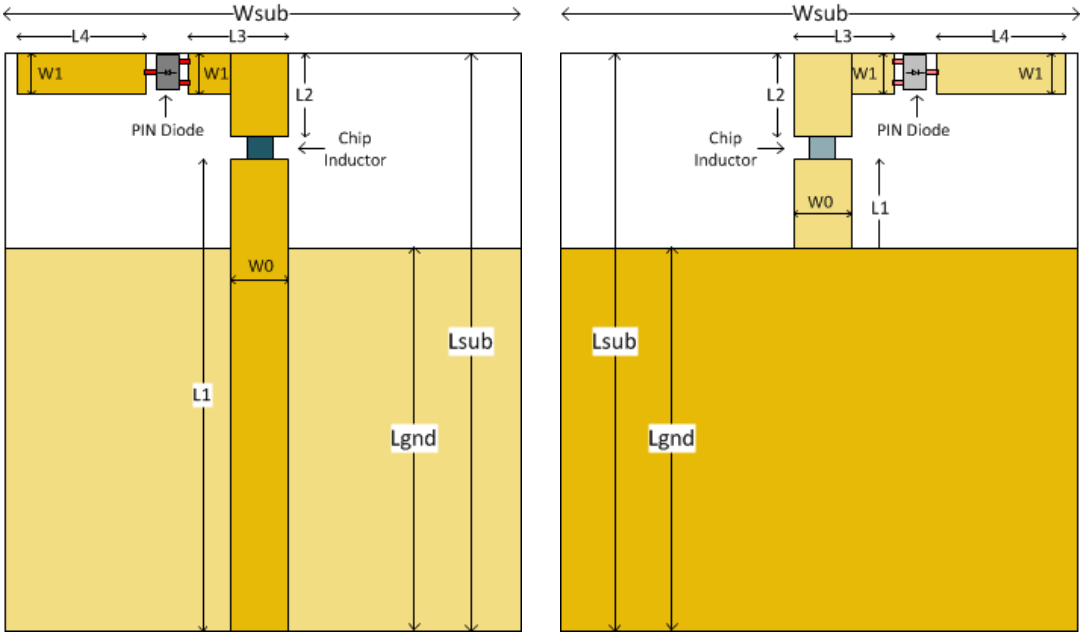

(a) (b)

FIGURE 5.1: Miniaturized reconfigurable L-monopole model (a) front view, (b) back view.

TABLE 5.1: Miniaturized reconfigurable L-monopole dimensions.

Parameter	**Value [mm]**
L0	26.0
L1	3.25
L2	4.50
L3	8.00
W0	3.0
W1	2.0
Lgnd	21.0
Lsub	30.0
Wsub	27.0
gap	0.50
gap2	2.00

That is not the case when the chip inductor and the PIN diode are used together on the same radiating element.

In Chapter 3 the influence of the chip inductor value on the resonating frequency was investigated and it was clear that the inductance value of the component was the determining factor for the resonant frequency of the antenna. At the time, the trial was conducted with no special attetion to a specific value, since the purpose was to study the effects of its usage. However, in this case, the resonant frequencies matter, since the purpose of this antenna is to work at UMTS, WLAN and LTE frequencies. In that sense,

after antenna optimization and regarding the available values for the chip inductor, the best response was obtained with the 0402HP-8N2 chip inductor from Coilcraft©, which exhibits a series resistance of 1.8 Ω and an inductance of 8.2 nH at 2.5 GHz.

The return loss for this monopole is presented in Figure 5.2. It is not very good, for various reasons. First, neither the WLAN nor the UMTS band are all covered. A little frequency shift and the narrow bandwidth dictated this failure. And second, the difference in the impedance match for both operating modes. Matching both modes in this antenna is a big challenge, even harder then the examples for the reconfigurable antennas in the previous chapter, for reasons that will be exploited further.

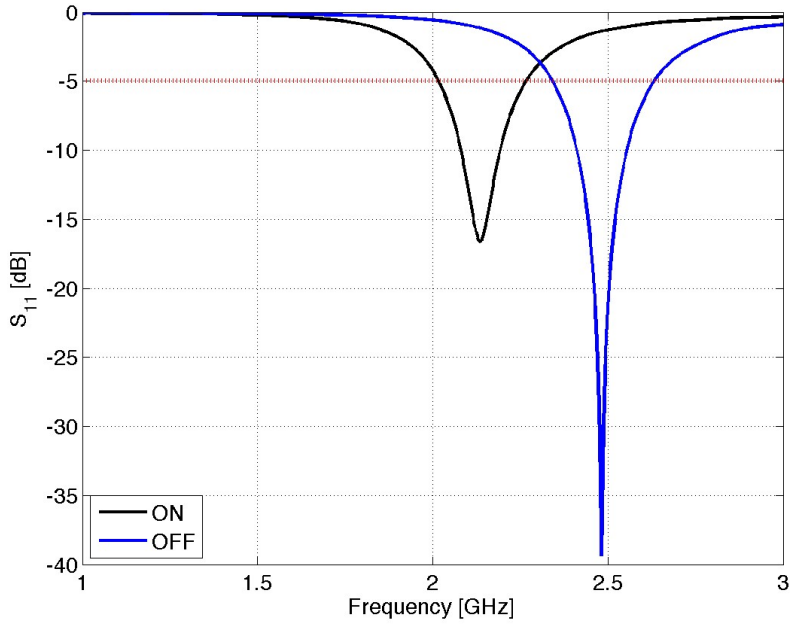

FIGURE 5.2: Return loss for the miniaturized reconfigurable L-monopole in 'ON state' (black) and 'OFF state' (blue).

From the results obtained in the previous chapter, it was clear that the introduction of the chip inductor or the PIN diodes, would produce a slight reduction in the antenna gain. However, when this two components are used together the reduction is steeper. Luckily the radiation pattern doesn't seem to suffer any considerable changes when compared to the L-monopole in the second chapter.

The radiation pattern simulated for this antenna is presented in Figure 5.3. Both modes of operation show the same response, has expected. However, the gain for the highest frequency is around 0.71 dBi, as the gain for the lowest frequency is around 0.27 dBi.

This has consequences to the radiation efficiency too. In this case the radiation efficiency is 69% and 65% for the highest and lowest frequency respectively.

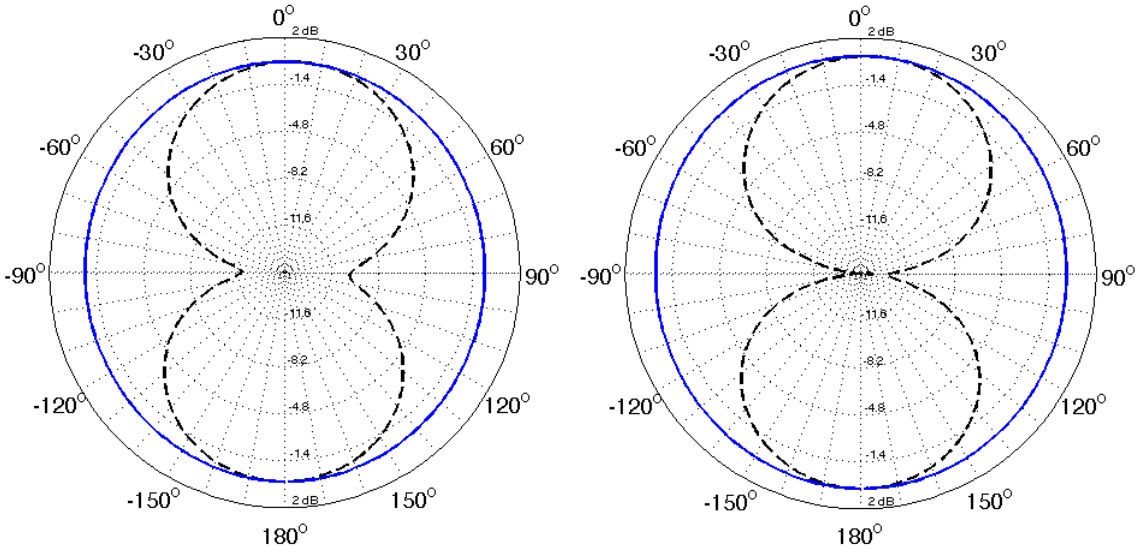

FIGURE 5.3: Radiation pattern for the miniaturized reconfigurable L-monopole on E plane (dashed) and H plane (continuous) at (a) 2.0 GHz, (b) 2.4 GHz.

This results lead to a mischief conclusion regarding the loss in efficiency. In Chapter 3, the radiation efficiency of the antenna was severely decreased by the introduction of the chip inductor. This result was hard to explain, and not at all expected. Nonetheless, the fact that this antenna, that adds the PIN diode to the radiator, have an higher radiation efficiency, makes the obtained results in Chapter 3 even less plausible.

As shown before, the introduction of the chip inductor and/or the PIN diodes in the radiation element of the antenna has an effect on radiation characteristics. For instance, the radiation efficiency decreases due to them. If we consider that the PIN diode, introduces a loss of roughly 15 to 20% to the radiation efficiency, as seen in previous chapter, then, the simulation results obtained for this miniaturized reconfigurable monopole are credible.

This particular monopole, although simplistic, ended up being problematic to the application of this technique. However, it proved the concept and it became clear that it is possible to use PIN diodes and inductors to allow reconfigurability of very small antennas. Nonetheless, a careful dimensioning and a very large set of simulations is needed in order to succesfully design this kind of antennas.

One of the issues with the miniaturized reconfigurable L-monopole is the impedance mismatch between modes of operation. In Figure 5.4, a sweep to the feeding line width for both operating frequencies is shown, and the differences in the corresponding variations can be observed.

From the graphic in Figure 5.4 one can see that the impedance has a similar variation for both modes. If the width of the feeding line is increased, the impedance is lowered, and if the impedance drops 20 Ω in the antenna 'ON' state, then it also drops close to 20 Ω in the 'OFF' state. This is an expected behavior, but the impedance in the lower frequencies is always higher then at the higher frequencies, that is why it's impossible to perfectly match both modes, using this method.

Another issue about this variation, is that the width of the feeding line not only changes the impedance absolut value, but it also shifts the resonating frequency. And this shift is not linear, at the highest width tested the frequency shifts outwards and that contradicts a possible prediction. This behavior is a reflection of the influence of the components used, these became determinant to define the resonating frequency and the impedance response of the antenna is completely different from a normal printed monopole.

Figure 5.5 shows a variation of the feeding line width for the printed monopole from section 2.3.2. In this case, the expected response was obtained in which only the absolut impedance value is changed, mantaining the resonating frequency of the antenna.

In Section 3.4.2, there's a graphic about the influence of the inductor value on the resonant frequency. In the following Figures 5.6 and 5.7, a similar sweep is presented, but for the monopole proposed in this chapter. Bases on this, one can see the effect of having the inductor and the PIN diode together, which is an increased influence of the inductor value on the resonating frequency. Besides that, it's also possible to compare the influence when the diode is 'ON' and 'OFF'.

As concluded in Chapter 3, the increased inductor value reduces the resonating frequency of the antenna and increases the impedance. However, the frequency shift occuring because of the inductor value is in this case higher. This arises from the increased complexity of the impedance response due to the introduction of the PIN diode.

The results obtained for both modes of operation, present in Figure 5.6 and 5.7, are somewhat similar. The main difference is the impedance steps, the impedance variation

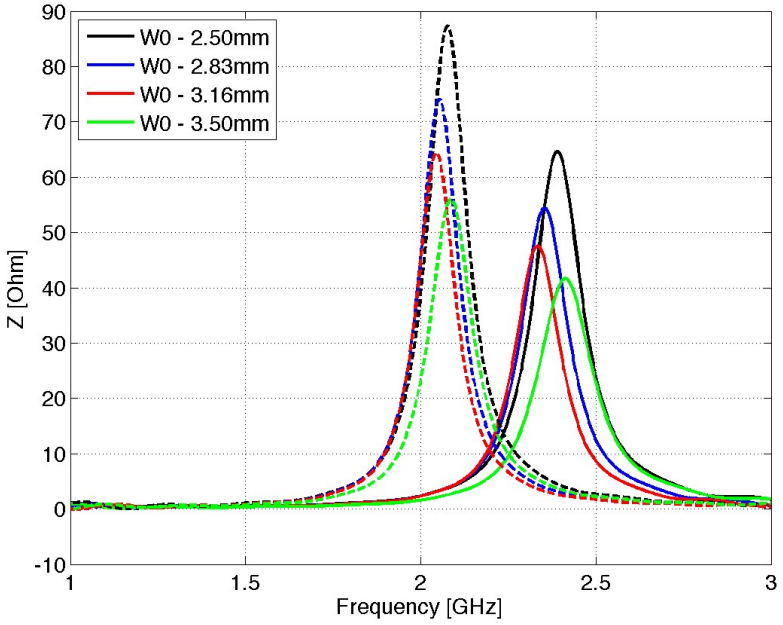

(a)

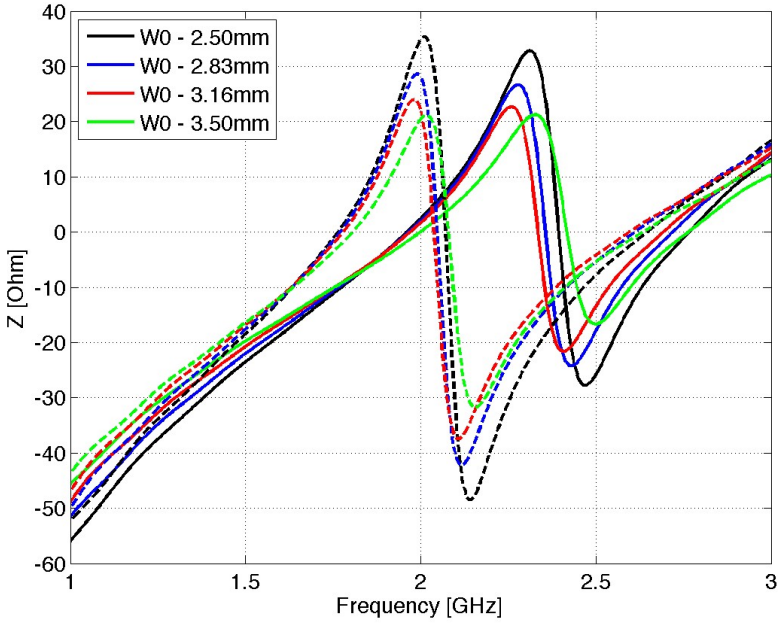

(b)

FIGURE 5.4: Impedance for the feeding line width sweep of the miniaturized reconfigurable L-monopole with diode in 'ON' state (dashed) and 'OFF' state (solid) (a) resistance, (b) reactance.

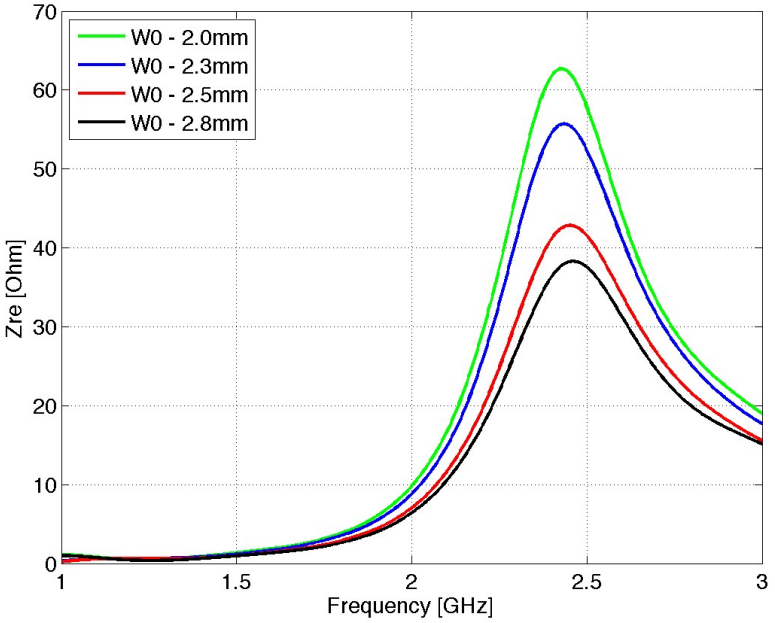

(a)

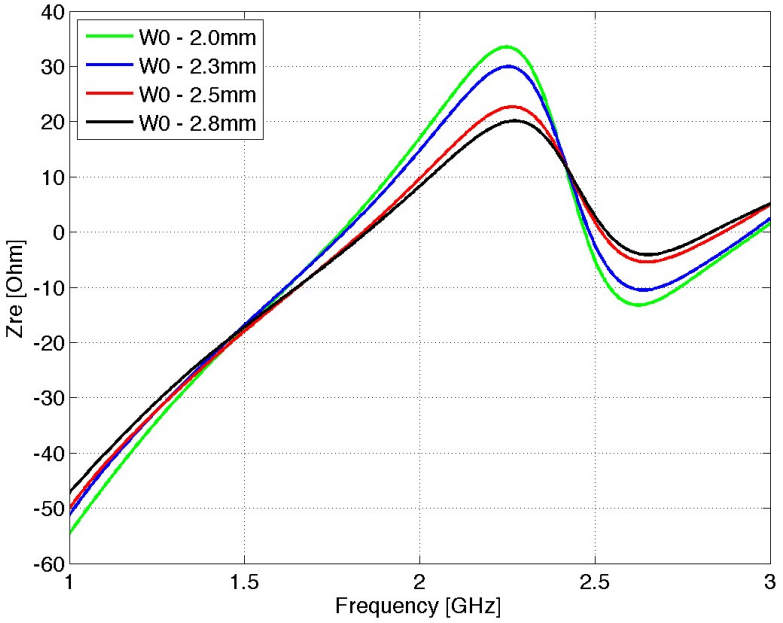

(b)

FIGURE 5.5: Impedance for the feeding line width sweep of the printed L-monopole (a) resistance, (b) reactance.

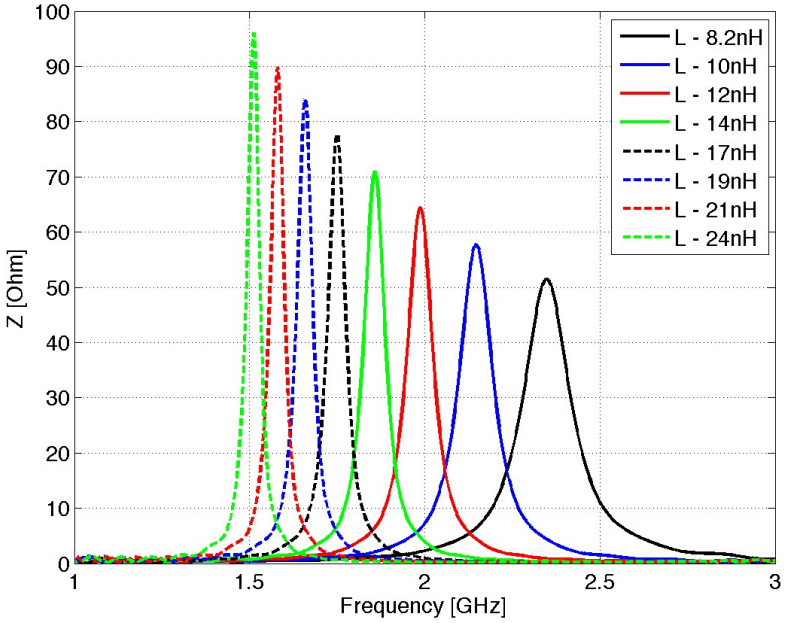

(a)

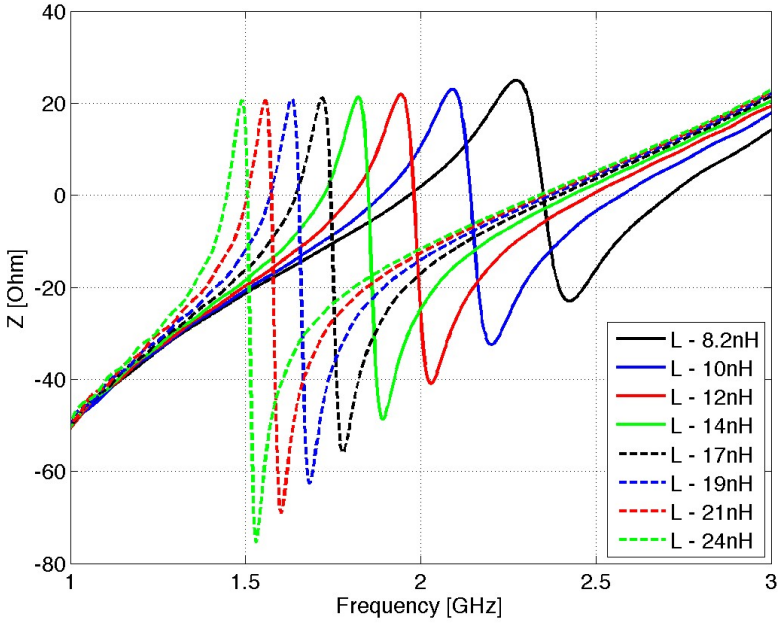

(b)

FIGURE 5.6: Impedance for a chip inductor's value sweep of the miniaturized reconfigurable L-monopole with diode in 'OFF' (a) resistance, (b) reactance.

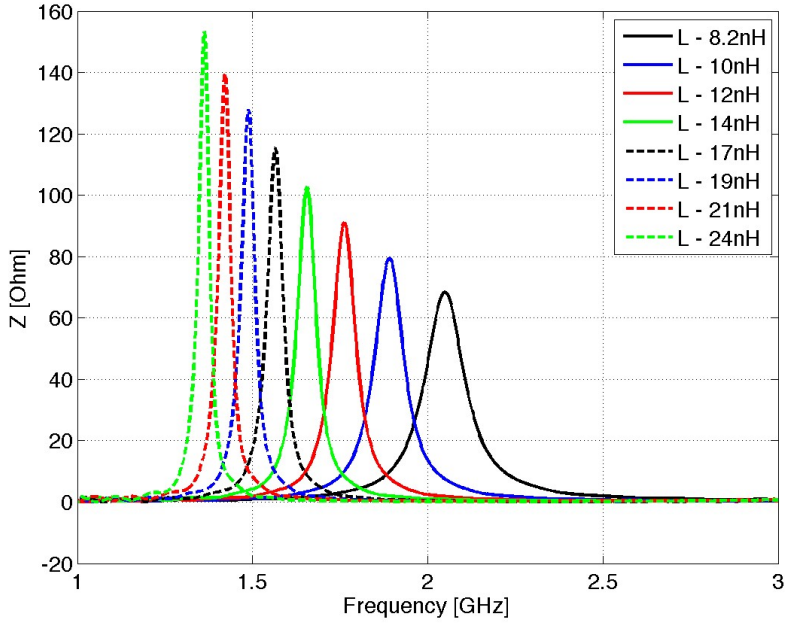

(a)

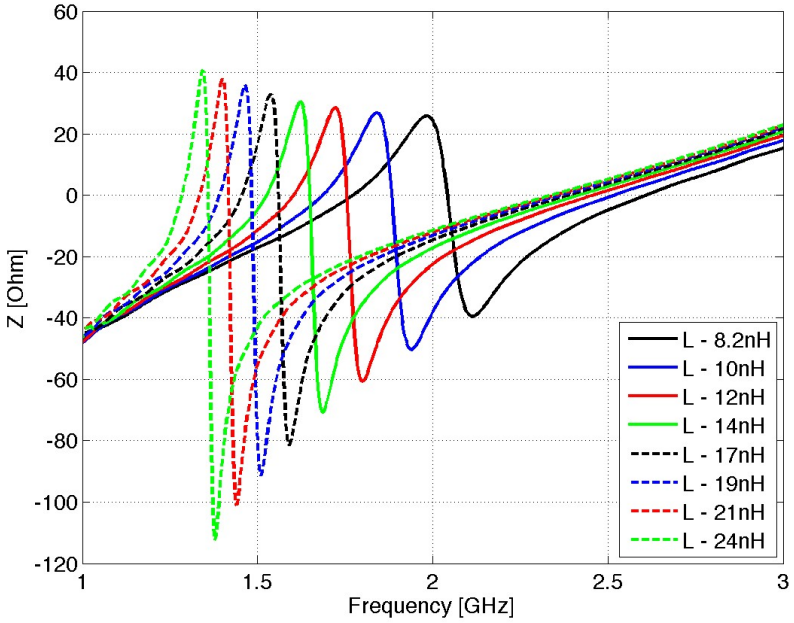

(b)

FIGURE 5.7: Impedance for a chip inductor's value sweep of the miniaturized reconfigurable L-monopole with diode in 'ON' state (a) resistance, (b) reactance.

is more severe when the diode is forward biased ('ON' mode). When in 'OFF' mode, the resistance is of approximately 50 Ω and 95 Ω for the lowest and highest inductor value respectively. When in 'ON' mode, the resistance is of approximately 70 Ω and 150 Ω for the lowest and highest inductor value respectively, this is a difference of 80 Ω, considerably higher that the 45 Ω difference for the 'OFF' mode.

This differences in the impedance response to the matching line, justify the dificulty, almost impossibility in some cases, in achieving a good impedance match for both modes of operation.

The prototype of this antenna was fabricated according to the design specifications mentioned earlier. These can be seen in Figure 5.8

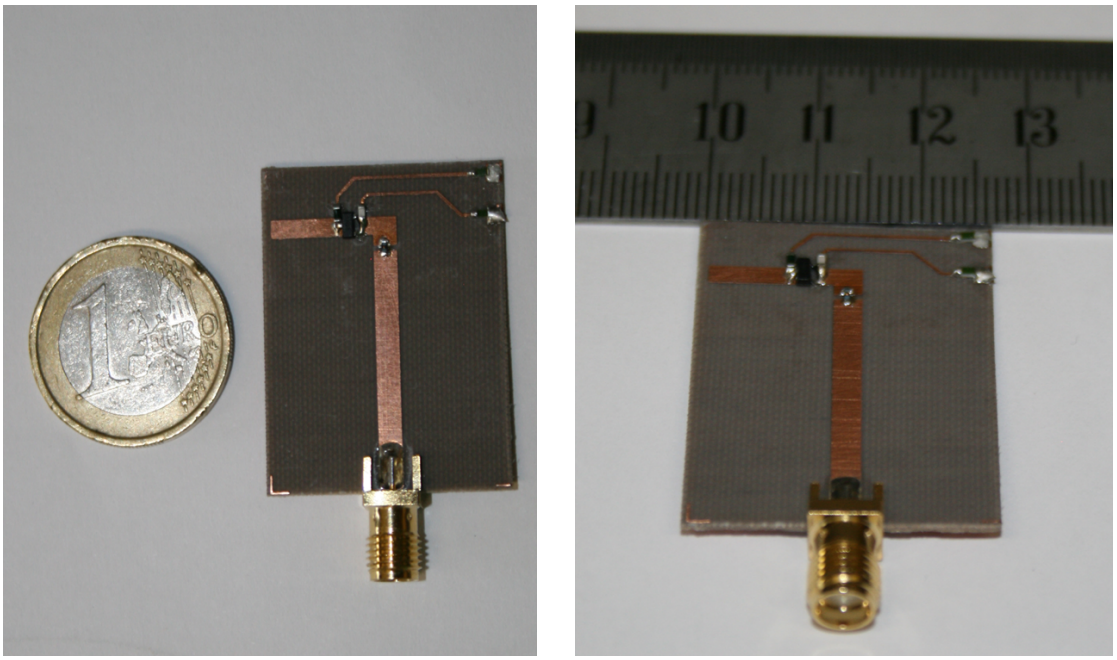

(a) (b)

FIGURE 5.8: Prototype miniaturized reconfigurable L-monopole.

The really small size of the antennas can be perceived by the comparisons in the photographs. The prototype has a few add-ons when compared to the simulated design presented in Figure 5.1. That circuit, that can be seen in Figure 5.9, is the PIN diode biasing circuit. A simple circuit of a RF SPST (Single Pole Single Throw) switch based on the PIN diode, as the schematic in Figure 5.10.

The measured return loss for this antenna is shown in Figure 5.11. In the graphic both simulated and measured return losses are presented for comparison. It resulted in a

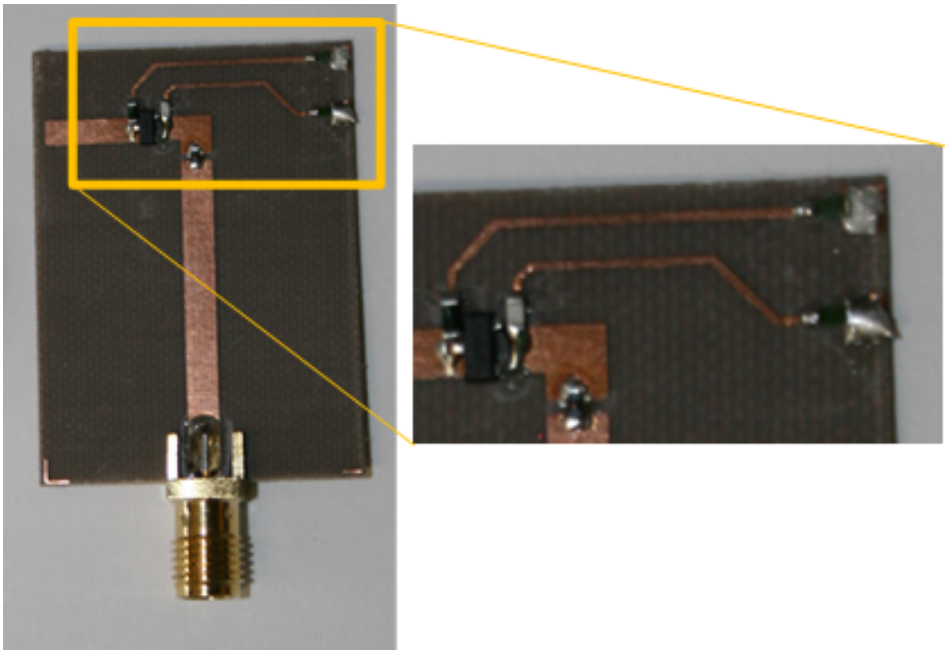

FIGURE 5.9: Prototyped miniaturized reconfigurable L-monopole close up.

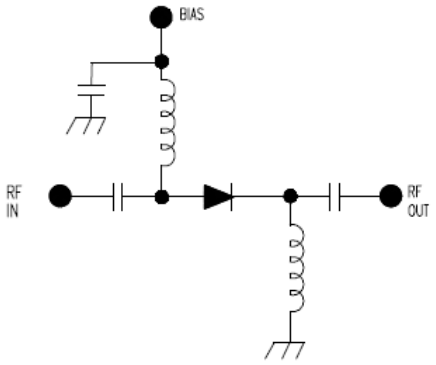

FIGURE 5.10: Schematic of a PIN diode as an RF SPST switch [47].

deviaton of the resonating frequencies of the prototype model to the simulation results. Both operating modes of the antenna were shifted up, with a larger effect on the lowest band.

As shown before, the inductor and the PIN diode have a large influence on the antenna resonating frequencies. The effects of the PIN diode in combination with the chip inductor on this antennas is further investigated. However, from the results obtained so far, it's easy to conclude that small variations on the parasitic characteristics and tolerances of this components can change the operating frequencies of this antenna. That is, therefore, one explanation for the measured results being so different from the simulated.

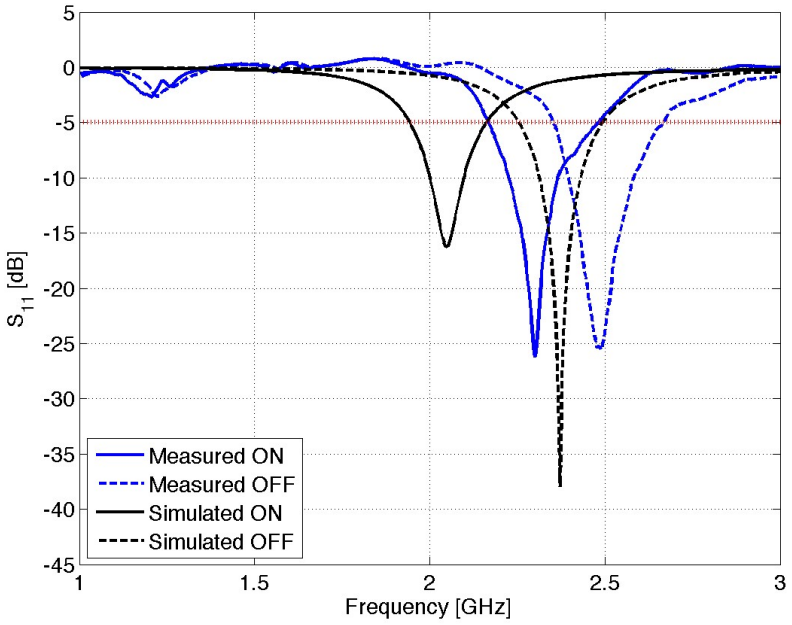

FIGURE 5.11: Simulated (Black) and Measured (Blue) return loss for the miniaturized reconfigurable L-monopole in 'ON state' (solid) and 'OFF state' (dashed).

The diode activation circuit was not considered in the simulated model. This is another possible source for the obtained deviations in frequency. Although RF chokes and bandpass capacitor were used to reduce the interference of it.

5.2.2 C-monopole

The first attempt to create a very small reconfigurable antenna using a printed L-monopole was not very succesful. Although the concept of reconfigurability in small antennas using PIN diodes and inductors was proved, the antenna structure doesn't have a great degree of freedom to perform adjustments. And thus, the frequencies proposed for this antenna were not attained.

In that sense, a second approach was made, this time with a printed C-monopole. The C-monopole, not only allows for an even smaller antenna, but has more branches, which means more degrees of optimization that can be made in order to obtain the proposed results.

The proposed antenna design is presented in Figure 5.12 and the corresponding dimensions are presented in Table 5.2. The size of this antenna is exactly the same as the C-monopoles presented in Chapters 2 and 3.

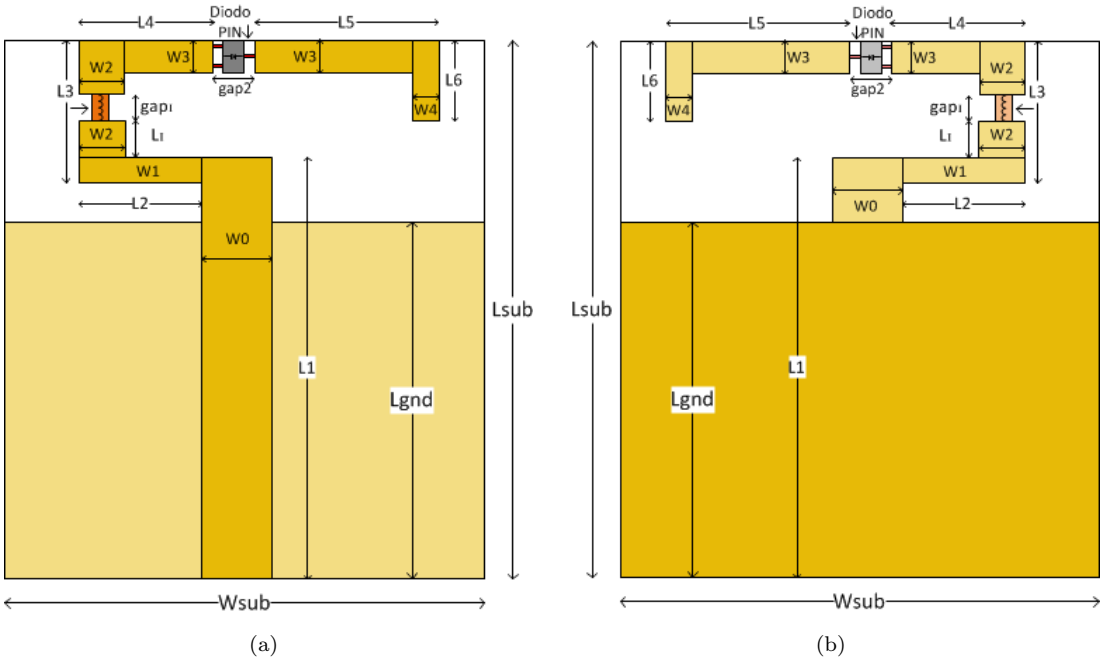

FIGURE 5.12: Miniaturized reconfigurable C-monopole (a) front view, (b) back view.

TABLE 5.2: Miniaturized reconfigurable C-monopole dimensions.

Parameter	**Value [mm]**
L1	24.0
L2	3.35
L3	6.00
L4	4.00
L5	7.60
L6	5.00
Lgnd	21.0
Lsub	28.5
Wsub	20.0
W0	3.30
W1	1.50
W2	1.50
W3	2.00
W4	1.50
gap	2.00
gap_I	0.50
L_I	1.00

The simulated return loss for both operating states of the PIN diode, can be seen in Figure 5.13. When comparing to the results obtained for the printed C-monopole in Chapter 2, the resonant frequencies reduction is obvious, with a reduction of 1 GHz and 4.3 GHz respectively for the diode 'ON' and 'OFF' state. But, has occured in Chapter 3, the chip inductor also reduces the bandwidth of the antenna.

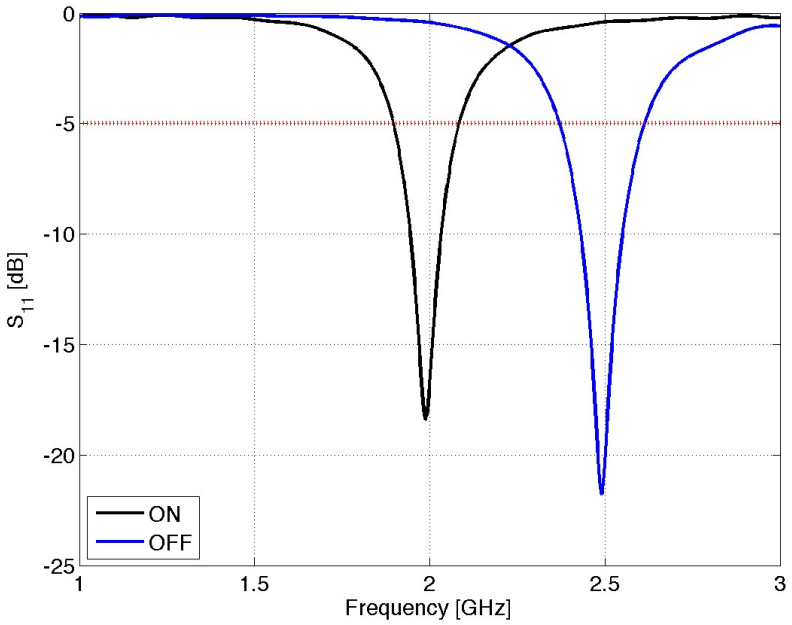

FIGURE 5.13: Return loss for the miniaturized reconfigurable C-monopole in 'ON state' (black) and 'OFF state' (blue).

When in 'OFF' state, the reduction in frequency is in fact 4.3 GHz, because in the C-monopole presented in Chapter 2, the impedance matching of the shorter monopole was only achieved for the second resonating mode, around 6.7 GHz. While for this monopole, roughly good impedance matching was achieved for the fundamental mode in both antenna states.

When compared to the reconfigurable C-monopole in Chapter 4 one can see a clear size reduction. Whilst the antenna presented in section 4.4.4 has an area of $16.1 \times 18.5\text{mm}^2$ and the a total area of $25.0 \times 38.0\text{mm}^2$, the reconfigurable C-monopole presented in the current section, as mentioned before, has an area of 13.6×7.5 mm^2 and a total area of 20.0×28.5 mm^2. This is equivalent to a 65% antenna area reduction, and a 40% total antenna size reduction. These are very expressive results.

The impedance response of the miniaturized reconfigurable C-monopole presents the same behavior as the L-monopole in the previous section. This can be observed in Figure 5.14.

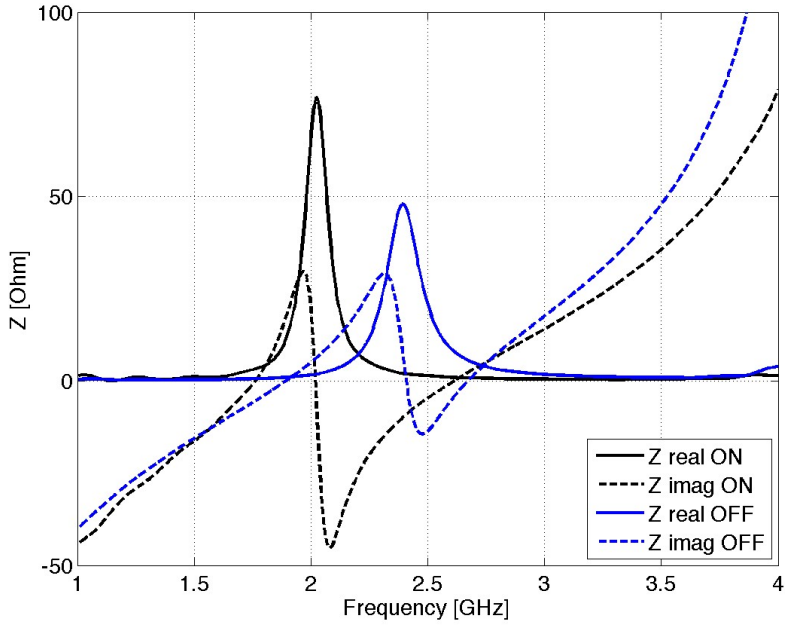

FIGURE 5.14: Impedance for the miniaturized reconfigurable C-monopole in 'ON state' (black) and 'OFF state' (blue).

The resonant frequency of the miniaturized reconfigurable C-monopole is, as the previous section example, very dependant on the lumped components. However, it seems the C-monopole geometrie has an advantage for this kind of development when compared to the L-monopole. Besides the even smaller area of the antenna, this geometrie shows higher gains and efficiencies in both diode operation states. The simulated gain for this C-monopole is of 0.4 dBi and 1 dBi for the 'ON' and 'OFF' state, respectively. These are higher than the obtained for the L-monopole in the previous section, by a factor of 0.15 dB and 0.3 dB, for both states respectively.

The radiation pattern was not significantly affected, still presenting an omnidirectional characteristic, as can be seen in Figure 5.15.

In the previous chapter, a small analysis to the effect of the PIN diode in the monopole, led to the conclusion that small variations on the parasitic elements of the component would have a determinant but not very severe effect on the antenna response. In the next few graphics, it is shown that when the PIN diode and the inductor are used together,

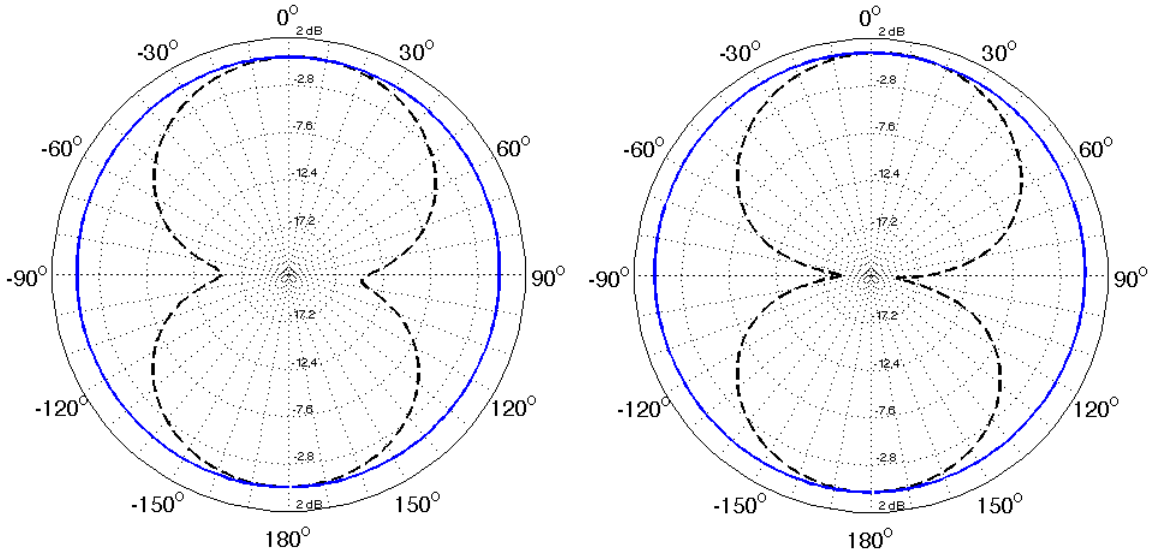

(a) (b)

FIGURE 5.15: Radiation pattern for the miniaturized reconfigurable C-monopole on YZ plane (dashed) and XZ plane (continuous) at (a) 2.0 GHz, (b) 2.5 GHz.

the impedance response is so dependant on these components that slight changes in their values, have a large effect on the entrance impedance of the antenna.

The parasitic inductance of the PIN diode, has the same effect as in the reconfigurable monopole presented in the previous chapter. As the inductance value increases, the resonating frequency is reduced. This happens for both modes of operation of the antenna, with more influence on the 'ON' state. Figure 5.16 shows the PIN diode parasitic inductance value sweep, for both modes of operation.

The series resistance value does not change the resonating frequency. In fact when in 'ON' mode, the influence is very small, the results were very close to the observed in section 4.4.3. However, when in 'OFF' mode, the variation in the absolut value of the impedance is much more noticeable in this case, when compared with the results from section 4.4.3. Figure 5.17 shows the variation of the impedance to the series resistance value sweep when the diode is reversed biased.

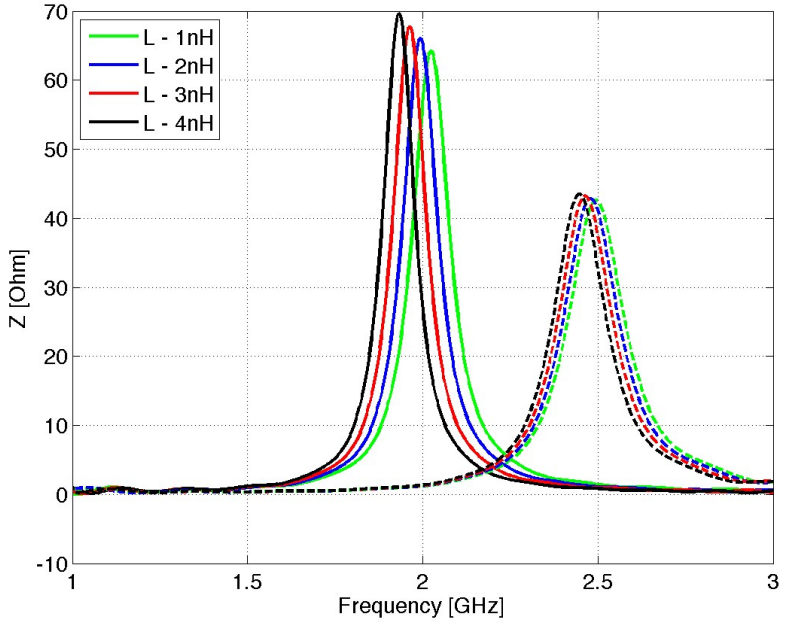

(a)

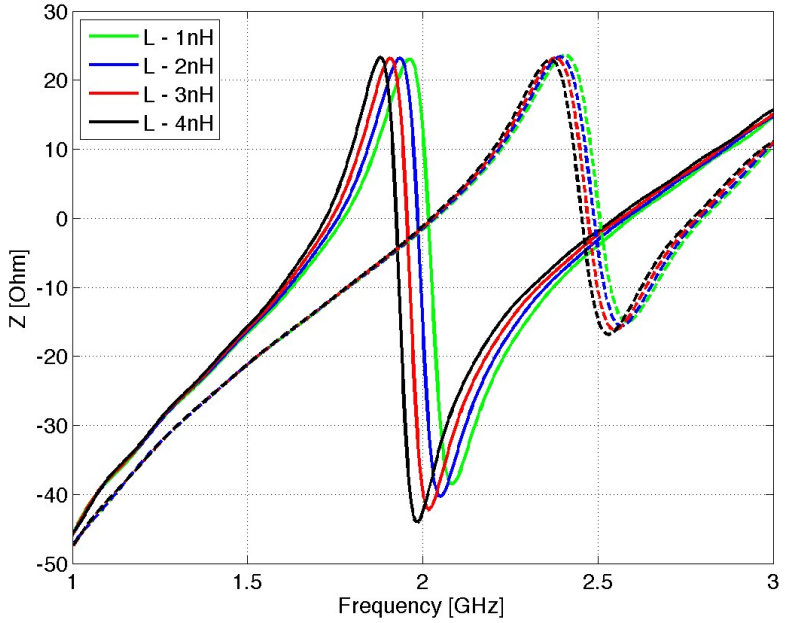

(b)

FIGURE 5.16: Impedance for the PIN diode's parasitic inductance value sweep of the miniaturized reconfigurable C-monopole (a) resistance, (b) reactance.

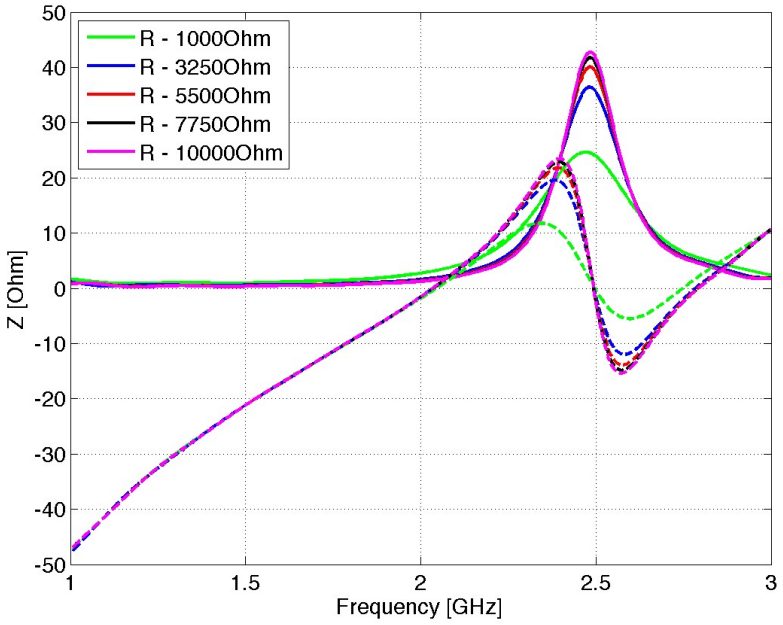

FIGURE 5.17: Impedance for the PIN diode's series resistance value sweep of the miniaturized reconfigurable C-monopole.

The effect of the PIN diode capacitance's variation is presented in Figure 5.18. As before, this influences the resonating frequency as the absolut value of the impedance. This means, that this parasitic element of the PIN diode, which has a value that is not always accurate in the components datasheets since it's hard to measure, can be, the major responsible for the deviations occuring in the prototyped antennas when compared to simulation results.

The prototype of this antenna was also fabricated, according to the design specifications mentioned earlier on this section. These can be seen in Figure 5.19

Photographs are always misleading in proportions. Still, with the comparison elements introduced one can perceive, once again, the small size of this antenna.

Same as the L-monopole in the previous section, for the correct measurement of the return loss of the antenna, a network analyzer and a power source in order to activate the PIN diode is needed. In Figure 5.20 the measurements setup and the equipment used to perform them is shown.

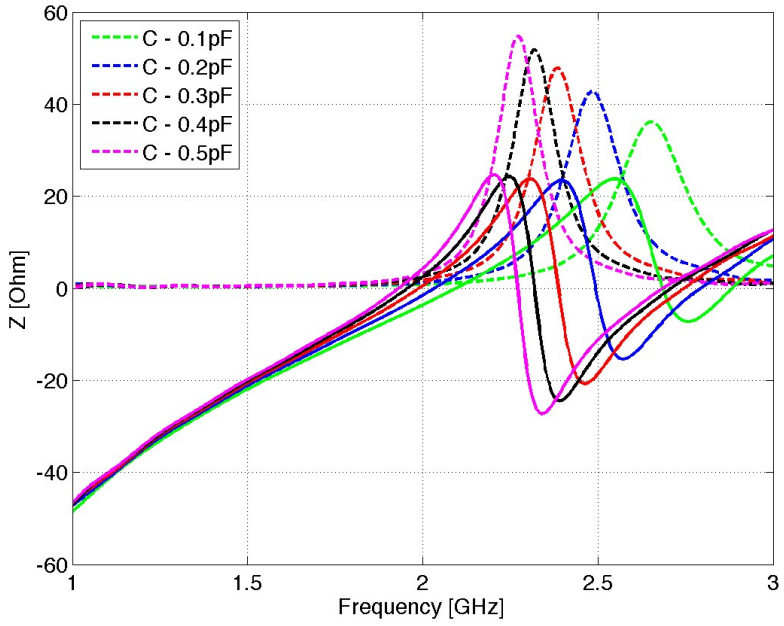

FIGURE 5.18: Simulated impedance for the PIN diode's capacitance value sweep of the miniaturized reconfigurable C-monopole.

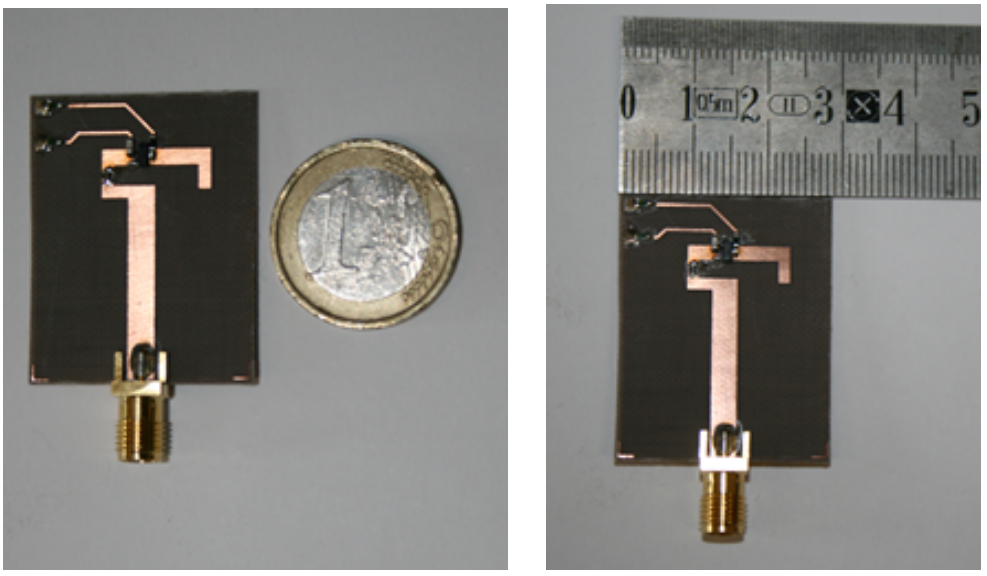

(a) (b)

FIGURE 5.19: Prototype miniaturized reconfigurable C-monopole.

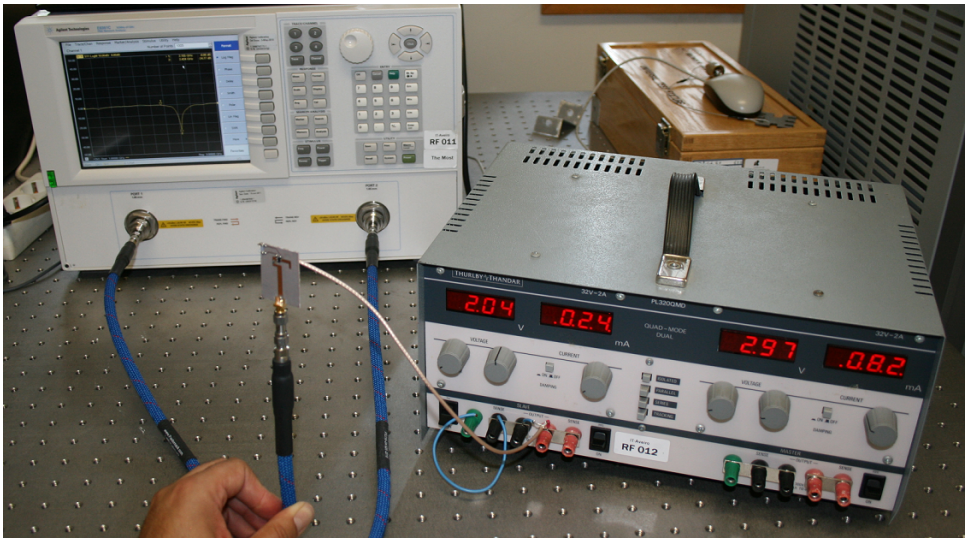

FIGURE 5.20: Measurements setup.

A special care was taken in order to minimize interference from the power source on the antenna operation and to protect the power source from the antenna RF signal. This was done by protecting the antenna from the rest of the circuit with RF chokes and a capacitor for filtering. Besides, a very slim coax cable was used for the circuit feeding, since during the tests it was concluded that simple copper wires would produce a considerable interference with the antenna.

The measured return loss is shown in Figure 5.21, in which one can compare the simulated with the measured results.

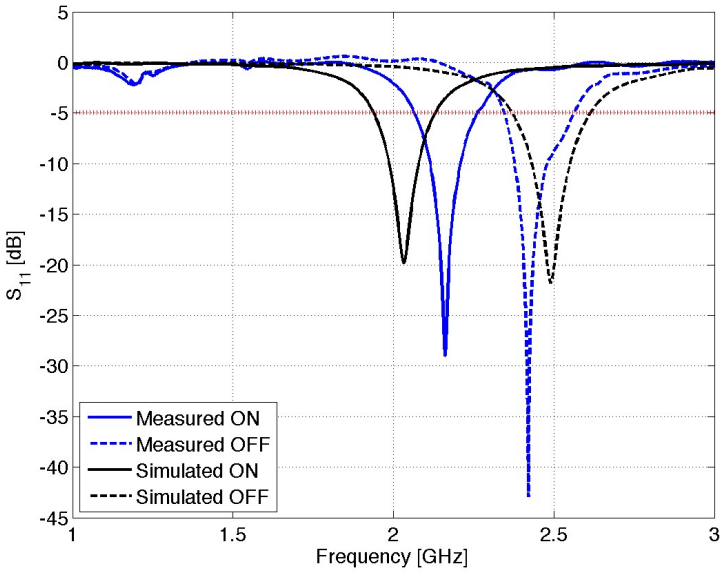

FIGURE 5.21: Simulated (Black) and Measured (Blue) return loss for the miniaturized reconfigurable C-monopole in 'ON state' (solid) and 'OFF state' (dashed).

Once again, some deviations to the simulated results were observed. However, in this case the upper band as shifted down slightly and the lower band shifted up. However, the prototype upper band ('OFF' state) is between 2.39 and 2.5 GHz, which means it covers the WLAN band, one of the proposed applications. Therefore, the results obtained for the C-monopole prototype can be considered better than the ones obtained for the L-monopole prototype in the previous section.

One fact about both prototype measurements is that the impedance matching shows much better agreement for the prototyped antennas, than the simulated antennas. This might be due to the PIN diode variations with current. When testing both prototypes it was observed, that the return loss would vary when the voltage and current applied to the PIN diode change. The best results were achieved with a source of 3 V and 35 mA.

The measured radiation pattern for this prototype presents the expected omnidirectional characteristic, as shown in Figure 5.22. The protuberances present in the obtained pattern may arise from the presence of the wires for the polarization circuit, besides the shadow zone of the anechoic chamber which is noticable in the XZ plane measurement.

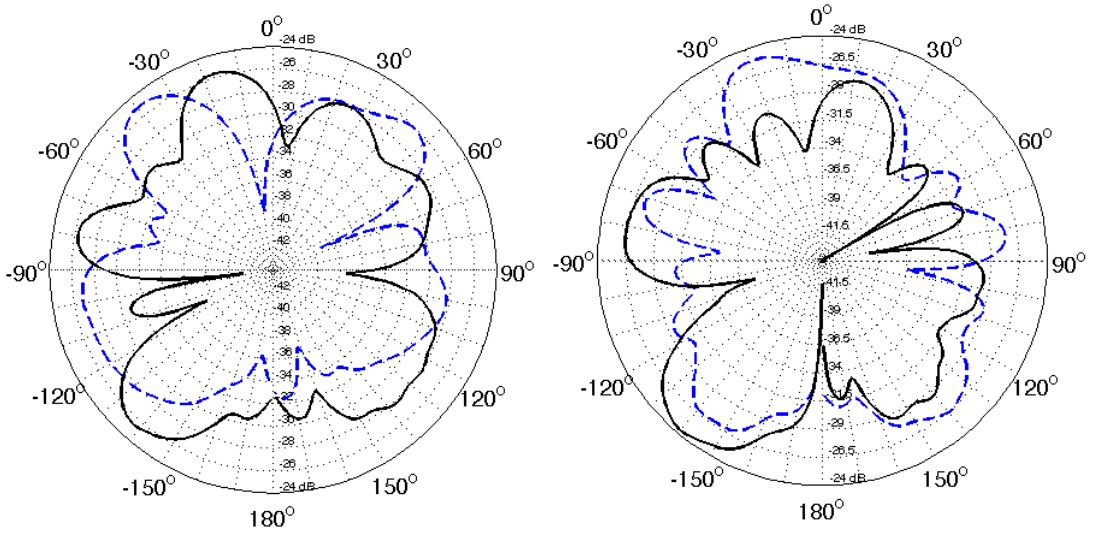

FIGURE 5.22: Radiation pattern for the miniaturized reconfigurable C-monopole on YZ plane (solid) and XZ plane (dashed) at (a) 2.2 GHz, (b) 2.4 GHz.

Chapter 6

Conclusion

6.1 Conclusion

The purpose of this thesis work was to study reconfigurability and miniaturization of printed antennas, for mobile communication equipments.

There are limitations in what concerns the miniaturization of antennas. The physical limitations of small antennas were described, and the effects on radiation performance were discussed, based on some designed models to achieve it. Two miniaturization techniques were proposed, one based on a shorting pin to the end of the antenna, and another with the use of chip inductors, embedded in the antenna structure. The first attempt was not very successful, the use of a shorting pin for the miniaturization of a printed monopole, results in very poor radiation efficiencies and a complete degradation of the radiation pattern. The second approach showed better results, since the radiation efficiencies and the radiation pattern of the antenna were barely affected, however, the use of the chip inductor committed the bandwidth of the antenna.

Reconfigurability has received a lot of research attention in the past few years. In this work, frequency reconfigurability with PIN diodes was investigated, and used efficiently, to create a frequency reconfigurable printed monopole for multi-band operation. An ideal monopole was simulated and prototyped, in order to compare simulation to actual response of the antennas. A few differences were detected in the resonating frequencies obtained, but it could work in most of the proposed bands.

A line connection however, cannot properly emulate a PIN diode, since the diode is characterized for certain values of resistance, capacitance and inductance, that are very different from the line values. In that sense, new simulations were performed, in which a PIN diode was emulated by its equivalent circuits. A clear change in the antenna characteristics was observed, particularly in the resonating frequencies. A new prototype was built to compare the results of simulation, and again a few deviations of the operating frequencies were observed.

For last, these two techniques were employed together in order to create very small antennas for selectable dual-band operation. A C-monopole and an inverted L-monopole were designed with this techniques. Simulation results shown that both show dual-band operation, although narrower bandwidths were obtained in comparison with the reconfigurable monopoles, both operate in the WLAN and UMTS bands.

As regards the research, this two techniques were never used together to achieve this purpose, and so this contributed to some original content publications.

6.2 Future Work

The bandwidth of the proposed monopoles is very narrow in both cases. It would be interesting to apply bandiwdth enhancement techniques, in order to achieve good operation for more services. A starting point would be to verify the substrate height influence and try to increase. This would mean increasing the antenna size, but a trade-off could probably be achieved.

Besides the bandwidth, the prototyped antennas need some tunning to further aproximate the obtained results with the simulation. The lumped elements have a large influence over the operation of the antenna that could be further investigated and modeled to close the gap between simulations and measurements.

Besides all this, it is possible to further miniaturize the proposed antennas, if a 3D approach is considered. In this work, only planar structures were considered due to the lower cost and ease of fabrication. A 3D antenna structure is harder to design, and can degrade the radiation characteristics, however it's a possibility for future research, the use of the techniques discussed in this dissertation, for volumetric antennas.

Appendix A

Printed Transmission Lines

The field of study of transmission lines is vast, and its not the objective of this document to give a profound knowledge about it. However, printed transmission lines are largely used to feed printed antennas, and so some basic concepts must be considered to design them effectively.

A.1 Microstrip Line

The microstrip line is probably the most common and most used printed transmission line used in radio frequency applications. This structure can be applied to guide signals, its most common application, but can also be used to create filters, couplers and other microwave structures. The operation of such structures is contrary to the operation of a printed antenna. Whereas in the design of printed antennas, we should privilege the existence of space and leakage waves, in the design of printed transmission lines, we should privilege the existence of more guided waves. In this sense, the perfect dimensioning of an antenna leads to a faulty operational transmission line. Because of the propagation method associated with the microstrip line, which causes such dispersion, these are considered quasi-TEM (Transverse Electromagnetic) transmission lines, which means they don't propagate a full TEM wave at a given time. An example of a microstrip line is shown in Figure A.1. The impedance of this type of transmission line is rather complex to calculate, however it has been widely studied and according to [7] the best approximation if given by A.1.

FIGURE A.1: Printed microstrip transmission line example.

$$Z_0 = \frac{\eta_0}{2\sqrt{2}\pi\sqrt{\epsilon_{eff}+1}} \ln\left\{1+\frac{4h}{w'}\left[\frac{4h\left(14+\frac{8}{\epsilon_{eff}}\right)}{11w'}+\sqrt{\left(\frac{14+\frac{8}{\epsilon_{eff}}}{11}\right)^2\left(\frac{4h}{w'}\right)^2+\frac{1+\frac{1}{\epsilon_{eff}}}{2}\pi^2}\right]\right\}[\Omega] \tag{A.1}$$

Where η_0 is the dielectric constant of free space of value 120π, w' is the effective width of the microstrip line, with a slight correction based on the thickness (t) of the conductor material, so w' becomes w if the thickness of the conductor is disregarded as seen in A.2, and ϵ_{eff} is the effective dielectric constant which can be calculated according to A.3 and A.4.

$$w' = w + t\frac{1+\frac{1}{\epsilon_r}}{2\pi}\ln\left[\frac{4e}{\sqrt{\left(\frac{t}{h}\right)^2+\left(\frac{\frac{1}{\pi}}{\frac{w}{t}+1.1}\right)^2}}\right][mm] \tag{A.2}$$

$$\epsilon_{eff} = \frac{\epsilon_r+1}{2}+\frac{\epsilon_r-1}{2}\left[\left(1+\frac{12h}{w}\right)^{-0.5}+0.04\left(1-\frac{w}{h}\right)^2\right] \quad when\ {}^{w}/_{h} \leq 1 \tag{A.3}$$

$$\epsilon_{eff} = \frac{\epsilon_r+1}{2}+\frac{\epsilon_r-1}{2}\left(1+\frac{12h}{w}\right)^{-0.5} \quad when\ {}^{w}/_{h} > 1 \tag{A.4}$$

To the design of printed antennas, these are very useful to create the antenna feeding. Since theyre easily integrated in the structure and can be simulated and modeled with the antenna at the same time. Besides they're very useful to create quarter-wavelength adapters to match the input impedance of the antennas, on single elements and especially the feeding mesh of printed antenna arrays.

A.2 Coplanar Line

The coplanar waveguide is another example of printed transmission line. In this case the ground plane is in the same plane as the conductor, as is shown in Figure A.2. This

is rather good to save money since the feeding line and the antenna can be built on single layer PCBs. However, this is not a great advantage nowadays, due to the fact that most substrates are covered in conductive material in both sides. In this case, the

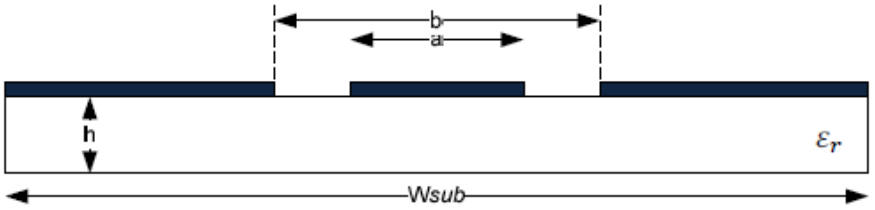

FIGURE A.2: Printed coplanar transmission line example.

best approximation for the characteristic impedance of the line is, once again according to [7], given by A.5.

$$Z_0 = \frac{30\pi}{\sqrt{\epsilon_{eff}}} \frac{K'(k_1)}{K(k_1)} [\Omega] \tag{A.5}$$

$$\epsilon_{eff} = 1 + \frac{\epsilon_r - 1}{2} \frac{K(k_2)}{K'(k_2)} \frac{K'(k_1)}{K(k_1)} \tag{A.6}$$

$$\begin{cases} k_1 = \frac{a}{a+(b-a)} & 0 < k < \frac{1}{\sqrt{2}} \\ k_2 = \frac{\sinh(a\pi/4h)}{\sinh(\pi(a+(b-a))/4h)} & \frac{1}{\sqrt{2}} < k < 1 \end{cases} \tag{A.7}$$

$$\begin{cases} \frac{K(k)}{K'(k)} = \frac{\pi}{\ln\left(2\frac{1+\sqrt[4]{1-k^2}}{1-\sqrt[4]{1-k^2}}\right)} & 0 < k < \frac{1}{\sqrt{2}} \\ \frac{K(k)}{K'(k)} = \frac{\ln\left(2\frac{1+\sqrt[4]{1-k^2}}{1-\sqrt[4]{1-k^2}}\right)}{\pi} & \frac{1}{\sqrt{2}} < k < 1 \end{cases} \tag{A.8}$$

To ensure that the values calculated with these expressions are correct it should be guaranteed that the ground plane around the line is five times the length of the gap b.

A.3 Coplanar line with ground plane

As mentioned before, most of the substrates nowadays are covered in both sides with conductive material, so another transmission line that can be considered is the grounded coplanar waveguide. This is very similar to the coplanar waveguide, but in this case theres ground plane on both layers, as shown in Figure A.3.

This structure is better than the simple coplanar waveguide since it can perform the wave propagation in different configurations, by changing the design of the elements.

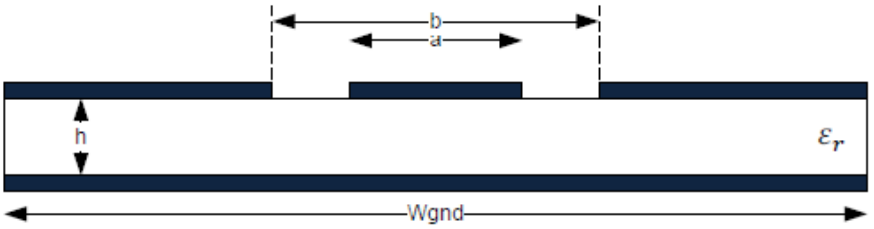

FIGURE A.3: Printed coplanar line with ground plane example.

This leads to a more versatile and less dispersive line than the coplanar waveguide or the microstrip transmission line [7]. Although this transmission line shows better performance than the last two examples, its a worse case when considering its application in printed antennas design, since the larger areas of ground plane will certainly affect the radiation.

A.4 Stripline

Albeit there are other types of printed transmission line designs, the stripline is the last one that shall be presented in this document. This is common feeding line found in slot fed printed antennas. The guide line is buried in the substrate and there are ground planes above and below it, which should be shorted together, as shown in Figure A.4. Although the guide line in the example shown is centered in relation to the ground planes, it doesnt have to be like that.

The stripline, contrary to the microstrip line, is a TEM transmission line media. So it behaves much like a coax cable, due to the fact that the conductor is surrounded by ground plane, its non-dispersive for almost all frequencies. [52] However there's a few disadvantages regarding the stripline, it is more expensive since its harder to fabricate, the introduction of lumped elements or active components can be tricky and the widths of the strips is much narrower when comparing to a microstrip line and the substrates are much thicker.

Considering the case that the guide is buried in the center of the substrate, than the characteristic impedance of this transmission line can be obtained with A.9.

$$Z_0 = \frac{\eta_0}{2\pi\sqrt{\epsilon_r}} \ln\left\{1 + \frac{4h}{\pi w'}\left[\frac{8h}{\pi w'} + \sqrt{\left(\frac{8h}{\pi w'}\right)^2 + 6.27}\right]\right\}[\Omega] \tag{A.9}$$

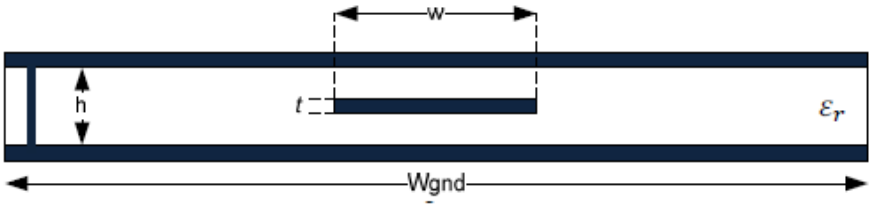

FIGURE A.4: Stripline example.

Where w' is the width of the guide with a correction due to its thickness and the height of the substrate, which becomes simple w when considering an infinitely thin guide.

Appendix B

Chip Inductor Characteristics

In this appendix the chip inductor SPICE model values, of the 0402HP family from Coilcraft are presented in Table B.1.

Table B.1: Coilcraft chip inductor 0402HP family values.

Part Number	**R1 (Ω)**	**R2 (Ω)**	**C (pF)**	**L (nH)**	***k***	**Upper Limit (MHz)**
0402HP-2N0	5	0.038	0.050	2.00	5.22E-6	20000
0402HP-2N2	4	0.038	0.040	2.20	5.70E-6	20000
0402HP-2N4	13	0.042	0.044	2.40	6.20E-6	20000
0402HP-2N7	11	0.056	0.044	2.70	6.46E-6	20000
0402HP-3N3	15	0.045	0.032	3.30	7.80E-6	20000
0402HP-3N6	10	0.045	0.022	3.60	8.10E-6	20000
0402HP-3N9	12	0.045	0.042	3.90	9.70E-6	14000
0402HP-4N3	10	0.040	0.048	4.30	1.12E-5	12000
0402HP-4N7	13	0.060	0.052	4.70	1.29E-5	12000
0402HP-5N1	15	0.100	0.044	5.10	1.45E-5	12000
0402HP-5N6	1	0.048	0.032	5.60	1.27E-5	12000
0402HP-6N2	15	0.050	0.047	6.20	1.43E-5	12000
0402HP-6N8	15	0.055	0.049	6.80	1.65E-5	12000
0402HP-7N5	12	0.080	0.049	7.50	2.04E-5	10000
0402HP-8N2	17	0.054	0.049	8.20	2.04E-5	10000
0402HP-8N7	11	0.058	0.048	8.70	2.13E-5	10000
0402HP-9N0	18	0.070	0.039	9.00	2.21E-5	10000
0402HP-9N5	10	0.075	0.048	9.50	2.43E-5	10000
0402HP-10N	4	0.085	0.051	10.0	2.57E-5	10000
0402HP-11N	10	0.065	0.042	11.0	2.67E-5	10000
0402HP-12N	10	0.070	0.043	12.0	2.84E-5	10000
0402HP-13N	4	0.140	0.047	13.0	3.40E-5	9000
0402HP-15N	15	0.078	0.038	15.0	4.00E-5	9000
0402HP-16N	18	0.130	0.044	16.0	4.50E-5	8000
0402HP-18N	5	0.120	0.040	18.0	5.40E-5	8000
0402HP-19N	22	0.145	0.040	19.0	4.70E-5	7000

Part Number	R1 (Ω)	R2 (Ω)	C (pF)	L (nH)	*k*	Upper Limit (MHz)
0402HP-20N	18	0.155	0.038	20.0	5.63E-5	7000
0402HP-22N	22	0.160	0.035	22.0	6.28E-5	7000
0402HP-23N	18	0.160	0.036	23.0	6.42E-5	7000
0402HP-24N	30	0.170	0.039	24.0	6.80E-5	7000
0402HP-27N	30	0.275	0.026	27.0	6.70E-5	7000
0402HP-30N	22	0.275	0.035	30.0	7.20E-5	7000
0402HP-33N	30	0.330	0.034	33.0	7.78E-5	7000
0402HP-36N	32	0.360	0.028	36.0	9.40E-5	7000
0402HP-37N	26	0.480	0.032	37.0	9.70E-5	7000
0402HP-39N	38	0.380	0.033	39.0	8.60E-5	6000
0402HP-40N	30	0.380	0.032	40.0	1.00E-4	6000
0402HP-43N	44	0.520	0.035	43.0	1.10E-4	6000
0402HP-47N	48	0.580	0.029	47.0	1.35E-4	6000
0402HP-51N	40	0.700	0.034	51.0	1.41E-4	6000
402HPH-56N	30	1.00	0.041	56.0	1.36E-4	5000
0402HPH-68N	25	1.20	0.035	68.0	1.72E-4	5000
0402HPH-82N	40	1.25	0.035	82.0	2.28E-4	4000
0402HPH-R10	20	1.20	0.039	100	2.71E-4	4000
0402HPH-R12	20	1.20	0.038	120	3.26E-4	3000
0402HPH-R15	40	2.00	0.041	150	3.72E-4	3000
0402HPH-R18	40	2.10	0.041	180	4.20E-4	3000
0402HPH-R22	20	3.10	0.037	220	5.10E-4	3000

Bibliography

[1] Wikipedia Community. http://en.wikipedia.org/wiki/Internet_of_Things, Retrieved March 2012.

[2] G. A. Deschamps. Microstrip microwave antennas. *3rd USAF Symposium on Antennas*, 1953.

[3] Iradilson Ferreira da Costa. *Antenas e Superfícies Selectivas de Frequência Reconfiguráveis para Sistemas de Comunicação Sem Fio*. PhD thesis, Universidade Federal do Rio Grande do Norte, 2009.

[4] Constantine A. Balanis. *Antenna Theory: Analysis and Design*. Wiley Interscience, 3 edition, 2005.

[5] R. F. Schwartz. Input impedance of a dipole or monopole. *Microwave Journal*, Vol. 15(12):22+, December 1972.

[6] Arlon©. http://www.arlon-med.com/Cuclad.pdf, Retrieved March 2012.

[7] Brian C. Wandell. *Transmission Line Design Handbook*. Artech House, Inc., 1991.

[8] J. L. Volakis. *Antenna Engineering Handbook*. McGraw-Hill, 4 edition, 2007.

[9] J. L. Volakis, C. Chen, and K. Fujimoto. *Small Antennas Miniaturization Techniques & Applications*. McGraw-Hill, 1 edition, 2010.

[10] Kin-Lu Wong. *Compact and Broadband Microstrip Antennas*. Wiley Interscience, 2002.

[11] Xueyi Yo, Guolin Li, and Zhihua Wang. Design of compact 2.45 ghz microstrip antenna. *IEEE International Symposium on Microwave, Antenna, Propagation and EMC Technologies for Wireless Communications*, Beijing, 2005.

[12] C. Delaveaud and S. Sufyar. A miniaturization technique of a compact omnidirectional antenna. *3rd European Conference on Antennas and Propagation (EUCAP)*, Berlin, 2009.

[13] Pradeep Kumar and G. Singh. Microstrip antennas loaded with shorting post. *Engineering*, Vol. 1(1-54), 2009.

[14] Ouedraogo R. O., Rothwell E. J., Diaz A. R., Fuchi K., and Temme A. Miniaturization of patch antennas using a metamaterial-inspired technique. *IEEE Transactions on Antennas and Propagation*, Vol. 60(5):2175 – 2182, 2012.

[15] Yonghun Cheon, Jungyub Lee, and Joonghee Lee. Quad-band monopole antenna including lte 700 mhz with magneto-dielectric material. *IEEE Antennas and Wireless Propagation Letters*, Vol. 11:137 – 140, 2012.

[16] Gaikwad S. S., Singh M., Ajey A., and Karthikayen S. S. Size miniaturized fractal antenna for 2.5 ghz application. *IEEE Students Conference on Electrical, Electronics and Computer Science*, 2012.

[17] Homayoon Oraizi and Shahram Hedayati. Circularly polarized multiband microstrip antenna using the square and giuseppe peano fractals. *IEEE Transactions on Antennas and Propagation*, Vol. 60(7):3466 – 3470, 2012.

[18] Homayoon Oraizi and Shahram Hedayati. Miniaturization of microstrip antennas by the novel application of the giuseppe peano fractal geometries. *IEEE Transactions on Antennas and Propagation*, PP, Early access articles(99):1 – 8, 2012.

[19] Qi Luo and J. R. Pereira. Compact printed c-shaped monopole antenna with chip inductor. *IEEE International Symposium on Antennas and Propagation (APS)*, Spokane, WA, 2011.

[20] Qi Luo, J. R. Pereira, and H. M. Salgado. Compact printed monopole antenna with chip inductor for wlan. *IEEE Antennas and Wireless Propagation Letters*, 2011.

[21] H. A. Wheeler. Fundamental limitations of small antennas. *Proceedings of the IRE*, Vol. 35(12):1479 – 1484, 1947.

[22] R. C. Hansen. Fundamental limitations in antennas. *Proceedings of the IEEE*, Vol. 69(2):170 – 182, 1981.

[23] A. D. Yaghjian and S. R. Best. Impedance, bandwidth, and q of antennas. *IEEE Transactions on Antennas and Propagation*, Vol. 53(4):1298 – 1234, 2005.

[24] Coilcraft©. http://www.coilcraft.com/0402hp.cfm, Retrieved April 2012.

[25] M. F. Ismail, M. K. Rahim, H. A. Majid, M. R. Hamid, M. R. Kamarudin, and N. A. Murad. Frequency reconfigurable aperture coupled antenna. *6th European Conference on Antennas and Propagation (EUCAP)*, Prague, 2012.

[26] Jeen-Sheen Row and Chuang-Jiashih Shih. Polarization-diversity ring slot antenna with frequency agility. *IEEE Transactions on Antennas and Propagation*, PP, Early access articles(99):1 – 5, 2012.

[27] Y. Tawk, J. Constantine, and C. G. Christodoulou. A rotatable reconfigurable antenna for cognitive radio applications. *IEEE Radio and Wireless Symposium*, Phoenix, AZ, 2011.

[28] M. Unlu, Y. Damgaci, H. S. Mopidevi, O. Kaynar, and B. A. Cetiner. Reconfigurable, tri-band rf mems pifa antenna. *IEEE International Symposium on Antennas and Propagation (APS)*, Spokane, WA, 2011.

[29] T. Yamagajo and Y. Koga. Frequency reconfigurable antenna with mems switches for mobile terminals. *IEEE-APS Topical Conference on Antennas and Propagation in Wireless Communications (APWC)*, Torino, 2011.

[30] Risto Valkonen, Cyril Luxey, Jari Holopainen, Clemens Ichlen, and Pertti Vainikainen. Frequency-reconfigurable mobile terminal antenna with mems switches. *Proceedings of the 4th European Conference on Antennas and Propagation (EUCAP)*, Barcelona, 2010.

[31] Chi-Yuk Chiu, Jichao Li, Sichao Song, and Ross D. Murch. Frequency-reconfigurable pixel slot antenna. *IEEE Transactions on Antennas and Propagation*, PP, Early access articles(99):1 – 5, 2012.

[32] N. Haridas, A. T. Erdogan, T. Arslan, A. J. Walton, S. Smith, T. Stevenson, C. Dunare, A. Gundlach, J. Terry, P. Argyrakis, K. Tierney, A. Ross, and T. O'Hara. Reconfigurable mems antennas. *NASA/ESA Conference on Adaptive Hardware and Systems*, Noordwijk, 2008.

[33] Qi Luo. *Design Synthesis and Miniaturization of Multiband and Reconfigurable Microstrip Antenna for Future Wireless Applications.* PhD thesis, Faculdade de Engenharia da Universidade do Porto, 2012.

[34] M. Fallahpour, M. T. Ghaspr, and R. Zoughi. A multiband reconfigurable cpw-fed slot antenna. *IEEE International Symposium on Antennas and Propagation (APS)*, Chicago, 2012.

[35] A. Ghasemi, N. Ghavehchian, A. Mallahzadeh, and S. Sheikholvaezin. A reconfigurable printed monopole for mimo application. *6th European Conference on Antennas and Propagation (EUCAP)*, Prague, 2012.

[36] M. G. S. Hossain and T. Yamagajo. Reconfigurable printed antenna for a wideband tuning. *Proceedings of the 4th European Conference on Antennas and Propagation (EUCAP)*, Barcelona, 2010.

[37] Y. K. Park and Y. Sung. A reconfigurable antenna for quad-band mobile handset applications. *IEEE Transactions of Antennas and Propagation*, Vol. 60(6):3003–3006, 2012.

[38] Faouzi Romdhani, Mohsen Denden, and Abdelaziz Samet. A printed reconfigurable antenna for communication system. *Mediterrannean Microwave Symposium (MMS)*, Tangiers, 2009.

[39] Trong Duc Nguyen, Yvan Duroc, Van Yem Vu, and Tan Phu Vuong. Novel reconfigurable 8-shap pifa antenna using pin diode. *International Conference on Advanced Technologies for Communications (ATC)*, Da Nang, 2011.

[40] Jong-Hyuk Lim, Gyu-Tae Back, Young-Il Ko, Chang-Wook Song, and Tae-Yeoul Yun. A reconfigurable pifa using a switchable pin-diode and a fine-tuning varactor for uspcs/wcdma/m-wimax/wlan. *IEEE Transactions on Antennas and Propagation*, Vol. 58(7):2404 – 2411, 2010.

[41] Symeon Nikolaou, Boyon Kim, and Photos Vryonides. Reconfiguring antenna characteristics using pin diodes. *3rd European Conference on Antennas and Propagation (EUCAP)*, Berlin, 2009.

[42] M. I. Lai, T.Y. Wu, J. C. Hsieh, C. H. Wang, and S. K. Jeng. Design of reconfigurable antennas based on an l-shaped slot and pin diodes for compact wireless devices. *IET Microwaves, Antennas & Propagation*, Vol. 3(1):47 – 54, 2009.

[43] M. S. Nishamol, V. P. Sarin, D. Tony, C. K. Aanandan, P. Mohanan, and K. Vasudevan. An electronically reconfigurable microstrip antenna with switchable slots for polarization diversity. *IEEE Transactions on Antennas and Propagation*, Vol. 59(9):3424 – 3427, 2011.

[44] Manoj S. Parihar, A. Basu, and S. K. Koul. Polarization reconfigurable microstrip antenna. *Asia Pacific Microwave Conference*, Singapore, 2009.

[45] C. Sai-Xiong, Y. Xue-Xia, G. Bo, and S. Bing-Cheng. A reconfigurable microstrip antenna with agile polarization using diode switches. *IEEE International Symposium on Antennas and Propagation (APS)*, Spokane, WA, 2011.

[46] D. Jiawei, W. Anguo, and L. Hang. A simple radiation pattern reconfigurable printed dipole antenna. *IEEE International Symposium on Microwave, Antenna, Propagation and EMC Technologies for Wireless Communications*, Beijing, 2009.

[47] Jr. W. E. Doherty and R. D. Joos. *The PIN diode circuit designer's handbook*. Microsemi Corporation, 1 edition, 1998.

[48] Application Note 922. *Applications of PIN diodes*. Hewlett Packard Company.

[49] Application Note 1002. *Design with PIN diodes*. Alpha Industries Inc.

[50] Avago Technologies©. http://www.avagotech.com/docs/AV02-0293EN, Retrieved April 2012.

[51] NXP©. http://www.nxp.com/documents/data_sheet/BAP64-03.pdf, Retrieved April 2012.

[52] P-N Designs Inc. Stripline. http://www.microwaves101.com/encyclopedia/stripline.cfm, Retrieved March 2012.